SUPPORTING SPACE TRAFFIC MANAGEMENT

A ROAD TO COLLISION AVOIDANCE MANOEUVRING FOR CONSTELLATIONS

GIGI LAAN.

nlr

TU Delft

Cover art by Isabel Offenberg

Supporting Space Traffic Management

A Road to Collision Avoidance Manoeuvring for Constellations

by

Gigi Laan

March 25, 2021

Student number: 4229274
Supervised by: ir. M. C. Naeije, TU Delft, supervisor
ir. M. Snijders, NLR, supervisor

TU Delft

Preface

From the beginning of my Masters already, I noticed the pressing worries of space contamination. Even though I did not know this would be the topic of my thesis, it had stayed with me. It was therefore also an unintended but good reminder when I was presented with this subject again by NLR, that I could still go this direction for my thesis. Not only has this topic been great in terms of what I want to focus on in life, which is to make the world a better place (cheesy but true), where I am also grateful that I had the opportunity to do this in collaboration with NLR. They were able to provide me with the background information and resources to do my research, where they also gave me the freedom to choose which way I wanted to go.

Writing a thesis has its ups and downs, where the highs are high and the lows can feel pretty low, which is why I couldn't have done this without the support I got. I want to thank my mom, dad and brother for all their love and support. I also want to thank all my friends, who helped me in keeping my head clear and stay focused on the goal through the good and the bad times. Next to my family and friends I also want to thank my supervisors, Merle and Marc, for their guidance and supervision throughout this process. Not only do I want to thank Merle for the technical support but also the emotional support that was needed sometimes. It has been great to work with you and I truly hope our paths will cross again in the future.

Gigi Laan
Berlin, March 2021

Abstract

With the increase of satellite constellations in orbit, the need for a Space Traffic Management (STM) is becoming undeniable. Within the scope of STM, an impartial and optimized collision avoidance advice based on the perspective of two manoeuvrable satellites could encourage more active collision avoidance and prevent on-orbit collisions. Using CDM data and operator input for the setup of the optimization, it was shown that in-track manoeuvres performed by either one or both of the satellites have a minimum usage of ΔV in combination with a small displacement and meet the collision probability threshold. Additionally, it was shown that the use of weights in the optimization cost function can influence the manoeuvre magnitude and the respective satellite that needs to perform the manoeuvre. Combining this optimization with a linearized propagation of the satellite states, a quick recommendation can be generated on the manoeuvre options for both satellites, which could help the development of an STM in terms of an impartial collision avoidance manoeuvre advice system.

“ *Even a correct decision is wrong when it was taken too late*”
- Lee Iacocca

Master Thesis
March 25, 2021
V2.0

Contents

List of Figures

List of Tables

List of Abbreviations

Abbreviation	Definition
18SPCS	18th Space Control Squadron
ASAT	Anti-Satellite Technology/Test
CDM	Conjunction Data Message
CNES	Centre National d'Etudes Spatiales
COTS	Commercial Off The Shelf
CSpOC	Combined Space operations Center
DE	Differential Evolution
ESA	European Space Agency
FCC	Federal Communications Commission
GEO	Geosynchronous Orbit
HASDM	High Accuracy Satellite Drag Model
IOS	In-Orbit Servicing
ISS	International Space Station
ITRF	International Terrestrial Reference Frame
JB08	Jacchia-Bowman-2008
JBH09	Jacchia-Bowman-HASDM-2009
JSpOC	Joint Space Operations Center
LEO	Low Earth Orbit
NASA	National Aeronautics and Space Administration
NEO	Near-Earth Objects
NORAD	North American Aerospace Defense Command
PF	Payload Fragmentation Debris
PL	Payload
PMD	Post Mission Disposal
RB	Rocket Bodies
RF	Rocket Fragmentation Debris
RIC	Radial, In-track, Cross-track
SGP4	Simplified General Perturbations 4
SSA	Space Situational Awareness
SST	Space Surveillance and Tracking
STK	Systems Tool Kit
STM	Space Traffic Management
STMX	State transition matrix
SWE	Space Weather
TCA	Time of Closest Approach
TLE	Two Line Element
U.S.	United States
UI	Unidentified
USSPACECOM	United States Space Command
USSTRATCOM	U.S. Strategic Command

List of Symbols

Greek Symbol	Definition	Unit
$\Delta\overline{r}_B$	Relative position vector in the B-plane	m
ΔC	Displacement in cross-track direction	m
ΔI	Displacement in in-track direction	m
Δr	Relative position	m
ΔV_C	Velocity change in cross-track direction	m/s
ΔV_I	Velocity change in in-track direction	m/s
ΔV_R	Velocity change in radial direction	m/s
ΔV_x	Velocity change in x-direction	m/s
ΔV_y	Velocity change in y-direction	m/s
ΔV_z	Velocity change in z-direction	m/s
ΔV	Change in spacecraft velocity, manoeuvre magnitude	m/s
Δv	Relative velocity	m/s
Δx	Relative position	m
ϵ	Residuals	-
Φ	State transition matrix	-
σ	Standard deviation	-

Latin Symbol	Definition	Unit
$\bar{C}$	Combined covariance matrix	-
$\hat{\bar{x}}$	State estimate	m, m/s
$\overline{h}$	Model observations vector	m, m/s
$\overline{r}$	Position vector	m
$\overline{v}$	Velocity vector	m/s
$\overline{X}_B$	B-plane x-direction unit vector	m
$\overline{x}$	State vector	m, m/s
$\overline{Y}_B$	B-plane y-direction unit vector	m
A_C	Collision sphere cross-section	m^2
C_0	Error Covariance Matrix at t_0	-
C_B	Error covariance matrix in B-plane	-
$C, \dot{C}$	Cross-track position and velocity	m, m/s
CN_N	Covariance Element Normal-Normal	m^2
CN_R	Covariance Element Normal-Radial	m^2
CN_T	Covariance Element Normal-Transverse	m^2
CR_R	Covariance Element Radial-Radial	m^2
CR	Probability threshold for trial vector selection	-
CT_R	Covariance Element Transverse-Radial	m^2
CT_T	Covariance Element Transverse-Transverse	m^2
D	Real parameters	-
F	Mutation factor	-
G	Generations	-
h_0	Disturbance step for central differencing	m, m/s
H	Jacobian matrix of modeled observations	-
I_{rand}	Random integer	-
$I, \dot{I}$	In-track position and velocity	m, m/s
J	Cost function	-
k	Normal distribution dimension	-
N	Population size	-
P_C	Collision probability	-
R_{X_B,Y_B}	Transformation matrix to B-plane	-
R_C	Collision sphere radius	m
R_r	Risk object sphere radius	m
R_t	Target object sphere radius	m
$R, \dot{R}$	Radial position and velocity	m, m/s
R	Transformation matrix	-
SF	Scaling factor	-
t_{tca}	Time of closest approach	s
t_0	Initial time	s
T_1	Transformation matrix to RIC frame	-
t	Time	s
U	Radial direction	-
$v_{i,G+1}$	Donor vector i from generation G	-
V_C	Collision sphere volume	m^3
V	In-track direction	-
W	Weighing Matrix	-
W	Cross-track direction	-
w	Cost function weight	-
$x_{r,G}$	Mutation vector r from generation G	-
x_B	Position in the B-plane x-direction	-
$x, \dot{x}$	Position and velocity in x-direction	m, m/s
X, X_DOT	Position and velocity in the X-direction	m, m/s
x^L	Lower bound value	-
x^U	Upper bound value	-
y_B	Position in the B-plane y-direction	-
$y, \dot{y}$	Position and velocity in y-direction	m, m/s
$z, \dot{z}$	Position and velocity in z-direction	m, m/s
Z, Z_DOT	Position and velocity in the Z-direction	m, m/s
Z, X_DOT	Position and velocity in the Y-direction	m, m/s

1 Introduction

Closely after the launch of the first artificial Earth satellite Sputnik 1, which initiated the space race, the *United Nations Committee on the Peaceful Uses of Outer Space* was established in 1958. The mission of the committee was to review international cooperation regarding peaceful uses of outer space, while studying and encouraging space research programmes as well as studying the legal problems resulting from the exploration of outer space. The aim was to govern the exploration of outer space and to simultaneously benefit all humanity of peace, security and development.[1]

Four decades after the launch of this committee a report was published on space debris, from when onward it was understood that the space debris environment poses a risk to the spacecraft that are orbiting the Earth. In this report, space debris was defined as all man-made objects, including fragments and mission-related debris. It was already understood that the amount of space debris is growing and at a significant higher count than the operational satellites in orbit, leading to higher collision risk and increasing potential risk of damage [1]. Another study was done on the effect of fragmentation events, where a collision including Earth orbiting satellites could cause a cascading chain reaction, rendering the space environment hazardous to space flight [2].

The evolution of objects in space can be seen in Figure 1.1. More than 8000 new objects are reported in orbit, being 40% of the current object count. Only 25% of the total object count are new operational satellites from the last 12 years, where the resulting objects are mainly debris [3]. Following the most recent numbers, as of January 1 2020 the catalogued on-orbit fragments from accidental explosions is 60% [4]. Figure 1.1 depicts this growth in the object count, where some sudden spikes can be seen in the count of objects. These sudden spikes are the result of satellite collisions, intentional as well as unintentional.

The first event happened in 2007, which was an intentional fragmentation event as a result of the test of an anti-satellite missile test (ASAT) done by China. This anti-satellite missile test destroyed the Chinese FengYun-1C weather satellite, creating orbital fragmentation debris that would take multiple decades to deorbit. The second event in 2009 was a result of two communication satellites colliding, Iridium 33 and Cosmos-2251, causing a large amount of collision fragments, which again will take multiple decades to deorbit [5].

A recent anti-satellite test was performed by India in 2019, where orbital debris was created that is posing a significant risk increase to the International Space Station.[2] Following this event, it became apparent that more regulated space traffic rules are needed, as these kinds of actions are posing a large risk to future space flight. Not only did this event spark a discussion regarding the safekeeping of space flight, a recent collision risk involving a European Space Agency (ESA) satellite and SpaceX constellation satellite (Aeolus and Starlink 44) was detected, which again indicated a need for a more centralised system. This collisions risk was eliminated by performing a successful collision manoeuvre by Aeolus (ESA) about half an orbit before the potential collisions would take place. It is expected that these kind of manoeuvres involving active satellites will need to happen more often with the increase in space traffic[3], confirming a higher need for Space Traffic Management (STM).

Looking at the level of technology in the space sector, it can be observed that a recent growth can be seen. Launch costs are being reduced, granting easier access to space, suborbital flights together with space

[1] https://www.unoosa.org/oosa/en/ourwork/copuos/index.html
[2] https://spacenews.com/op-ed-indias-asat-test-is-wake-up-call-for-norms-of-behavior-in-space/
[3] https://www.space.com/spacex-starlink-esa-satellite-collision-avoidance.html

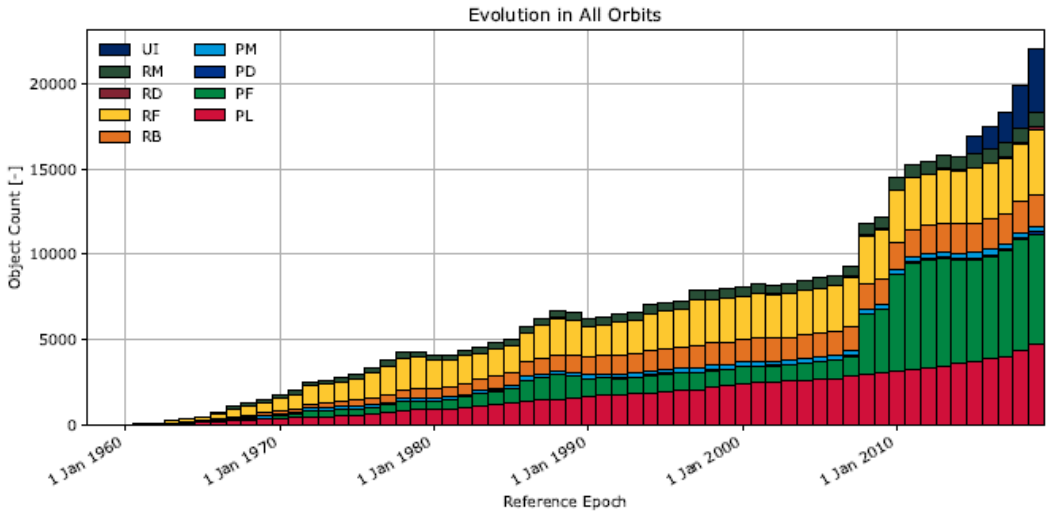

Figure 1.1: Evolution of objects in space in all orbits [1], (PL: Payload, PF: Payload Fragmentation Debris, PD: Payload Debris, PM: Payload Mission Related Object, RB: Rocket Body, RF: Rocket Fragmentation Debris, RD: Rocket Debris, RM: Rocket Mission Related Object, UI: Unidentified)

tourism is a growing interest, and the satellite technology is steering towards smaller satellites in the form of Cubesats or even in larger amounts together forming large constellations [6]. Hand-in-hand with the fourth industrial revolution 'Industry 4.0', the manufacturing, technology and utilization of the space sector is being optimized to accommodate for information transparency and decentralized systems. All these technological advances together are causing the space environment to see an exponential growth in accessibility to space for emerging start-ups as well as established companies.

An older idea with a newfound implementation of Cubesats is also evolving, where large (or even mega-) constellations are designed and put into orbit. The most well-known companies at the moment focused on setting up these mega constellations are SpaceX, Amazon, Telesat and OneWeb, who combined plan on putting thousands of satellites in orbit to accommodate for global communication. These constellations will allow for continuous coverage with low latency, being a large technical advantage, but will also bring challenges regarding design and collision hazards to other satellites and even other constellations. Again, as concluded above, a need for management in these space systems is needed to guide these launches and deployments of mega constellations.

Now that the biggest players in launching and putting spacecraft into orbit and the growing number of objects in space has been discussed, it is important to have a look at what is coming down. Figure 1.2 shows the amount of objects that has re-entered over the past decades. Comparing this figure to Figure 1.1, it can be easily concluded that more spacecraft (and therefore objects) are going to space than the amount of objects that is coming down.

To this end, space debris mitigation guidelines were set up in order to decrease the risk and damage to space systems, as well as objects and people on Earth. These guidelines were focused on the mission safety and the ecological cleanliness of the space environment for the three phases of functioning: launch, mission and disposal[7]. Multiple debris mitigation handbooks have been set up over the years, the fundamental three principles are similar:

1. Prevention of on-orbit break-ups
2. Removing spacecraft and rocket stages that reached the end of operations
3. Limiting the release of objects during nominal operations

Although the mitigation guidelines will help in reducing the collision risk and control the number of objects in space, it will not act as a managing force for space traffic.

The coming years may drastically change the space environment. As mentioned before, an increase in launches of hundreds of small satellites is observed. Next to this, a trend is seen in the launch and development of suborbital launch vehicles as well as that of large and mega constellations. If all these developed constellations would be deployed effectively, the amount of space objects in orbit will grow with one order

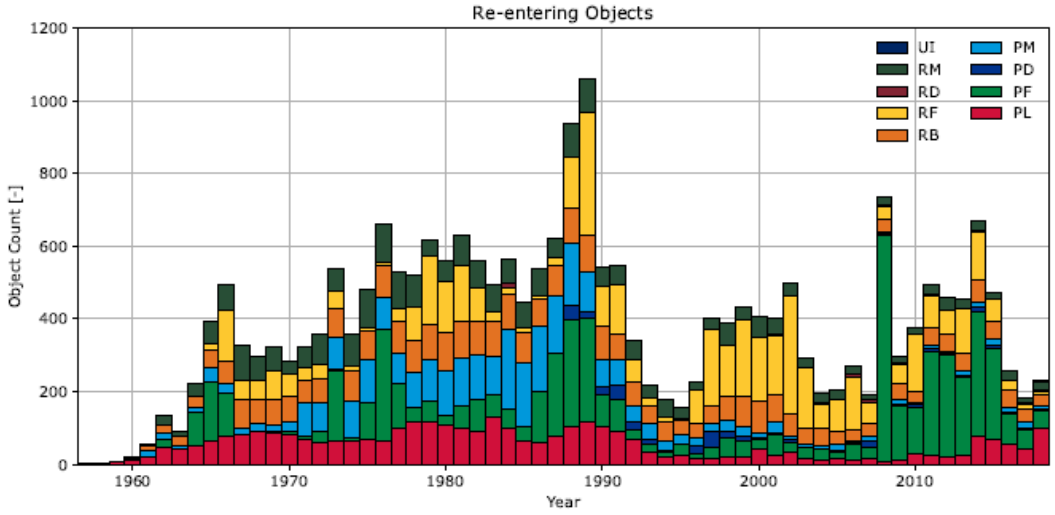

Figure 1.2: Evolution of objects re-entering the atmosphere [1], (PL: Payload, PF: Payload Fragmentation Debris, PD: Payload Debris, PM: Payload Mission Related Object, RB: Rocket Body, RF: Rocket Fragmentation Debris, RD: Rocket Debris, RM: Rocket Mission Related Object, UI: Unidentified)

of magnitude[3] and the amount of traffic passing airspace will need more attention in terms of safety and regulations. Given this growth in number of objects in space, multiple instances are also starting to realize the need for a more managed space environment.

As the future market is difficult to predict, the current trends can be seen moving towards smaller satellites (Smallsats) and constellations of small satellites. Together with the number of objects that already reside in space, the risk of collisions is increasing. This is also what follows from multiple research papers and simulations. Not only this, the collisions that are expected to be most dominant regarding the creation of new space debris are catastrophic intact-intact spacecraft. This means that collision avoidance manoeuvring will become more and more important in the near future where these intact satellites are able to manoeuvre (hereafter indicated with active satellites). Adding to this, the current way of working with collision warnings shows that the satellite operators need to be proactive and do much of the analyzing themselves before being able to say with certainty that the collision avoidance manoeuvre will be performed. Following this train of thought, combining this with the massive growth of constellation traffic, the research topic will be on the collision avoidance manoeuvres of two satellites from different constellation operators, where the constellation performance is taken into account as well. The relation of this research to Space Traffic Management will then be to provide an impartial technical view on the possibilities of collision avoidance manoeuvres.

Appendix A gives a more in-depth overview of the different aspects of Space Traffic Management as well as the developments that have been observed over the last few years. Next to the technical developments it will also give some insights in what efforts have been done to implement regulations. Last but not least some studies are discussed, in which future simulations have been done on the effect of constellation traffic on the space environment and what the relation of this is with respect to collision probabilities and collision counts.

1.1. Problem Summary

From a short introduction to the current evolution in the space market and space environment it can readily be seen that a steep growth in the space sector is taking place. This growth might cause a drastic change in the coming years, where the change can be seen on ground and in space. Hundreds of small satellites are being launched and deployed for single satellite missions as well as large constellations, where the launch infrastructure is also changing in the sense that the launch options are becoming more available and technologically advanced. This advancement of the space sector will result in a large growth, which can also be seen in the number of objects in space. The increasing number of objects in space and expansion of ground infrastructure means that there might come a point where regulations need to step in, in search of a system or management to set up guidelines. From this it can be concluded that the setup of a Space Traffic Management not only covers technical topics, but also requires a regulatory input on national and international

levels.

As was mentioned, Space Traffic Management consists of several sub branches, of which the two main branches are the orbital and the suborbital regime. The suborbital branch is expanding rapidly, where sub-orbital space travel as well as space tourism can be seen. Even though the suborbital regime is becoming more and more interesting regarding new technologies and the challenges in terms of integration of space traffic in air and maritime traffic, the focus of the further literature review was orientated towards the orbital regime, which is given the current pace of developments in a higher need of a Space Traffic Management than the suborbital regime. The orbital branch will cover three main subjects, being Space Situational Awareness (SSA), space debris mitigation and slot allocation.

With the clear evidence that the number of objects in space is growing, the three aspects of orbital space flight mentioned above become more and more important. Because of the relatively high speeds of the objects with respect to each other and the difficulty in precise orbit determination as well as precise tracking of the debris, the challenges are not that easy to overcome. Space Situational Awareness (SSA) on the other hand, being the largest branch of the three, is also gaining more interest. Research groups and consortia are formed to study the use and implementation of SSA. Simultaneously, a decline in deorbiting objects is observed. Additionally, there are still challenges in keeping track of all space objects of different sizes, especially those that are smaller than 10cm (which can still be lethal to spacecraft). From these aspects it could follow that an orbital congestion might happen, as more and more satellites are launched without some of those previously launched satellites coming down, where the largest growth is seen in constellations. With the technological advancements, the deployment of constellations is becoming an interesting playing field for commercial companies that want to partake in space activity.

Based on the fact that the number of objects in space is growing, especially between the 700km and 900km altitude bands, it became of importance to get a better understanding of these objects and how these are related to the market growth and mitigation guidelines. Results from multiple studies found that the growth of Smallsat traffic, in particular constellations, might cause risks for the future space environment. This risk is not only caused by an increased number of objects in space, but also resulting from a lack of compliance to the post mission disposal guidelines [8].

Next to the increasing amount of constellation launches, the higher expectancy rate of collisions was also dived into, where it appeared that the intact-intact collisions will be the most impacting type of collisions on the future space environment. Following a number of collisions in the past, it was seen that the debris cloud that is formed as a result of a collision poses a threat to other space traffic that is passing these orbital altitudes and inclinations. This means that the importance of being able to deorbit satellites that are no longer functioning, as well as being able to manoeuvre satellites that are still active will become a key part of avoiding catastrophic collisions. If this is not aimed for, the so called cascading effect could happen, where a shell of debris around the Earth will be the result. In terms of Space Traffic Management, this means that more regulations and guidelines need to be set up to accommodate for structuring of this future space environment, where 30% of the catastrophic intact-intact collisions can be prevented by collision avoidance manoeuvring [9]. In terms of the focus on constellations, the option to perform collision avoidance manoeuvres therefore also becomes more and more important in order to prevent future catastrophic events. Not only would this be beneficial for general space operations, this would also prevent the constellation from having catastrophic collisions with itself.

Adding to the need for collision avoidance between active and intact satellites to prevent catastrophic events from happening that could result in large debris clouds, a short review of the current process was done regarding collision detection. As was mentioned before, the ability to track objects in space is not as accurate as is desired, where propagation of the objects over a timeline of 7 days results in conjunction event alerts if passing a certain collision probability threshold. Depending on the probability and more precise orbit prediction and determination of the objects, a collision warning will be given to the operators. Depending on the willingness of the operators to act on these collision warnings, more propagations and assessments are done to determine the risk and cost of moving against the actual risk of collision. From this it can readily be seen that the decision to act lies completely in the hands of the operators and their willingness to perform a manoeuvre [10], [11].

Following the collision prediction, the collision avoidance phase is started. Depending on the probability of the collision, action needs to be taken to decide on a fitting manoeuvre to either lower the probability or to increase the miss distance. Given the way a collision avoidance manoeuvring problem needs to be solved, it is best solved with an optimization if the manoeuvre needs to be efficient and of low impact for the structure of the constellation.

Following all the steps summarized above, the proposed research means to investigate collision avoidance between constellations of different operators, with an eye on the ability to support Space Traffic Management.

1.2. Research Objective

As Space Traffic Management covers many aspects of spaceflight and with that covers all challenges mentioned above, this thesis will focus on the field of collision avoidance. With the growing number of objects in space there is a need for a more regulated space environment, where catastrophic events need to be prevented in order to allow for future access to space. Combining this aspect with the knowledge of the growing number of constellations and with that constellation satellites, this thesis aims to research the options of collision avoidance in combination with constellation satellites, as well as how this would fit into a Space Traffic Management. With that, the research objective can be formulated as follows:

> *Provide impartial collision avoidance manoeuvre advice for two satellites of different Low Earth Orbit constellations in support of the development of a space traffic management, by presenting multiple manoeuvre options as a result of an optimized parameter cost function that takes into account constellation performance.*

Following this research objective, the main research question can be formulated with the subquestions. This will be discussed more extensively in the next chapter.

1.3. Setup of report

After setting the background of the problem as described above as well as the research objective, the next chapter will describe the research questions and subquestions. It will then also be explained what aspects of the research each question covers and how this together will lead to the answer of the main research question. Following this, it will be explained what the approach is that was used and what methods and software are needed for this. The last section of this chapter will then explain how Conjunction Data Messages (CDM) work and how these are used throughout this research.

After the research has been defined, the research parameters will be set up and defined in Chapter 3. These parameters will be used and evaluated throughout the whole research.

Chapter 4 will make a selection of the parameters involved. This selection is needed for the way in which the collision avoidance manoeuvre problem will be solved.

This is followed by the setup of the cost function in Chapter 4 and what blocks of code are needed for this in Chapter 5. All input and output will be discussed, as well as how the blocks process the input and output and how they are connected. This chapter will also discuss the optimization method.

The next step is to verify and validate the blocks of code. This is done in Chapter 6, where the formulas and pieces of code will be checked against the CDMs and the software that is used. Additionally, the optimization will be tested with known formulas that can be used to check the validity of optimizations.

Following the verification and validation, the sensitivity of some of the code and formulas can be assessed. Next to that, additional sensitivity is checked of some of the given data that is used for the simulation.

This leads to Chapter 8, where the results will be shown of the simulations that have been done. These results will help in answering the research questions as well as give a broader understanding of the solution space. After the results have been shown, these results will be discussed in Chapter 9, where a more extensive look will be taken at the results.

From the results and discussion the research can be answered in Chapter 10, which will give the conclusions. This will then be followed by the recommendations for further research.

2

Problem Definition

This chapter will discuss the research questions, which follow the research objective and introduction of the problem in the previous chapter. After the research questions have been discussed, the approach will be explained. This is followed by which software is used to work out the approach.

The last section of this chapter discusses how Conjunction Data Messages get to the operators and what information is provided in these messages. These CDMs will form the basis of setup of the simulations.

2.1. Research Questions

As an increased number of objects in space is threatening to future space activity, the collision that can be avoided should therefore be avoided. As no clear guidelines and procedures exist on which of the two satellites needs to move or how this should be approached, a first setup of a method to support the manoeuvring decision is tried to be achieved, which will be based on an optimization. This method can then in it its turn provide support for Space Traffic Management in general, as it is an impartial way of looking at the problem and optimizes the possible manoeuvre advice.

As the research is meant to provide a supporting method for the development of a Space Traffic Management, the idea is to keep it impartial (as described in the research objective in Section 1.2. As was found before, operators are now informed on conjunction events through messaging services, where it is their own decision if they want to act on those messages or not. Additionally, the trade-off to manoeuvre depends on both parties, which needs to be discussed at their own initiative. It is therefore that an optimized pre-calculated set of options on which party would use what amount of resources might give an overall unbiased understanding of the situation. This means that the decision on who should move in order to prevent a catastrophic event is observed from a fully technical point of view and therefore disregards underlying non-technical motives.

Following the research objective, the main research question can be formulated as follows:

> *How could the result of an optimization based advice on collision avoidance manoeuvres for two satellites of different constellations in Low Earth Orbit be used to support the development of a Space Traffic Management?*

The main research question can be split in two research questions, from which sub question can be derived to structure the solution path of the main question. These two questions and sub questions are given below:

1. How does a collision avoidance manoeuvre optimization influence a predicted conjunction event between two satellites of different constellations?
   (a) What are the input and output parameters of a constellation focused collision avoidance manoeuvre optimization?
   (b) What requirements for the collision avoidance manoeuvre optimization would be needed from a constellation operator perspective?
   (c) What is the influence of the constellation satellites on an optimized collision avoidance manoeuvre?
   (d) What is the impact of an optimized collision avoidance manoeuvre on the constellation satellites?

2. How would the optimization of the collision avoidance manoeuvre between two satellites of different constellations support the development of a Space Traffic Management system?
    (a) How does the optimization of the collision avoidance manoeuvre impact the use of resources?
    (b) How do the results of the optimization compare to traditional collision avoidance manoeuvres?
    (c) How would the advised collision avoidance manoeuvres from the optimization and the operators of the constellations interact?

The first of the two questions target the more technical part of the research, where the interaction between the constellation and the cost function is tried to be determined, as well as the interaction between the cost function and the resulting collision avoidance manoeuvre. It needs to be noted here that question (a) and (b) are linked to each other, meaning that the required input and output parameters also depend on the influence of constellation parameters on the manoeuvre and vice versa. The results of question (c) will then provide the feedback loop for further improvements in case the impact of the manoeuvre is unacceptable. This means that indirectly this will also influence the boundary conditions and constraints of the collision avoidance manoeuvre optimization.

The second question will target the part where it relates to the development of a Space Traffic Management and where the interaction between the input/output and the eventual operator is investigated. This second question builds on the technical part in the first question, where the simulations and optimizations are performed and iterated. Question (a) refers to the use of resources, which can be taken as a broad description of material resources, but also costs or operation process time. As collision avoidance manoeuvres have been part of space activities for some time now, question (b) is aimed at comparing the results from the collision avoidance manoeuvre optimization with other collision avoidance manoeuvres that have been done in the past. Finalizing the second sub question is done by answering question (c), which looks into the communicative as well as the actionable aspects of the process and results. In the end, the goal is to support the development of a Space Traffic Management, which means that the results need to be communicated while at the same time being actionable for the operators.

The aim of the research is to get an extensive understanding of the answers to these sub questions, in order to be able to answer the main research question. As an STM is not yet in place, positive results of the research would help in preventing the formation of collision fragments in an impartial way. Given that current collision avoidance manoeuvres depend on actions of the operators themselves, the manoeuvre will be biased by the preferences of each operator, which could lead to the unneeded expense of resources. Even though the formation of collision fragments is a small part of the overall STM that is needed, a first step to limit the formation of debris will prevent the orbital environment from cascading into a shell of debris and making it difficult to access space. As the largest part of the satellites that will be launched are constellation satellites, the use of the research results is market oriented and therefore of interest for the future space operations.

2.2. Approach

The approach to answering the research question is made up of a combination of literature research and programming. Where the initial step is to focus on the literature to get an understanding of the fundamental setup of the formulas and to narrow down the research scope, the step that follows is the complete setup of the simulations which is a more practical approach. As a literature study has already been done before the start of this thesis, literature will not be discussed extensively in this report (see appendices for additional information from the literature study). Conclusions from this literature research will however be used throughout this report, such as the parameter space as well as which optimization will be used.

Five main steps can be defined when looking at the approach that is taken:

1. With the research questions defined above, it is important to understand what parameters are involved and which of those parameters are needed to find the answer to the research questions. Knowing that an optimization will be done in which the minimum is searched for, a cost function needs to be set up. This cost function is made up of different parameters. This is then also the first step in the approach, where a parameter overview is made from which the needed parameters will be chosen. The determination of parameters in this research is based on theory and research as well as getting an understanding of the process through stakeholder talks.
2. After the parameters have been chosen, the parameters can be combined into a cost function. As this cost function will be evaluated in the optimization through iterations, it is important to define if some parameters are more important than other parameters. Whilst setting up the cost function, it is there-

fore also important to have a look at penalty values that are needed or if other means of weighting are required. This is an analytical approach.

3. Following the determination of the cost function the code can be set up. With the determination of the parameters, the formulas are also known as well as how to solve these formulas. In order to set up the complete code, it is therefore needed to combine these separate formulas and pieces of code. From this step it will also become clear which input and output will be generated (based on the parameters that were defined) and how these blocks of code are linked together. With the setup of the code, the pieces of code that will be used are verified and validated before combining into the complete code. This is done using CDMs and Satellite Tool Kit (STK) (which will be described in the next sections).
   In order to do some simplifications, analytical methods will be used and set up to be run before the simulations can be started. Following these simplifications the optimization can be started. The optimization that is used is called Differential Evolution (DE), which is a form of a genetic algorithm and was decided on following the literature that was done. This setup of this optimization as well as all input and output will be further discussed in Chapter 5.
   As the simplification is done to limit the propagations that need to be done, the code is based on analytical methods only.
4. Following the analytical pieces of code and the setup of the code, the verification and validation is needed of the pieces of code that were written. All transformation methods and simplifications as well as the optimization are verified. Following the verifications the sensitivity of some of the pieces of code need to be checked. It needs to be noted here though that with the validation and verification as well as the result generation the sensitivity is checked. This will be indicated in the designated chapters and sections.
5. Using the completed code, results can then be generated. As the aim is to answer the research question, multiple scenarios will be simulated using the code, from which a broader sense of understanding of the problem and solution space. The results then need to be analyzed, which is done in the discussion, where a more extensive look will be taken at why the results are as they are and what can be said about those results.

The first step of this list reiterates the literature review that has been done, where from step two onwards the preparation for the results is done. After these five steps have been taken, a conclusion can be drawn and the research questions can be answered. Last but not least some recommendations will be made, based on the research simplifications and results, where more research might be needed.

2.3. Software

Two types of software will be used, which are only used for the simulations. The first one Satellite Tool Kit (STK), which is used to do the propagations of the satellites. As a large number of clicks would be needed in an iterative scheme, it was decided to use the MATLAB integration of STK. The second software that will be used is then MATLAB (R2020a), in which all the code is written that calls the STK commands. Also the collision probability code will be written in MATLAB, next to determining the resulting cost from the cost function. Additionally, all the different optimization code as well as some simplifications that are needed, run faster in MATLAB (Chapter 5 will describe the different simplifications and pieces of code).

MATLAB is therefore the main software, which calls commands and functionalities from STK to do the propagation. Both softwares are used from step two of the approach onwards, until the results are analyzed and discussed.

2.4. Conjunction Data Messages and Notification Process

Before the parameters important to the research problem can be discussed in the next chapter, first the background of Conjunction Data Messages needs to be explained. This will be done below, where the pieces of information will be shown that will be used throughout this thesis.

The United States (U.S.) government entity that is responsible for SSA is the United States Space Command (USSPACECOM). This entity is committed to promoting a safe, sustainable, stable and secure space environment by sharing SSA information. The party that is made responsible for the interface between the U.S. Department of Defense and satellite operators is the 18th Space Control Squadron (18SPCS). Previously this role was performed by the Joint Space Operations Center (JSpOC), which became the Combined Space Operations Center (CSpOC) in July 2018. SSA information is shared with the global space community through

```
CCSDS_CDM_VERS                  =1.0
COMMENT                         =CDM_ID:43057886
CREATION_DATE                   =2020-06-20T02:48:35
ORIGINATOR                      =JSPOC
MESSAGE_FOR                     =
MESSAGE_ID                      =000032789_conj_000044725_2020174050700_172035216866
TCA                             =2020-06-22T05:07:00.516
MISS_DISTANCE                   =459                    [m]
RELATIVE_SPEED                  =5748                   [m/s]
RELATIVE_POSITION_R             =96.4                   [m]
RELATIVE_POSITION_T             =415.4                  [m]
RELATIVE_POSITION_N             =170.7                  [m]
RELATIVE_VELOCITY_R             =4.2                    [m/s]
RELATIVE_VELOCITY_T             =-2175                  [m/s]
RELATIVE_VELOCITY_N             =5321.2                 [m/s]
COLLISION_PROBABILITY           =0.000001769128
COLLISION_PROBABILITY_METHOD    =FOSTER-1992
```

Figure 2.1: Conjunction Data Message Example 1

`www.space-track.org`, which is the primary method of sharing SSA information [12].

The conjunction assessment process from 18SPCS identifies and catalogues close approaches between all resident space objects. Initial tracking starts with observations from the U.S. Space Surveillance Network, which is done through sensors among other methods. These observations are then used as input in the mission system, which implements the 'Special Perturbations' propagation theory. Multiple times per day orbit determination is performed, where the updated states are also constantly updated in the High Accuracy Catalog.

Following this tracking, a Concern List is generated for follow up screenings. This list includes close approaches with a collision probability of $1 \cdot 10^{-7}$ and higher. These close approaches are reevaluated by the conjunction assessment team to make sure that all observations are included in the orbit determination. A refinement screening is then done to update the conjunction estimates that were identified in the initial screening.

If this close approach still falls within the criteria with which a close approach is identified and involves active satellites, 18SPCS will notify the operators of these satellites through email notifications. These email notifications are generated and transmitted through the Space-Track website as mentioned above. Based on the information received and from other data sources, the operator can decide to perform a collision avoidance manoeuvre or not. If the decision is to manoeuvre, the operator may send the predicted ephemeris data to 18SPCS to perform additional screenings. If it is decided not to manoeuvre, 18SPCS will continue to monitor the close approach and provide updates. Additionally, 18SPCS does not provide recommendations for the manoeuvre [12].

Figure 2.1 shows the first few lines of the a CDM. Here the message creation date is seen as well as to which operator it should be sent. It also shows the Time of Closest Approach (TCA), in this case about two days after the creation date. After the TCA a few other important parameters are shown, being the miss distance (the range between the two satellites) and the relative positions and velocities. It needs to be noted here that these relative distances and velocities are given in the Radial, In-track and Cross-track frame (RIC), which is indicated here with RTN (Radial, Normal and Tangential).

After the relative positions and velocities are given, the collision probability can be found for this conjunction. In this case, the collision probability is $1.769 \cdot 10^{-6}$. Below this it also shows the method with which it is calculated, being Foster-1992.

Looking a little bit further in the message, the information as in Figure 2.2 can be found. Starting from the first few lines in this figure it can be seen that it is indicated if the satellite is manoeuvrable and in what frame the parameters are given, in this case non-manoeuvrable and International Terrestrial Reference Frame (ITRF) respectively.

Below this the models are given with which the propagations are done upon creating the CDM. Important for the calculations that will be described in Section 3.2.2, the exclusion volume radius is needed.

What is further needed to set up the simulations, are the location of TCA and the corresponding covariance matrix values. This can also be found in Figure 2.2, where the position of TCA is indicated in X, Y, Z, X_DOT, Y_DOT and Z_DOT. This is then also in the ITRF frame. A little below that, the covariance matrix elements can be found. The values that are most important to the calculations are the position covariance values, which are the first six entries as seen here (CR_R, CT_R, CT_T, CN_R, CN_T and CN_N). Only six elements are given here, as the matrix is symmetric, meaning that the upper right side elements are the same as the lower left side elements in a 3x3 matrix.

The entries named above are used for the setup of the scenario, which will be described in Chapter 5.

```
MANEUVERABLE                    =N/A
REF_FRAME                       =ITRF
GRAVITY_MODEL                   =EGM-96: 36D 36O
ATMOSPHERIC_MODEL               =JBH09
N_BODY_PERTURBATIONS            =MOON,SUN
SOLAR_RAD_PRESSURE              =YES
EARTH_TIDES                     =YES
INTRACK_THRUST                  =NO
COMMENT Covariance Scale Factor = 1.000000
COMMENT Exclusion Volume Radius = 5.000000 [m]
TIME_LASTOB_START               =2020-06-19T02:48:35
TIME_LASTOB_END                 =2020-06-20T02:48:35
RECOMMENDED_OD_SPAN             =7.37                    [d]
ACTUAL_OD_SPAN                  =7.37                    [d]
OBS_AVAILABLE                   =188
OBS_USED                        =188
RESIDUALS_ACCEPTED              =99.7                    [%]
WEIGHTED_RMS                    =1.563
COMMENT Apogee Altitude = 559   [km]
COMMENT Perigee Altitude = 556   [km]
COMMENT Inclination = 97.4  [deg]
AREA_PC                         =0.12                    [m**2]
CD_AREA_OVER_MASS               =0.082356881561          [m**2/kg]
CR_AREA_OVER_MASS               =0.024826498465          [m**2/kg]
THRUST_ACCELERATION             =0                       [m/s**2]
SEDR                            =0.000261673             [W/kg]
X                               =4560.16072              [km]
Y                               =5192.240197             [km]
Z                               =-501.709793             [km]
X_DOT                           =0.756933827             [km/s]
Y_DOT                           =-1.388219496            [km/s]
Z_DOT                           =-7.500758917            [km/s]
COMMENT DCP Density Forecast Uncertainty = 1.947118720000000E-01
COMMENT DCP Sensitivity Vector RTN Pos = -1.373264236666561E+01 2.054306551858346E+03  4.700064382099635E-01  [m]
COMMENT DCP Sensitivity Vector RTN Vel = -2.254708140782168E+00 7.700670679789762E-03  1.457036028099783E-04  [m/sec]
CR_R                            =69.83596840885664       [m**2]
CT_R                            =-1291.603568317956      [m**2]
CT_T                            =175605.453084276        [m**2]
CN_R                            =-5.314552665639384      [m**2]
CN_T                            =8.585562252076247       [m**2]
CN_N                            =28.53619574456276       [m**2]
CRDOT_R                         =1.438284365848781       [m**2/s]
CRDOT_T                         =-192.8486793259243      [m**2/s]
CRDOT_N                         =-0.0202123720140508     [m**2/s]
CRDOT_RDOT                      =0.2118372201930982      [m**2/s**2]
CTDOT_R                         =-0.07231787914661612    [m**2/s]
CTDOT_T                         =0.8096049042760549      [m**2/s]
CTDOT_N                         =0.005715626901928783    [m**2/s]
CTDOT_RDOT                      =-0.000910902102000551   [m**2/s**2]
CTDOT_TDOT                      =0.000076760953674431 4  [m**2/s**2]
CNDOT_R                         =0.002130313721679392    [m**2/s]
CNDOT_T                         =0.04557681516348815     [m**2/s]
CNDOT_N                         =-0.01306723472367862    [m**2/s]
CNDOT_RDOT                      =-0.000031365631835035 57 [m**2/s**2]
CNDOT_TDOT                      =-0.000002364566332281778 [m**2/s**2]
CNDOT_NDOT                      =0.000034729752019840 09  [m**2/s**2]
```

Figure 2.2: Conjunction Data Message Example 2

3

Parameter Determination

Given the need of parameters on which the cost function will be based, this chapter will focus on the parameter options and the determination of the final parameters for the cost function. The parameters that will be looked at originate from different aspects of the problem, being station keeping, collision prediction and collision avoidance.

This chapter will also describe the analytical formulas that will be used to determine the parameters for the simulations.

One of the parameter groups that could also be included is that of constellation design. However, as it is assumed that the parameters that are involved in constellation design are set before the launch, the manoeuvre done by one of the satellites will not influence the design of the constellation. The constellation design parameters were part of the literature study and can be found in Appendix B.

3.1. Station Keeping

In order to keep the satellite in the place where it is supposed to be, station keeping is needed. This can be either relative to inertial space or relative to other satellites. In most constellations, the aim is to keep a relative position with respect to each other to reduce propellant utilization, as was already discussed in the literature study.

The decision of which type of station keeping will be done depends on multiple factors, of which the main one to save as much ΔV as possible. Another important factor that needs to be taken into account is if it is desired to maintain the system altitude or to let it decay slowly as a result of the drag. This directly influences the use of ΔV. Figure 3.1 shows the advantages and disadvantages of both relative and absolute station keeping.

From this it can be seen that the majority of the advantages are in favor of the absolute station keeping. This means that the satellite will be continuously pushed back, in order to restore the position that was taken out due to perturbations. The main advantage of the absolute station keeping is the minimization of the manoeuvre frequency. Another advantage, which is important for the scope of this thesis, is that the absolute position station keeping can be expressed in a control box. This will simplify planning and scheduling.

Absolute station keeping is therefore taken into account for further determination of the station keeping parameters, which means that the orbits will be controlled orbits. The position and attitude at a certain time and date will then be defined, which is done by using predefined mathematical algorithms as well as propagators. This also means that the elements of the orbit are kept the same, making it easier to predict the future position of the satellite.

Within the parameter group of station keeping there is also the difference in in-track station keeping and cross-track station keeping. Both types of station keeping control different components of the orbit:

- In-track station keeping: controlling the true anomaly or orbit phase. The main component of in-track station keeping is to maintain the altitude and therefore try to put back the ΔV that was taken out due to drag. This can be compared to a Ping-Pong ball that is bouncing on a paddle [13]. For the case of the satellite, the drag takes it down, where after it is using its thrusters to get back in position again. The station keeping box comes in play here, where the drag will make the satellite drift to the side of

Method	Additional Propellant Cost	Advantages	Disadvantages
Relative Stationkeeping	May be some added propellant cost depending on implementation	• Minimizes maneuver frequency	• Stationkeeping depends on interrelationship between all satellites in the system • Complex commanding may lead to command errors and greater risk • High operations cost • Different logic for system build-up than operations
Absolute Stationkeeping	None, assuming drag makeup is the only in-plane stationkeeping	• Simple commanding • Each satellite maintains itself in the pattern • Position of all other satellites are known without sending data around continuously • Can be fully autonomous • Same logic for build-up as for normal operations • Easily monitored from ground • Stationkeeping will not interfere with normal system operations	• More frequent stationkeeping (may be an advantage since burns will be smaller and more easily controlled).

Table 3.1: Relative and absolute station keeping advantages and disadvantages [13]

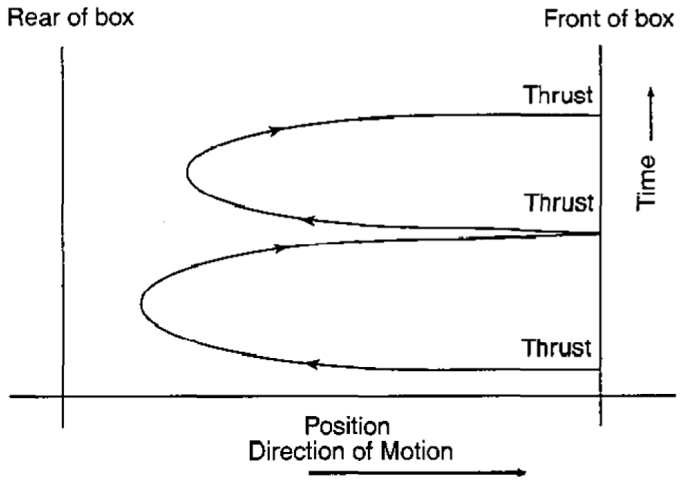

Figure 3.1: Satellite movement in station keeping box [13]

the box and the thrust is bouncing it back to the center of the box. Figure3.1 shows this station keeping process. This also means that the amount of ΔV that is used is not related to the number of times a station keeping manoeuvre is performed and that it is a function of the atmospheric drag. The way a station keeping box is set up is shown in Figure 3.2.
Radial station keeping also falls under in-track station keeping, as the altitude and therefore the semi-major axis directly determines the orbital period.

- Cross-track station keeping: controlling the inclination and the node, being the components that are perpendicular to the orbital plane. These two parameters are coupled because of the oblateness of the Earth and thus the J_2 effect (discussed in Appendix B). Because of this coupling, small differences in the inclination also cause a drift of the nodes, from which it can be implied that the inclination needs to be maintained to control the node rate. If the inclination is set to a sufficient accurate value, manoeuvres to adjust the inclination will take small amounts of propellant. It is however needed from time to time to perform burns in the cross-track direction, which is why thrusters are needed in this direction or a mechanism to use the in-track thrusters in this direction.

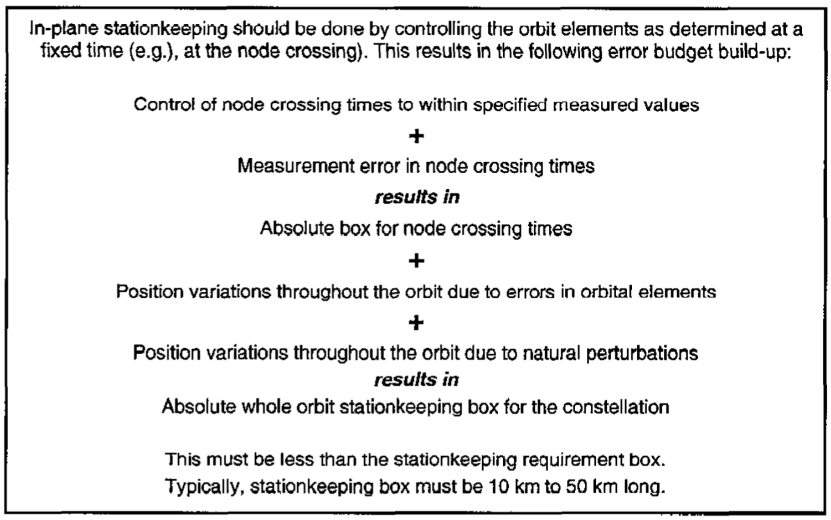

Figure 3.2: In-track station keeping box setup [13]

3.2. Collision Prediction

The accuracy of the spacecraft is tracked in multiple ways, of which one is by observation in the catalog and the other is by orbit determination from the operator. Given the current observation capabilities, the accuracy of the precise orbit determination is two orders of magnitude higher than that of the observed data that is tracked in the catalog. It is therefore better to work with precise orbit data than Two Line Elements (TLE). TLEs can be read through the Simplified General Perturbations 4 (SGP4) model and can be used as a good estimation of the position of the spacecraft, but are not meant to be used for precise orbit determinations.

However, as the precise orbit data is not always available (operator knows precise data of own satellite, but not of the other operators if not shared), the collision prediction most of the times comes to the data that is available through TLEs and the conjunction messages. With TLEs being an average estimated value of the orbit and the CDMs resulting from high precision propagations from the same provider as the TLEs (JSpOC), this research will base the collision prediction on the data that is available through the CDMs.

The parameters needed to assess the collision probability will be discussed in the sections below. One of these parameters is the covariance matrix of the residuals of the orbit prediction. As this covariance matrix largely depends on the accuracy of the orbit prediction model, there is an inaccuracy of the covariance matrix. Given that there is no precise orbit data used for this thesis and only the CDMs are available (and TLEs), with the same decision steps as done above, the covariance data will not be improved for the code. This will be discussed further in Chapter 7.2.

3.2.1. Error Covariance Matrix

Finding the covariance matrix is an important part of collision prediction as well as avoidance. As the covariance matrix is also used in precise orbit determination, the method is comparable. The steps below described how the covariance matrix can be found. This will, as stated above, not be done for this thesis. However, to get an understanding of how this parameter is build up a short description will be given on the steps to get a covariance matrix.

The error covariance matrix C_0 is found by performing a batch least-squares calculation of the Jacobian of the modeled observations H and the weighing matrix W:

$$C_0 = \left(H^T W H\right)^{-1} \tag{3.1}$$

where

$$H = \frac{\partial \overline{h}(\overline{x}_0)}{\partial \overline{x}_0}\Big|_{\overline{x}_0=\hat{\overline{x}}_0} \tag{3.2}$$

$$W = \text{diag}(\sigma_1^{-2}, \ldots, \sigma_n^{-2}, \ldots, \sigma_N^{-2}) \tag{3.3}$$

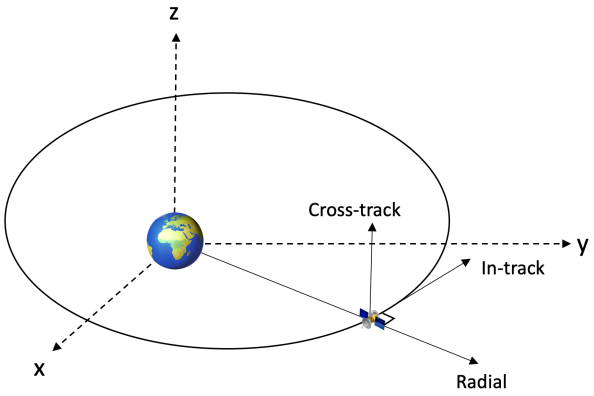

Figure 3.3: Radial, in-track and cross-track reference frame with respect to the x, y, z frame

$\overline{h}(\overline{x}_0)$ in Equation 3.2 is the vector containing the model observations and $\overline{x}_0$ is the vector $(\overline{r}_0, \overline{v}_0)$ at the starting epoch t_0. $\hat{\overline{x}}_0$ is then the initial state estimate. In Equation 3.3 the standard deviations of the uncorrelated measurement errors are found on the diagonal as σ_n.

Substituting both Equation 3.2 and 3.3 in Equation 3.1 for the initial state at the starting epoch will then give the inverse of the normal matrix $H^T W H$ and can be substituted in the following equation to map the covariance for the different epochs t_n:

$$C(t) = \Phi(t_0, t) C_0(t_0) \Phi^T(t_0, t) \tag{3.4}$$

where $\Phi(t_0, t)$ is the state transition matrix. It is described as the sensitivity of the response of the predicted state $\overline{x}(t)$ to the variation of the initial state $\overline{x}_0(t_0)$. To put this in mathematical notation:

$$\Phi(t_0, t) = \frac{\partial \overline{x}(t)}{\overline{x}_0(t_0)} \tag{3.5}$$

The equations that result of the right hand side of Equation 3.5 are also called vibrational equations, which can be expressed analytically.

The conjunction event will be described in a local coordinate frame, indicated with U, V and W (local coordinate frame expressed in radial (U), in-track (V) and cross-track (W) directions), where the orbit related coordinates are described in the X, Y and Z system. The orientation of the orbit is then described with the unit vectors $\overline{U}$, $\overline{V}$ and $\overline{W}$. This is seen in Figure 3.3.

These unit vectors can be found at a given orbital state $\overline{x} = (\overline{r}, \overline{v})$ at given time t with the following formulas:

$$\overline{U} = \frac{\overline{r}}{|\overline{r}|} \tag{3.6}$$

$$\overline{W} = \frac{\overline{r} \times \overline{v}}{|\overline{r} \times \overline{v}|} \tag{3.7}$$

$$\overline{V} = \overline{W} \times \overline{U} \tag{3.8}$$

These formulas can then be used to generate the transformation matrix $R_{U,V,W}$, which is needed to map the covariance matrix in the orbit related frame. Transformation matrix $R_{U,V,W}$ is found as follows using the previous equations:

$$R_{U,V,W} = \begin{pmatrix} U_X & U_Y & U_Z \\ V_X & V_Y & V_Z \\ W_X & W_Y & W_Z \end{pmatrix} \tag{3.9}$$

and can then be substituted in the following equation to map the covariance matrix $C_{X,Y,Z}$ in the $C_{U,V,W}$ plane:

$$C_{U,V,W} = R_{U,V,W} C_{X,Y,Z} R^T_{U,V,W} \tag{3.10}$$

where the elements on the diagonal of $C_{U,V,W}$ given the standard deviation 1σ of the position and velocity in the U, V and W frame.

3.2.2. Collision Risk Estimation

Before the collision risk can be calculated, the conjunction first needs to be detected. As this is not part of this research the parameters involved in this will not be described in this section. These parameters are however described in Appendix C. Conjunction Detection involves multiple steps in which sieving algorithms are used to find conjunction events.

The resulting conjunction events can be analyzed to assess the collision probability. This was already described in the literature study, but will be described again below for the assessment of the cost function parameters. It needs to be noted here again that not all steps below are done to find the conjunction events, as the CDMs will be the main source of data and already provide the relative state and corresponding parameters needed to compute the collision probability.

Looking at the conjunction geometry, the operational satellite is indicated as target (index 't'). The other object, the conjunction object, is then indicated as risk object (index 'r'). Another naming convention for these two satellites are primary and secondary satellite. A first order screening is done to assess close approaching satellites. Screening is done with three steps [14]. Now in order to be able to calculate the collision probability in the way it is done, four main simplifications were done [15]:

- The relative motion of the objects is assumed to be fast enough to be considered linear
- The positional errors are zero-mean, Gaussian and uncorrelated
- The covariance is assumed to be constant, because of the short encounter period
- The objects are modelled as spheres

Throughout this research, it is also assumed that the given covariance matrix values at TCA in the CDM do not change after the manoeuvre.

To find the collision probability the relative position $\Delta\overline{r}_{tca}$ and relative velocity $\Delta\overline{v}_{tca}$ are used at the time of closest approach t_{tca}. The relative risk object position can be found by substituting both in the following equation:

$$\Delta\overline{r}(t) = \Delta\overline{r}_{tca} + \Delta\overline{v}_{tca}(t - t_{tca}) \tag{3.11}$$

The propagated error covariance matrices of the target object state vector $\hat{\overline{x}}_{t,tca}$ and risk object state vectors $\hat{\overline{x}}_{r,tca}$ (6×6) can be found as in Equation 3.4 and gives the following matrices and state transition matrices as found in Equation 3.5:

$$\hat{C}_t(t_{tca}) = \Phi_t(t_0, t_{tca})\hat{C}_{t,0}(t_0)\Phi_t^T(t_0, t_{tca}) \tag{3.12}$$

$$\hat{C}_r(t_{tca}) = \Phi_r(t_0, t_{tca})\hat{C}_{r,0}(t_0)\Phi_r^T(t_0, t_{tca}) \tag{3.13}$$

As the errors of the state of both objects are expected to be uncorrelated, the separate covariance matrices of the target and risk object can be combined into one common covariance matrix:

$$\hat{C} = \hat{C}(t_{tca}) = \hat{C}_t(t_{tca}) + \hat{C}_r(t_{tca}) \tag{3.14}$$

where only the position error covariance will be taken into account in the next steps. This means that only the upper left (3×3) values are needed of the (6×6) full matrix, corresponding to the 1σ standard deviation error ellipsoid.

Assuming that the position error has a 3D normal distribution, the probability density function $p(\Delta\overline{r})$ at the point of closest approach can be found using the following equation (further discussed in Section 3.2.3):

$$p(\Delta\overline{r}) = \frac{1}{\sqrt{(2\pi)^3\det(C)}}\exp\left[-\frac{1}{2}\Delta\overline{r}^T C^{-1}\Delta\overline{r}\right] \tag{3.15}$$

Given the three-dimensional set-up of the closest approach as described above (the third order term in the denominator, further explained in Section 3.2.3), a similar way of defining the collision probability can be done resulting in a two-dimensional space and simplifies the calculations.

Both the target and risk object (primary and secondary object) will be enclosed with a sphere, having the radii R_t and R_r. When these two spheres intersect, a collision will occur. This can also be described with a collision sphere radius R_c, with volume V_c and cross-section A_c as in the equations below:

$$R_c = R_t + R_r \tag{3.16}$$

$$A_c = \pi R_c^2 \tag{3.17}$$

$$V_c = \frac{4}{3}\pi R_c^3 \tag{3.18}$$

The collision probability P_c can then be determined using the defined parameters above by determining the volume integral of the probability density function, which is three-dimensional. This integral needs to be evaluated over the sphere V_c with the center of the risk object as the point around which the integral will be evaluated. This leads to the following equation:

$$P_c = \frac{1}{\sqrt{(2\pi)^3 \det(C)}} \int_{(V_c)} \exp\left[-\frac{1}{2}\Delta\overline{r}^T C^{-1} \Delta\overline{r}\right] \mathrm{dV} \tag{3.19}$$

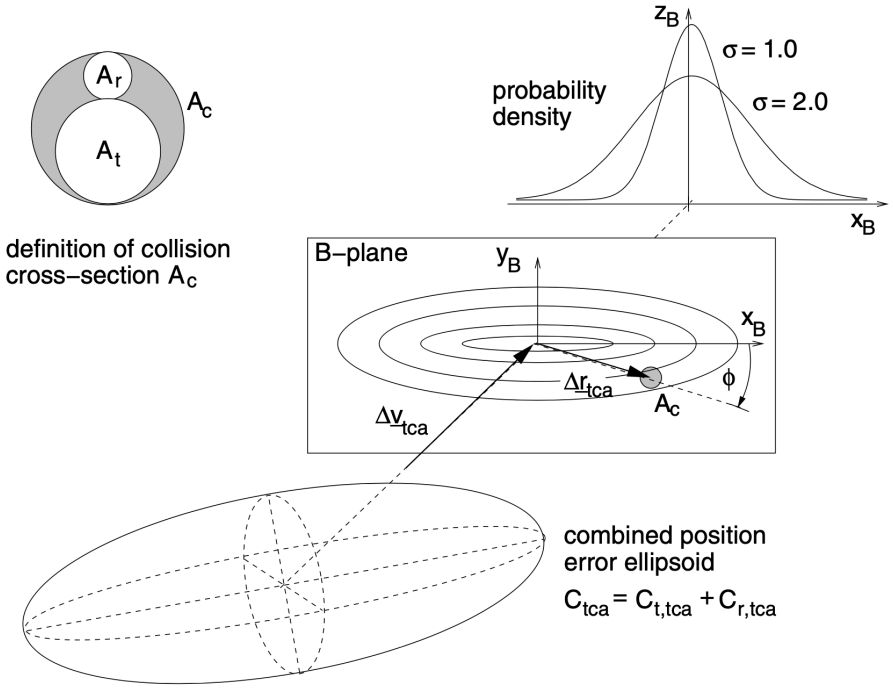

Figure 3.4: Definition of collision cross section and B-plane [14]

This volume integral can then be reduced to a surface integral. This is done by mapping the position error ellipsoid on a constant B-plane, which consist of elliptical contours with constant probability (see Figure 3.4). This B-plane is therefore perpendicular to the relative velocity vector at the time of closest approach $\Delta\overline{v}_{tca}$. The range vector at time of closest approach $\Delta\overline{r}_{tca}$ then lies within the B-plane, as can also be seen in Figure 3.4. The unit direction vectors can then be found using the following equations:

$$\overline{X}_B = \frac{\Delta r_{tca}}{|\Delta r_{tca}|} \tag{3.20}$$

$$\overline{Y}_B = \frac{(\Delta r_{tca}) \times (\Delta v_{tca})}{|(\Delta r_{tca}) \times (\Delta v_{tca})|} \tag{3.21}$$

$$\tag{3.22}$$

The transformation vector R_{X_B,Y_B} is used here again to create the covariance matrix C_B in the B-plane. This covariance matrix will be a 2D matrix, as only two unit vectors are taken into account, hence mapping the 3D covariance matrix $C = C_{X,Y,Z}$ onto the 2D plane:

$$R_{X_B,Y_B} = \begin{pmatrix} X_{B,X} & X_{B,Y} & X_{B,Z} \\ Y_{B,X} & Y_{B,Y} & Y_{B,Z} \end{pmatrix} \tag{3.23}$$

$$C_B = C_{X_B,Y_B} = R_{X_B,Y_B} C R^T_{X_B,Y_B} \tag{3.24}$$

The last step before continuing with the full collision probability formula is the determination of the orientation of the elliptic contour. This is determined with the eigenvalues and the eigenvectors of the covariance matrix in the B-plane. The semi-major axis of the ellipse is defined by the highest value of the two eigenvalues

and the semi-minor axis of the ellipse is defined by the lowest of the two values. Using this orientation, the eigenvectors can then be used to translate the conjunction position to coordinates in the B-plane.

The probability integral can then be reduced from a 3D integral to a 2D integral by integrating $\Delta\overline{r}_B$, which is the conjunction position in the B-plane:

$$P_c = \frac{1}{2\pi\sqrt{\det(C_B)}} \int_{-R_c}^{+R_c} \int_{-\sqrt{R_c^2-x_B^2}}^{+\sqrt{R_c^2-x_B^2}} \exp\left[-A_B\right] \mathrm{d}y_B \mathrm{d}x_B \tag{3.25}$$

where R_c is the circular collision cross-section radius, which is centered at the fly by location $\Delta\overline{r}_{tca}$. A_B is then defined as:

$$A_B = \frac{1}{2}\Delta\overline{r}_B^T C_B^{-1} \Delta\overline{r_B} \tag{3.26}$$

3.2.3. Simplification Collision Probability

Given the difficulty in solving the collision probability integral analytically, a different approach was used to define the collision probability, by making some simplifications and assumptions. Looking at the main setup of the collision probability function altogether, the idea is that a multivariate normal distribution is used to compute this probability in 3D space with the formula below:

$$\text{PDF} = (2\pi)^{-\frac{k}{2}} \det(\Sigma)^{-\frac{1}{2}} \exp^{-\frac{1}{2}(x-\mu)^T \Sigma^{-1}(x-\mu)} \tag{3.27}$$

which will be integrated for the area that the probability needs to be found for. For a 3D setup, k represents the amount of dimension and in this case should be 3. Filling in the parameters corresponding to a satellite collision event ($\Sigma = C$ and $x - \mu = \Delta\overline{r}$), a formula for the satellite collision probability can be formed. This was represented with the following formula [14] as was also shown above in Equation 3.19:

$$P_c = \frac{1}{\sqrt{(2\pi)^3 \det(C)}} \int_{(V_C)} \exp\left[-\frac{1}{2}\Delta\overline{r}^T C^{-1} \Delta\overline{r}\right] dV \tag{3.28}$$

Following some simplifications as were described above to find the form in a 2D plane, the formula was simplified to Equation 3.25. However, looking at this formula it is still made up of a double integral containing the exponential function, making it a difficult formula to solve analytically. Comparing this equation to the multivariate normal distribution in Equation 3.27, it can be seen that this represents the 2D equation ($k = 2$).

To simplify even more, it was assumed that instead of the collision area to be an elliptical form, the collision area could be a square form. This means that the collision probability does not have to be integrated over a sphere anymore, but instead can be done more straightforwardly by integrating over a rectangle. The last step that will be added is to rewrite the whole formula in error function terms. This simplifies the implementation in code, which can be seen later on. This simplification is also mentioned by 18SPCS, which provides the CDMs to operators [12].

The first step is to set up the problem in a different way. To simplify the double integral, instead of a circle, a rectangle is assumed to be the collision plane. This simplifies the problem by changing the integral limits. The limits as seen in Equation 3.25 are found when integrating over the limits for a circle: $x^2 + y^2 = R_C^2$. However, when assuming the collision plane to be a rectangle, the limits can be changed to $\pm R_C - y_B$ and $\pm R_C - x_B$.

The next step is to analyze the part in front of the double integrals in Equation 3.25, being the fraction containing the covariance matrix in the B-plane. Writing this as follows, a different form can be found:

$$C_B = \begin{bmatrix} \sigma_1^2 & 0 \\ 0 & \sigma_2^2 \end{bmatrix} \tag{3.29}$$

Taking the determinant of this matrix, followed by taking the root square of this results, the following is found:

$$\det(C_B) = \sigma_1^2 \times \sigma_2^2 - 0 \times 0 = \sigma_1^2 \sigma_2^2 \tag{3.30}$$

$$\sqrt{\det(C_B)} = \sqrt{\sigma_1^2 \sigma_2^2} = \sigma_1 \sigma_2 \tag{3.31}$$

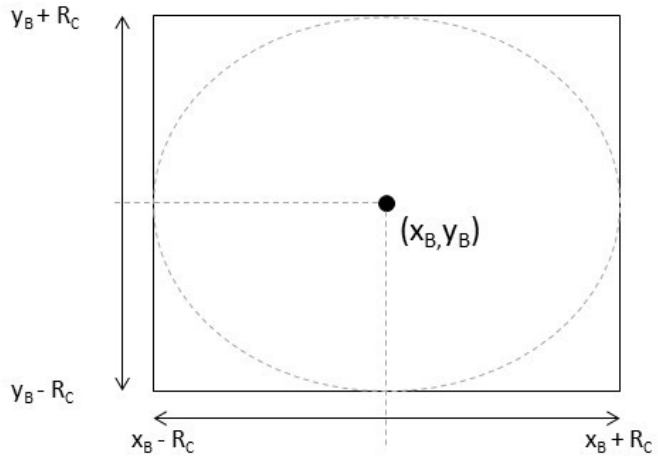

Figure 3.5: Simplification of collision area in the 2D plane

Filling this in for the complete fraction, it can be rewritten as seen below. With an eye on simplification in later steps, this can also be split in two terms:

$$\frac{1}{2\pi\sqrt{\det(C_B)}} = \frac{1}{2\pi\sigma_1\sigma_2} \tag{3.32}$$

$$= \frac{1}{\sigma_1\sqrt{2\pi}}\frac{1}{\sigma_2\sqrt{2\pi}} \tag{3.33}$$

Now looking at the part in between brackets of the exponent, A_B, it can also be simplified using Equation 3.34. Writing out $\Delta\overline{r}$, this leads to a vector containing the two coordinates of collision center, here indicated with s_1 and s_2. Fully written:

$$A_B = -\frac{1}{2}\begin{bmatrix} s_1 \\ s_2 \end{bmatrix}^T \begin{bmatrix} \sigma_1^2 & 0 \\ 0 & \sigma_2^2 \end{bmatrix}^{-1} \begin{bmatrix} s_1 \\ s_2 \end{bmatrix} \tag{3.34}$$

$$= -\frac{s_1^2}{2\sigma_1^2} - \frac{s_2^2}{2\sigma_2^2} \tag{3.35}$$

Combining all the simplifications above, the following formula is found:

$$P_c = \frac{1}{\sigma_1\sqrt{2\pi}}\frac{1}{\sigma_2\sqrt{2\pi}}\int_{x_B-R_C}^{x_B+R_C}\int_{y_B-R_C}^{y_B+R_C}\exp\left[-\frac{s_1^2}{2\sigma_1^2} - \frac{s_2^2}{2\sigma_2^2}\right] ds_1\, ds_2 \tag{3.36}$$

The formula above can then be split into two parts:

$$P_c = \left[\frac{1}{\sigma_1\sqrt{2\pi}}\int_{x_B-R_C}^{x_B+R_C}\exp\left[-\frac{s_1^2}{2\sigma_1^2}\right] ds_1\right]\left[\frac{1}{\sigma_2\sqrt{2\pi}}\int_{y_B-R_C}^{y_B+R_C}\exp\left[-\frac{s_2^2}{2\sigma_2^2}\right] ds_2\right] \tag{3.37}$$

Now looking at the error function, where the error lies between a and b, the following definition is found:

$$\left(\frac{c}{\pi}\right)^{\frac{1}{2}}\int_a^b e^{-cx^2}\, dx = \frac{1}{2}\left(\text{erf}(b\sqrt{c}) - \text{erf}(a\sqrt{c})\right) \tag{3.38}$$

where a and b are the limits as given in Equation 3.37. c can then be formulated in terms of the error function

as follows:

$$\left(\frac{c}{\pi}\right)^{\frac{1}{2}} = \left(\left(\frac{1}{\sigma_1\sqrt{2\pi}}\right)^2\right)^{\frac{1}{2}} \tag{3.39}$$

$$= \left(\frac{1}{\sigma_1^2 2\pi}\right)^{\frac{1}{2}} \tag{3.40}$$

$$c = \frac{1}{2\sigma_1^2} \tag{3.41}$$

Evaluating c for the position in the integral, this equation for c also holds. Rewriting Equation 3.37 as in the equation containing the error function, the following form is found:

$$P_C = \frac{1}{2}\left(\text{erf}\left((x_B + R_C)\sqrt{\frac{1}{2\sigma_1^2}}\right) - \text{erf}\left((x_B - R_C)\sqrt{\frac{1}{2\sigma_1^2}}\right)\right) \times \tag{3.42}$$

$$\frac{1}{2}\left(\text{erf}\left((y_B + R_C)\sqrt{\frac{1}{2\sigma_2^2}}\right) - \text{erf}\left(((y_B - R_C)\sqrt{\frac{1}{2\sigma_2^2}}\right)\right) \tag{3.43}$$

This is also the analytical expression that will be used in this thesis to compute the collision probability in the simplified 2D plane.

3.3. Collision Avoidance

As described earlier, the station keeping box is given in the RIC frame of the primary satellite. Together with the CDM information also given in this reference frame, it was therefore chosen to express the collision avoidance manoeuvre in this frame as well. As the state of the satellites are given in the Cartesian frame, using x, y and z coordinates, a transformation is needed to go from one to the other and the other way around. This conversion will be done through a transformation matrix, which can be multiplied with the position and velocity vector to get the RIC coordinates expressed in the frame of the primary satellite [16] (see Figure 3.3).

Using the position vector $\overline{x}$ and the velocity vector $\overline{v}$ (from the propagated states in STK) to get the unit vectors, the transformation matrix can be found:

$$u_R = \frac{\overline{x}}{|\overline{x}|} \tag{3.44}$$

$$u_C = \frac{\overline{x} \times \overline{v}}{|\overline{x} \times \overline{v}|} \tag{3.45}$$

$$u_I = u_C \times u_R \tag{3.46}$$

where u_R, u_I and u_C are the unit vectors of the radial, in-track and cross-track directions respectively. These vectors combined give the 3×3 transformation matrix (indicated with T and as seen in Equation 3.47), which multiplied with the position vector $\overline{x}$ gives the RIC position and multiplied with the velocity vector $\overline{v}$ gives the RIC velocity.

$$T = \begin{bmatrix} u_{R1} & u_{R2} & u_{R3} \\ u_{I1} & u_{I2} & u_{I3} \\ u_{C1} & u_{C2} & u_{C3} \end{bmatrix} \tag{3.47}$$

Now in order to find the relative positions and velocities as seen from the primary satellite, this transformation matrix needs to be based on the position and velocity of the primary satellite. The next step is to multiply this matrix with the difference in the positions and velocities as follows:

$$\begin{bmatrix} R \\ I \\ C \end{bmatrix}_{\text{relative}} = T_1 \cdot \begin{bmatrix} x_2 - x_1 \\ y_2 - y_1 \\ z_2 - z_1 \end{bmatrix} \tag{3.48}$$

$$\begin{bmatrix} \dot{R} \\ \dot{I} \\ \dot{C} \end{bmatrix}_{\text{relative}} = T_1 \cdot \begin{bmatrix} \dot{x}_2 - \dot{x}_1 \\ \dot{y}_2 - \dot{y}_1 \\ \dot{z}_2 - \dot{z}_1 \end{bmatrix} \tag{3.49}$$

$$\tag{3.50}$$

where T_1 is the transformation matrix (as in Equation 3.47) based on the primary satellite. The left side of the equal sign indicates the relative positions and velocities in RIC frame and on the right of matrix T_1 is the difference in position and velocity in Cartesian frame.

This way the collision avoidance manoeuvre ΔV can be expressed in the radial, in-track and cross-track direction, and will be taken into account in the setup of the simulations.

4

Cost Function

Following all the parameters that have been described which are important to station keeping and collision detection and avoidance, the most important parameters need to be included in a cost function that will be subject to the minimization algorithm. From this minimization of the cost function the most optimal collision avoidance option will result in terms of the boundary conditions and assumptions made for this research problem.

First a selection will be made from the parameters that were described in the previous chapter. This is then followed by how these parameters should be fitted into a cost function and if penalty functions need to be included for these parameters. Last but not least, the final form of the cost function will be described and how the different parameters in this cost function are computed.

4.1. Parameters

The previous chapter discussed the parameters from three different aspects, being station keeping, collision prediction and collision avoidance. For station keeping the parameters it could be concluded that the dimensions of the station keeping box are important parameters. Collision prediction included a multitude of different parameters, including the position and velocity standard deviation, error covariance matrix, time of closest approach, velocity and position at closest approach, collision probability, collision radius and collision volume. Adding to the collision prediction, there is the actual collision avoidance manoeuvre, which includes the changes in orbital parameters as a result of the ΔV impulse in a certain direction. This would then also result in the total ΔV that is needed for the manoeuvre. All the parameters can be seen in Table 4.1.

As not all these parameters can and need to be included in the cost function, it is important to determine the most important parameters to the problem. It needs to be kept in mind here that the importance of the parameters need to be assessed as a result of a position change from the manoeuvre. The distinction can

Table 4.1: Problem related parameters

Station Keeping	Collision Prediction	Collision Avoidance
- Box dimensions in radial direction	- Position standard deviation	- ΔV impulse in radial direction
- Box dimensions in in-track direction	- Velocity standard deviation	- ΔV impulse in in-track direction
- Box dimensions in cross-track direction	- Error covariance matrix	- ΔV impulse in cross-track direction
	- Time of closest approach	
	- Position at closest approach	
	- Velocity at closest approach	
	- Collision probability	
	- Collision radius	
	- Collision volume	

be made between two types of impact these parameters will have on the satellite, where one is the effect on the operations of the satellite and the other effect is on the operational lifetime of the satellite. Considering that the satellite is already in orbit and is operational, a reduction in lifetime is in this case assumed to have a bigger implication than the operational effect, as the lifetime that is saved by not performing a certain action takes away from overall operations (because of the collision risk) and the reduction of the operational period during a certain action is assumed to be for only a short period of time.

As was mentioned before, for constellation design some assumptions will be made here that will be used for the remainder of this research. As the constellations that are considered in this research have already been launched, it is assumed that the satellites are in position and do not have an orbit insert offset. Additionally, it is assumed that the constellation was designed to have the optimal node spacing and swath width for the purpose of the constellation, where the satellites will return to after the manoeuvre has been performed. The swath width and node spacing are assumed to be restored to their optimal state again. This will therefore not be taken into account in the distinction between the effect it has on operations or lifetime, as it has been predesigned. Even though it can be concluded that the swath width as well as the node spacing are influenced by the altitude and inclination, and have a negative impact on the operation of the constellation due to the use of ΔV, this will not be taken into account for the cost function parameter tradeoff. Additionally, given that the station keeping box takes into account the displacements that are allowed for altitude and inclination to have the least disturbance in operations, these parameters will be taken into accounted for indirectly in the station keeping. For more information on constellation design parameters, see Appendix B.

The first group of parameters that are evaluated are the station keeping parameters. In order to be able to maintain the station keeping box parameters, ΔV is needed. This general ΔV expression can be split in three different direction, being the ΔV in the radial, in-track and cross-track direction. As mentioned before, ΔV influences the lifetime of the satellites, therefore making station keeping also such that it influences the lifetime of the satellite.

Looking at the parameters that are involved in the collision prediction, most of the parameters are linked and depend on each other. The standard deviation of the position and velocity for example influences the error covariance matrix. The error covariance matrix in its turn influences the collision probability. Using the distinction that is used previously, being the influence on the lifetime and the influence on operations, it can be said that the collision probability does not directly influence either one. However, if a collision were to happen, it influences both the lifetime and operations as there is no coverage anymore due to the satellite having a high chance of not surviving the collision. It can therefore be said that the collision probability is one of the main parameters that need to be taken into account for the cost function. Additionally, the time of closest approach influences the collision parameters, which are based on the time of closest approach. The time of closest approach also indicates how much time is left to perform additional computations as well as the time that is left to perform the manoeuvre, but results from the observation of a possible collision and is therefore an effect of the detected collision. It needs to be kept in mind here that the collision warning and detection is done separately and is not part of the initial setup of the problem.

Continuing with the collision prediction parameters concerning the collision radius and volume, these are values that are set and do not change over time once the satellite is in orbit. It is therefore that these parameters are needed, but are not important for the cost function to take into account. The position and velocity at closest approach are important again for the collision prediction, but are not direct drivers for the cost function, as these are also directly taken into account in the collision probability. It is therefore that these values will not be taken into account directly in the cost function, but are reflected in the cost function in other restrictions and penalties (like the manoeuvre time, direction or station keeping box and collision probability as mentioned).

The last set of parameters belonging to the collision avoidance part of the problem consist of ΔV impulses in the three directions. Making the same considerations as above, it can be concluded that the ΔV impulse in radial, in-track and cross-track direction have a negative influence on the satellite lifetime.

Summing up the parameters that have an impact on the lifetime of the satellite, the following parameters are left:

- Station keeping boundaries
- Collision Probability
- ΔV impulse in radial, in-track and cross-track direction

These parameters will be combined in a cost function, which will serve as the function that needs to be optimized. As the goal is to minimize the amount of fuel as well as lower the collision probability and to keep

within the station keeping box, the station keeping box serves more as a boundary value than as a direct value that needs to be minimized next to the other parameters. It is therefore that the station keeping box parameter will be implemented with a penalty function, which will be described in Section 4.2.

Apart from the main parameters that are named above, additional parameters can be used for specific cases and scenarios. These additional parameters can then be included in the cost function by assigning a certain penalty to this parameter, with which it influences the optimal outcome of the cost function. The following parameters could be thought of:

- Orbit accuracy over time, where the collision probability is more certain the closer TCA gets
- The operational lifetime that is left for that particular satellite
- Degree in loss of coverage for that particular constellation

These parameters will not be taken into account in the basic form of the cost function, which includes the three parameters that are mentioned above. This is because these parameters are not primarily related to the operations of the satellite and constellation when a manoeuvre is performed and would therefore only serve as an additional decision-making parameter next to the necessary parameters. Recommendations for further research will be discussed in Chapter 11.

4.2. Parameter Involvement and Penalty Functions

As described above, three main parameters will be taken into account for the cost function, being the station keeping box, the collision probability and the ΔV that is used to perform the manoeuvre in either of the three directions. This section will describe how these parameters will be determined as well as what some threshold values will be.

4.2.1. Collision Probability Cost

As the collision probability needs to be lowered to a certain threshold in order to not be considered a thread anymore, this value is a hard limit. This means that the new calculated value is either a pass or a fail. The way to take this into account in the cost function is to either not have an additional value to the result of the cost function, or if the collision probability threshold is passed that a very high value is added to the total cost, making the solution unusable.

The value that will be added in case the threshold is passed depends on the outcome of the other cost function parameters and needs to surpass that value by a large amount. As mentioned earlier, there are different levels of severity for the collision probability. In most cases, when the threshold of $1 \cdot 10^{-4}$ is reached, a manoeuvre will be considered directly. A collision probability between $1 \cdot 10^{-4} < P_C < 1 \cdot 10^{-7}$ can become serious and is therefore further analyzed for possible manoeuvres. A collision probability lower than $1 \cdot 10^{-7}$ is practically ignored [17].

Depending on what value is chosen in the final cost function as threshold (which also differs per operator), an initial value of $1 \cdot 10^{6}$ is chosen as penalty value, as it is expected that the displacement in the station keeping box can reach multiple kilometers depending on when the manoeuvre is initiated. The penalty of the collision probability needs to pass the maximum value of the station keeping box, as the collision probability is the most determining factor in this research.

4.2.2. ΔV Cost

As one of the biggest players in the whole constellation design and satellite design is the ΔV budget, this is a parameter that needs to be minimized. Using the optimization method that was chosen, the combined minimum value of this ΔV is estimated, while passing the corresponding boundaries.

Based on that this value needs to be minimized, it is important to know what minimal ΔV can be applied to do a collision avoidance manoeuvre. The minimum amount of ΔV depends on how fast the valve can open and close, which determines the minimum impulse bit. This impulse bit is given in [N·s], where values as low as 2.6mN·s and as high as 460 mN·s can be observed for chemical propulsion for smallsats [18]. Dividing these numbers by the weight of the satellites gives an idea of how much [m/s], where assuming a mass of 100 kg (smallsat indicating masses below 500 kg) gives a ΔV ranging from 0.000026 m/s to 0.0046 m/s. Other values of minimum impulse bit for Commercial Off The Shelf (COTS) smallsat thrusters found were ranging from 50 mN·s to 400 mN·s[1,2]. From papers it was found that the minimum amount of ΔV needed for orbit

[1] https://www.dawnaerospace.com/products/p/smallsat-propulsion
[2] https://www.ecaps.space/products-1ngp.php

control ranges from 0.01 m/s to 0.025 m/s [19], [20].

Given the wide range of values, a minimum ΔV value of 0.01 m/s was chosen. This value is one order of magnitude smaller than the amounts found for orbit control and one order of magnitude larger than the values found for the thrusters taking into account a satellite mass of 100 kg, therefore giving a more conservative result.

Combining this value into the cost function, it can be concluded that the separate values of the cost function need to be scaled to carry enough weight to the final solution of the cost function. This will be tested and discussed in Chapter 7 and 8.

4.2.3. Station Keeping Box Cost

As mentioned before, the station keeping box is used as a measure as to which degree the satellite needs to be kept at its position in orbit. Following the discussion above, the station keeping box requires ΔV to account for corrections and to stay within this box. It needs to be noted here that it is possible that the manoeuvre with least ΔV needed to lower the collision probability, passes the station keeping box boundaries. As this cannot be set as a hard limit like the collision probability itself in order to allow for possible low values of ΔV, a penalty function will again be used here to determine the cost of crossing the station keeping box. This however consists of two different directions that needs to be taken into account.

In the in-track direction the movement of the satellite can be seen as a ping pong ball as described before (Chapter 3). As this in-track disturbance is a function of the atmospheric drag and the correction therefore strongly depends on the size and shape of the satellite as well as the altitude, a standard value is chosen as a simplification for the in-track dimension of the station keeping box. It was found that the length of the station keeping box varies between 10 and 50 kilometers, where a first estimation of 35 km is chosen as the box in-track length [13]. This means that the maximum displacement is 17.5km, as the box is centered around the satellite.

The next direction that is considered is the cross-track direction, used to maintain the orbital plane of the satellite. As only a small disturbance in the cross-track direction of the orbit can cause a large offset in the orbital plane [13], the constraint for this direction can be looked at in a different way than the in-track constraint because there is no direct value that can be linked to this direction. It is therefore assumed that the disturbance in the cross-track direction should be kept to a minimum, where a penalty function will assess the cost that comes with a large disturbance in this direction.

As the radial direction influences the altitude of the satellite and therefore indirectly is managed by the orbital period through the orbital plane, the radial component of the station keeping will also be controlled in the in-track constraints [13].

4.3. Final form of the Cost Function

Combining all the above named costs and penalties, the following parameters need to be combined to get the final cost function:

- Collision Probability - In the form of a hard limit penalty
- ΔV Cost - Value that needs to be minimized
- Station Keeping Box - Penalty for the in-track direction and minimization in the cross-track direction

which combined will lead to the following cost function:

$$J = P_{c,penalty} + (\Delta V_1 + \Delta I_1 + \Delta C_1) + (\Delta V_2 + \Delta I_2 + \Delta C_2) \tag{4.1}$$

where $P_{c,penalty}$ is the collision probability penalty:

$$P_{c,penalty} = \begin{cases} 0, & \text{if } P_c > 1 \cdot 10^{-7} \\ 1 \cdot 10^6, & \text{otherwise} \end{cases} \tag{4.2}$$

This means that if the collision probability value passes the allowed threshold, a penalty will be added to the total cost and if the collision probability threshold is not passed, no penalty is needed as the situation can be deemed allowable. Continuing with the parameters in the cost function, ΔV is the manoeuvre magnitude value that needs to be minimized in m/s. The next two parameters for the station keeping box are defined as follows:

$$\Delta I = \begin{cases} 0, & \text{if } \Delta I < 17.5\text{km} \\ (|\Delta I - 17.5\text{km}|)^2 + 17.5\text{km}, & \text{otherwise} \end{cases} \tag{4.3}$$

defining the in-track offset that is created by the manoeuvre and ΔC represents this in the cross-track direction, both with respect to the original orbit. The penalty function chosen here for the in-track direction is quadratic, where the penalty will only be added when passing the boundary of the station keeping box. This way a value for the in-track displacement will be taken into account and also minimized (depending on the magnitude of the other values), but will weigh more when crossing the boundary of the station keeping box. It is therefore also taken into account that the optimal manoeuvre could be passing the station keeping boundary with a certain value, but will not be dismissed due to a penalty which is too high as is the case for the collision probability. Similar to ΔV, ΔC needs to be minimized and is therefore not bound to a penalty function.

As can be seen from the values that need to be minimized, the magnitudes might not be of the same order. For this reason the parameters that are not bound to a penalty may need to be multiplied with weights to allow for an actual minimization. Three types of weights can be added to influence the difference in magnitude of the different values. The first type of weight is that of the two satellties, where the two satellites can have different priority with respect to eachother. The second type of weight is that for ΔV, where is is expected that the magnitude of ΔV is much smaller than that of the displacements and could therefore lead to a minimization which does not focus on the impulse magnitude. The last and third type is the weight for the cross-track displacement. As it was mentioned earlier, the magnitude of the cross-track displacement needs to be as small as possible, which is achieved by adding a weight to this value. The in-track displacement is however less of a priority in minimization, where some allowance is possible due to the length of the station keeping box.

This would then lead to the following formula:

$$J = P_{c,penalty} + w_1(w_3\Delta V_1 + \Delta I_1 + w_4\Delta C_1) + w_2(w_3\Delta V_1 + \Delta I_1 + w_4\Delta C_1) \tag{4.4}$$

where w_1 and w_2 are the weights per satellite, w_3 is the weight for the ΔV usage and w_4 is the weights for the cross-track displacement. These values will be determined and tested in Chapter 7 and 8. It needs to be noted that the base cost function is one where all weights are equal to one.

It needs to be noted here that it was found from a study that the collision probability was mostly influenced by the manoeuvre timing and manoeuvre velocity increment. Both of these variables parameters in their turn influence the relative distance and period of the orbit [11]. It was therefore chosen in this study to use the manoeuvre timing and velocity increment as input values, which is similarly done in this thesis.

5

Code Setup

This chapter will describe the code that was written to simulate the problem and to optimize the results. This code was written in Matlab, where the execution is both in Matlab as well as STK. First the overall idea of the code will be described, after which each block of code will be discussed separately, what inputs are needed and what outputs are generated.

Following the setup of the cost function in the previous section, the first part of this chapter describes the different blocks of code are needed to come to the final values needed as input for the cost function. This is then followed by a description of the optimization algorithm that is used, being Differential Evolution. After the optimization has been described, the input and output generation to obtain the final converged values will be described, where also an overview will be given on which formula is used in which block of code.

5.1. Code Blocks

This section will give an overview of the code blocks, from which the code it is built and what variations are in the code that can be implemented.

The code can be split in multiple blocks of code, where the main sequence is made up of

1. Initialize baseline scenario
2. Generate input values to start the optimization
3. Assess penalty values and cost of the generated input values
4. Evaluate cost function results to find lowest values
5. Generate new input values (using results from previous iteration)

These 5 blocks are the main setup of the code, where the last four blocks run in a loop until convergence is reached. These four blocks are thus the blocks that run within the optimization loop. Each block of code holds multiple functions, which will be described in the sections below.

The input for step 1 is the CDM, from which the baseline state at every time step is propagated. The CDM that is used for input should have a collision probability higher or equal than $1 \cdot 10^{-7}$. The information taken from the CDM is the following:

- TCA
- Exclusion volume radius satellite 1
- Position and velocity at TCA satellite 1
- Position covariance values satellite 1
- Exclusion volume radius satellite 2
- Position and velocity at TCA satellite 2
- Position covariance values satellite 2

As these propagation steps take a significant amount of time, two options are possible for further propagation for the evaluation of the manoeuvre. From these two options two versions of the code can be set up, where one uses STK for propagation and therefore takes longer and the other propagates the states in a linearized way (using a state transition matrix, indicated with stmx), minimizing the convergence time to

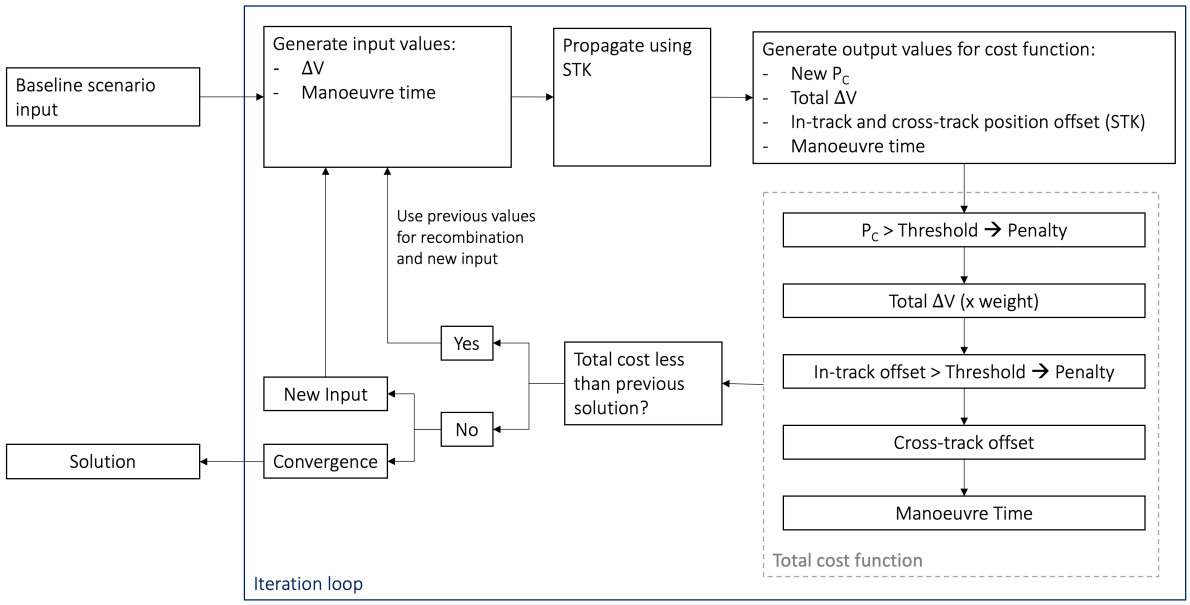

Figure 5.1: Code schematic using STK propagations

about a minute. As these two ways of propagation require a different setup, the first step is already to make the distinction which way the propagation will be done. Both code setups can be seen in Figure 5.1 and 5.2 respectively.

Following this setup and the propagation of the baseline scenario the iteration can be started, which is done using the Differential Evolution method. This method will be described in more detail in the sections below. Following the setup of the first iteration, the results and penalties will be assessed for the total final cost. After the cost is known, the results will be compared with the results of the previous iteration to see which input values give the lowest cost (as the minimization requires the cost to be as low as possible). Once the results of 3 subsequent iterations remain the same, convergence is reached.

With this convergence the minimal ΔV and direction is found with the corresponding minimum displacement, as well as at what time this gives the most optimal solution.

The sections below will describe the subsequent blocks of code in more detail.

5.1.1. Scenario Input and Orbit Propagation

The initialization of the code is done in Matlab, which then uses this input for STK. This initialization needs time of simulation as well as satellite states. The states of the satellites are taken directly from the CDM, which gives the closest approach state in the ITRF frame. This reference frame is the similar frame as the fixed frame in STK. Following this input, the propagation of the satellites will be done in the Cartesian frame.

As mentioned above, two ways of propagation methods can be used. The propagation of the baseline scenario is done in STK for both methods, after which the two methods diverge in setup.

For the method in which the propagation is done by STK only, only the propagation of the baseline scenario in STK is needed for initialization. The method in which the linearized propagation method is used needs six more propagations in STK, needed to set up the state transition matrices.

As the propagation of the satellite orbits takes a significant amount of time, a linearization of the dynamics was implemented to speed the propagation time up. This means that the system is assumed to behave in a linear way. As the problem is a non-linear dynamical system, the state transition matrix was used to find the approximate dynamics of the system.

The state transition matrix is defined as shown below, where $X(t)$ is the state of the spacecraft at time t

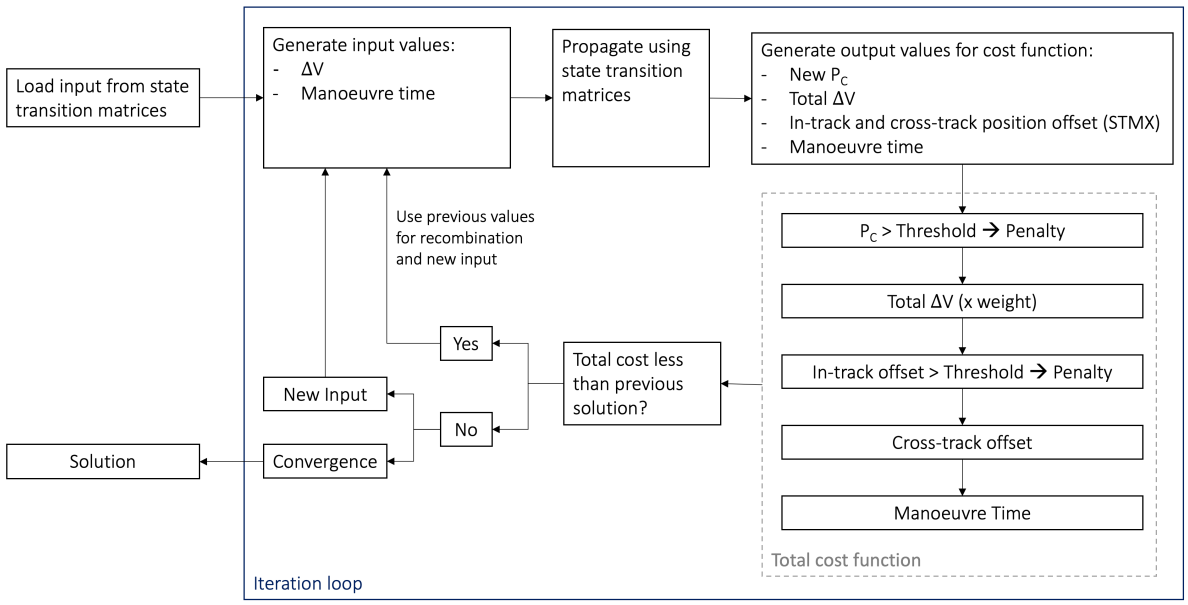

Figure 5.2: Code schematic using state transition matrix propagations

and $X(t_0)$ is then the state of the spacecraft at time t_0 [16]:

$$\Phi(t,t_0) = \frac{\partial X(t)}{\partial X(t_0)} = \begin{bmatrix} \frac{\partial x}{\partial x_0} & \frac{\partial x}{\partial y_0} & \frac{\partial x}{\partial z_0} & \frac{\partial x}{\partial \dot{x}_0} & \frac{\partial x}{\partial \dot{y}_0} & \frac{\partial x}{\partial \dot{z}_0} \\ \frac{\partial y}{\partial x_0} & \frac{\partial y}{\partial y_0} & \frac{\partial y}{\partial z_0} & \frac{\partial y}{\partial \dot{x}_0} & \frac{\partial y}{\partial \dot{y}_0} & \frac{\partial y}{\partial \dot{z}_0} \\ \frac{\partial z}{\partial x_0} & \frac{\partial z}{\partial y_0} & \frac{\partial z}{\partial z_0} & \frac{\partial z}{\partial \dot{x}_0} & \frac{\partial z}{\partial \dot{y}_0} & \frac{\partial z}{\partial \dot{z}_0} \\ \frac{\partial \dot{x}}{\partial x_0} & \frac{\partial \dot{x}}{\partial y_0} & \frac{\partial \dot{x}}{\partial z_0} & \frac{\partial \dot{x}}{\partial \dot{x}_0} & \frac{\partial \dot{x}}{\partial \dot{y}_0} & \frac{\partial \dot{x}}{\partial \dot{z}_0} \\ \frac{\partial \dot{y}}{\partial x_0} & \frac{\partial \dot{y}}{\partial y_0} & \frac{\partial \dot{y}}{\partial z_0} & \frac{\partial \dot{y}}{\partial \dot{x}_0} & \frac{\partial \dot{y}}{\partial \dot{y}_0} & \frac{\partial \dot{y}}{\partial \dot{z}_0} \\ \frac{\partial \dot{z}}{\partial x_0} & \frac{\partial \dot{z}}{\partial y_0} & \frac{\partial \dot{z}}{\partial z_0} & \frac{\partial \dot{z}}{\partial \dot{x}_0} & \frac{\partial \dot{z}}{\partial \dot{y}_0} & \frac{\partial \dot{z}}{\partial \dot{z}_0} \end{bmatrix} \tag{5.1}$$

With this definition above, a disturbance or error can be used as input and multiplied with the state transition matrix for that particular section of the orbit, to find the total disturbance at time of evaluation. This is done as follows:

$$\begin{bmatrix} \Delta x \\ \Delta y \\ \Delta z \\ \Delta \dot{x} \\ \Delta \dot{y} \\ \Delta \dot{z} \end{bmatrix} = \begin{bmatrix} \frac{\partial x}{\partial x_0} & \frac{\partial x}{\partial y_0} & \frac{\partial x}{\partial z_0} & \frac{\partial x}{\partial \dot{x}_0} & \frac{\partial x}{\partial \dot{y}_0} & \frac{\partial x}{\partial \dot{z}_0} \\ \frac{\partial y}{\partial x_0} & \frac{\partial y}{\partial y_0} & \frac{\partial y}{\partial z_0} & \frac{\partial y}{\partial \dot{x}_0} & \frac{\partial y}{\partial \dot{y}_0} & \frac{\partial y}{\partial \dot{z}_0} \\ \frac{\partial z}{\partial x_0} & \frac{\partial z}{\partial y_0} & \frac{\partial z}{\partial z_0} & \frac{\partial z}{\partial \dot{x}_0} & \frac{\partial z}{\partial \dot{y}_0} & \frac{\partial z}{\partial \dot{z}_0} \\ \frac{\partial \dot{x}}{\partial x_0} & \frac{\partial \dot{x}}{\partial y_0} & \frac{\partial \dot{x}}{\partial z_0} & \frac{\partial \dot{x}}{\partial \dot{x}_0} & \frac{\partial \dot{x}}{\partial \dot{y}_0} & \frac{\partial \dot{x}}{\partial \dot{z}_0} \\ \frac{\partial \dot{y}}{\partial x_0} & \frac{\partial \dot{y}}{\partial y_0} & \frac{\partial \dot{y}}{\partial z_0} & \frac{\partial \dot{y}}{\partial \dot{x}_0} & \frac{\partial \dot{y}}{\partial \dot{y}_0} & \frac{\partial \dot{y}}{\partial \dot{z}_0} \\ \frac{\partial \dot{z}}{\partial x_0} & \frac{\partial \dot{z}}{\partial y_0} & \frac{\partial \dot{z}}{\partial z_0} & \frac{\partial \dot{z}}{\partial \dot{x}_0} & \frac{\partial \dot{z}}{\partial \dot{y}_0} & \frac{\partial \dot{z}}{\partial \dot{z}_0} \end{bmatrix} \begin{bmatrix} \Delta x_0 \\ \Delta y_0 \\ \Delta z_0 \\ \Delta \dot{x}_0 \\ \Delta \dot{y}_0 \\ \Delta \dot{z}_0 \end{bmatrix} \tag{5.2}$$

where the vector on the right side of the state transition matrix is the disturbance at t_0 and the vector on the left side of the equal sign represents the total disturbance at time of evaluation. The starting time of the orbit is at t_0 and the disturbance is introduced at t_1. The time of evaluation where the total disturbance needs to be computed for is then indicated with t_2. This is expressed as:

$$\Phi(t_2,t_1) = \frac{\Delta X(t_2)}{\Delta X(t_1)} \tag{5.3}$$

$$\Phi(t_2,t_1)\Delta X(t_1) = \Delta X(t_2) \tag{5.4}$$

For the dynamics at hand, the goal is to know the total disturbance at t_2 (which is the TCA) as a result of an impulse that is done at time t_1. However, the state transition matrix is computed for an evaluation starting at t_0. This means that the state can be computed to t_1 and t_2, based on t_0 and not based on the disturbance that is introduced at t_1. However, the state transition matrix from t_1 to t_2 can be found by multiplying the state transition matrices.

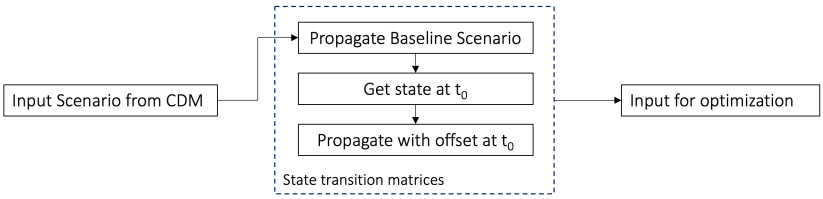

Figure 5.3: Initialization for state transition matrix propagations

The first two state transition matrices which can be found are defined as follows:

$$\Phi(t_1, t_0) = \frac{\Delta X(t_1)}{\Delta X(t_0)} \tag{5.5}$$

$$\Phi(t_2, t_0) = \frac{\Delta X(t_2)}{\Delta X(t_0)} \tag{5.6}$$

where the state transition matrix that needs to be found is defined as

$$\Phi(t_2, t_1) = \frac{\Delta X(t_2)}{\Delta X(t_1)} \tag{5.7}$$

Multiplying the state transition matrices as described above then leads to the following equation to find the state transition matrix from t_1 to t_2:

$$\Phi(t_2, t_1) = \Phi(t_2, t_0)\Phi^{-1}(t_1, t_0) \tag{5.8}$$

$$= \frac{\Delta X(t_2)}{\Delta X(t_0)} \frac{\Delta X(t_0)}{\Delta X(t_1)} \tag{5.9}$$

$$= \frac{\Delta X(t_2)}{\Delta X(t_1)} \tag{5.10}$$

Now that the state transition matrix can be used to find the total displacement of the satellite with respect to its originally estimated position at TCA, the state transition matrix needs to be found. This was done using central differencing, where a small disturbance in all positions and velocities is introduced at t_0 and propagated to find the state at each time step. The total disturbance per time step is assessed and divided by the disturbance that was applied, which can be written as follows for the state in x direction:

$$\frac{\partial x}{\partial x_0} = \frac{x_{+h_0} - x_{-h_0}}{2 \cdot h_0} \tag{5.11}$$

where h_0 indicates the disturbance in the x direction at t_0. This step is then repeated for all six matrix entries, from which the state transition matrix follows.

As this will be done for both satellites that are simulated, the propagation can be done using the state transition matrices. The propagation in STK is therefore not needed anymore if propagation is done this way. Zooming into the first block of code for initialization of the state transition matrix (STMX) method, the sequence as seen in Figure 5.3 is used. Comparing Figure 5.1 and Figure 5.2 it can be seen that the STMX are generated at initialization and later needed for propagation and computation of the in-track and cross-track displacements as well as the relative distances and velocities for the collision probability.

The next step is to start the optimization. The next section will first explain the optimization method that is chosen, after which the step by step implementation is explained.

5.1.2. Differential Evolution Optimization

Before the explanation of the next steps can be done, the setup of the optimization code needs to be explained. The blocks of code that are needed for the generation of input and output values as well as the cost function results are steps within the optimization.

The optimization that is used is the Differential Evolution method. Following earlier studies that were found regarding the use of certain optimization methods, it was seen that the Differential Evolution method gave the most optimal results [10]. Based on this study, it was therefore decided to make use of the differential evolution algorithm for the optimization of the problem in this research.

The advantages of heuristic algorithms, to which DE belongs, is that it is applicable and accessible for practical applications and that it has a simple structure, therefore being easy to use. Next to the solutions being found quickly, where the algorithm also has a high robustness[10].

The DE algorithm is a stochastic and population based optimization algorithm, which was introduced in 1996 [21]. Similarly to the Genetic Algorithm and Evolutionary Programming, it is an evolutionary algorithm. The procedure consists of four steps, which will be described below. The problem that needs to be optimized consists of D real parameters and has a population size of N, which needs to be at least 4. The parameter vector then has the following form:

$$x_{i,G} = \left[x_{1,i,G},\, x_{2,i,G},\, \ldots,\, x_{D,i,G}\right] \qquad i = 1,2,\ldots,N \tag{5.12}$$

where G is the number of generations. The block diagram of the DE optimization algorithm can be seen in Figure 5.4, where the four subsequent steps can be seen that need to be followed. A loop can be seen from the selection step back to the mutation step. This is the iteration loop where the results are evaluated each generation until a certain accuracy and convergence is reached. This will be described below, where each step will be defined [21].

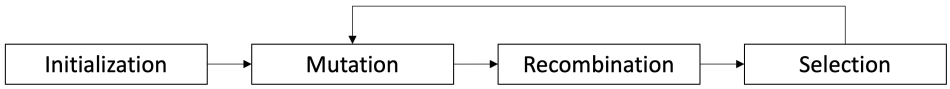

Figure 5.4: Differential Evolution algorithm process

The following process is followed after the setup of the problem:

1. Initialization

   This step initiates the algorithm and is therefore only needed in the first iteration. The upper and lower bounds per parameter are defined in this step

   $$x_j^L \leq x_{j,i,1} \leq x_j^U \tag{5.13}$$

   where also the initial parameters are selected randomly based on the upper and lower boundary interval

   $$\left[x_j^L, x_j^U\right] \tag{5.14}$$

   which will be used in the first iteration round. This step will not be revisited again during the iteration process and serves only as an initialization for the whole process.

2. Mutation

   The next step in the process is the mutation. Each vector of parameters from the population undergoes mutation, recombination and selection. The reason for using mutation in these algorithms is to expand the search space from the initially randomly chosen parameters. The mutation in this algorithm is done by going over the vectors $x_{i,G}$ and selecting three other vectors $x_{r1,G}$, $x_{r2,G}$ and $x_{r3,G}$, such that a distinction can be made between vector i, $r1$, $r2$ and $r3$.
   Using these four vectors the weighted difference is taken to generate a mutation vector

   $$v_{i,G+1} = x_{r1,G} + F(x_{r2,G} - x_{r1,G}) \tag{5.15}$$

   where F is the mutation factor, which is chosen in the range $[0,2]$. The mutated vector that results, $v_{i,G+1}$ is called the donor vector.

3. Recombination

   From the donor vectors that are found from the mutation step, the recombination step evaluates the found donor vectors with the solutions from the previous iteration (or in the case of the first iteration it will be compared to the initially generated vectors). From this evaluation, the trial vector can be

found. This trial vector, $u_{i,G+1}$, is therefore a combination of the previous vectors $x_{i,G}$ and the donor vectors $v_{i,G+1}$. The elements that are allowed to continue in the trial vector are selected by a probability threshold CR in the range of $[0,1]$. This is done by implementing the following step:

$$u_{j,i,G+1} = \begin{cases} v_{j,i,G+1} & \text{if rand}_{j,i} \leq CR \text{ or } j = I_{\text{rand}} \\ x_{j,i,G} & \text{if rand}_{j,i} > CR \text{ or } j \neq I_{\text{rand}} \end{cases} \qquad i = 1,2,\ldots,N; j = 1,2,\ldots,D \tag{5.16}$$

where $\text{rand}_{j,i} \in U[0,1]$ and I_{rand} is a random integer from the range $[1,2,\ldots,D]$. the second requirement per entry is to make sure that $v_{i,G+1} \neq x_{i,G}$.

4. Selection
The last step in the process is the selection step, where depending on function value from the trial vector a new generation can be formed with the found vectors. This is done by comparing the target vector $x_{i,G}$ with the trial vector $v_{i,G+1}$, where the lowest cost function outcome determines which vector can go to the second iteration round

$$x_{j,i,G+1} = \begin{cases} u_{j,i,G+1} & \text{if } f(u_{i,G+1}) \leq f(x_{i,G}) \\ x_{i,G} & \text{otherwise} \end{cases} \qquad i = 1,2,\ldots,N \tag{5.17}$$

where the second iteration starts at the mutation step again.

The process described above will be continued until a certain stopping criteria is reached.

Looking at the initially set values for the number of vectors within a population as well as the mutation factor and probability threshold, some rules of thumb are advised based on practical experience [22]. The number of vectors in the population, N, is advised to be 5 to 10 times the number of parameters D in the problem. The second advice that is given is to choose $F = 0.5$, where in case the solutions get stuck to increase either F or N. It is mentioned that the range for F is most effective in $[0.4,1]$. Additionally, when a quick solution is required, the probability threshold CR is best chosen between 0.9 or 1 for a quick convergence.

5.1.3. Input Generation and Propagation

As described above in step 1 of the optimization, the boundaries of the parameters need to be chosen for the generation of the random variables (Equation 5.13). In this case the parameters for which the boundaries need to be determined are the ΔV in radial, in-track and cross-track direction and the manoeuvre time, added together 8 parameters ($D = 8$ for the optimization setup). Some things need to be kept in mind for the determination of these boundaries, which are the limitations of the spacecraft and the propagation method.

Given the limitations of the spacecraft as well as the boundary which is deemed to be the maximum for the operator, the ΔV may need to be specified per wishes of the operator (it needs to be noted here that the manoeuvre will probably have a lower value, as it is a minimization). This could also depend on the minimum impulse bit as explained in Section 4.2.2. Additionally, the propagation method also needs to be taken into account when choosing these boundaries, as the linearized state transition matrix method has a higher inaccuracy. Choosing a high boundary value for ΔV could lead to incorrect results for the resulting displacement. This will be checked in Chapter 6 and 7.

The randomized number generator will determine the starting population of the ΔV in the three directions and the manoeuvre time. Following this step the recombination and mutation will be determined as described in Equation 5.15 and 5.16. Based on the resulting population parameters, the manoeuvres can be propagated either using STK or using the state transition matrix, where the propagation using the state transition matrices will be used to generate the results as will be described in Chapter 8.

Before the ΔV in RIC can be used, the conversion needs to be done to the Cartesian frame. This is done using the equations as described in Section 3.3. After this the propagation steps can be started.

The propagation in STK requires the input of the new velocity in the three directions as a result of manoeuvre ΔV at the time of manoeuvre (as mentioned before, it is assumed that the manoeuvre is impulsive and therefore a direct change of velocity at moment of manoeuvre). This is done by taking the position and velocity at the time of manoeuvre and adding the change in velocity to create the new state at time of manoeuvre. This can then be used as input directly and be propagated to find the state at time of closest approach.

The propagation using the state transition matrix works a little different. As explained earlier, the state transition matrix needs to be found to propagate the disturbance in the state from t_1 (time of manoeuvre)

to t_2 (time of closest approach). With this matrix, a multiplication can be done with the disturbance vector, which will look as follows:

$$\begin{bmatrix} 0 \\ 0 \\ 0 \\ \Delta V_x \\ \Delta V_y \\ \Delta V_z \end{bmatrix} \tag{5.18}$$

Here the first three entries of the vector are zero, as the position is not changes from the manoeuvre. The last three entries have a value depending on which direction the manoeuvre is performed in, where an instantaneous change in velocity is assumed. From the use of the state transition matrix the direct displacement is calculated from the reference point, in this case being the time of closest approach.

5.1.4. Output Value Generation

The output generation is also done differently for the two propagation methods. For the STK output, some additional steps are needed to obtain the relative states, whereas the state transition matrix method directly gives the displacement as a result of the ΔV impulse.

Following the propagation in STK, the relative states need to be obtained as well as the displacements of the original state of the satellites at TCA. This is done using the 'Relative Motion' report, querying the relative distance between:

- Satellite 1 and new satellite 1 - for the displacement of satellite 1
- Satellite 2 and new satellite 2 - for the displacement of satellite 2
- New satellite 1 and new satellite 2 - for the collision probability calculation

It is these reports, together with the propagation of the satellite states, that make the process take longer than compared to the state transition matrix method. These relative states that are found for the three points above then need to be converted to the RIC frame at TCA. Following the relative positions of the in-track and cross-track direction, the penalty function can be filled in and included in the cost function.

Following the state transition matrix method, the displacement resulting from the manoeuvre is a direct result of the multiplication of STMX with ΔV vector. Just as for the STK method, this needs to be converted to RIC frame to find the final solution which can be used in the penalty and cost function. To find the relative distance between satellite 1 and 2 the displacements need to be added to the baseline state to find the new states.

As the new states are now determined, the only remaining parameter that is not known yet is the collision probability for the new states. This will be calculated as was mentioned in Chapter 3.

5.1.5. Cost Function Output and Evaluation

With the values known the penalty functions can be filled in and with that the cost function itself (Equation 4.4) and the results can be evaluated. Per item in the population the cost function will be determined (the values determined for the displacements and collision probability were also done per item in the population). Each item will then be evaluated against the cost of the previous iteration as seen in Equation 5.15.

Depending on which cost is lower, the input of the lowest of the two will be used as new input for the next iteration. For the input values of the result that is higher, the same item will be used as input for the next iteration, which will then also be used in the recombination and mutation step.

This iterative process continues until convergence is reached. Convergence is reached when three subsequent iterations have the exact same results and all entries in the population are the same value.

5.2. Code Overview

Combining all the previously discussed blocks of code as well as the setup of the different blocks with respect to each other, the equations can be coupled to the blocks of code for the complete setup.

Figure 5.5 and 5.6 show the first steps needed for the setup of the scenario, similar to 5.3. Figure 5.5 shows how the state transition matrices are set up and Figure 5.6 shows how the first steps are done to import the scenario and the initial collision probability is computed. Following this setup, the STK input as well as the loading of the scenario is used to setup the base script.

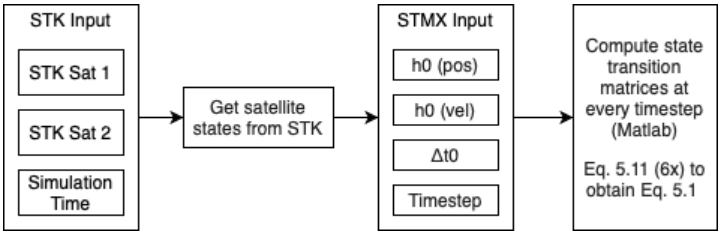

Figure 5.5: Setup and computation of the state transition matrices

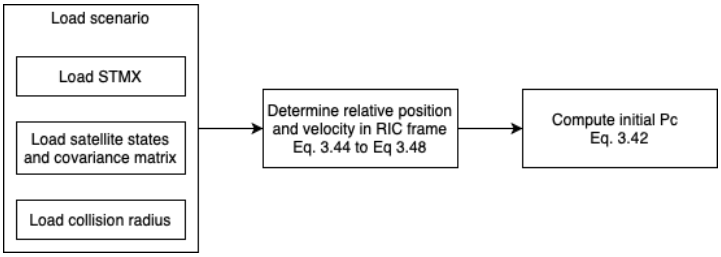

Figure 5.6: Setup and computation of the initial collision probability and input files to start simulation including formulas

Figure 5.7 shows the complete loop with equations from iteration initialization up to convergence. It can be seen here that the initialization needs to be done only once to set the parameters. Using this code the information in the following chapters is generated and tested.

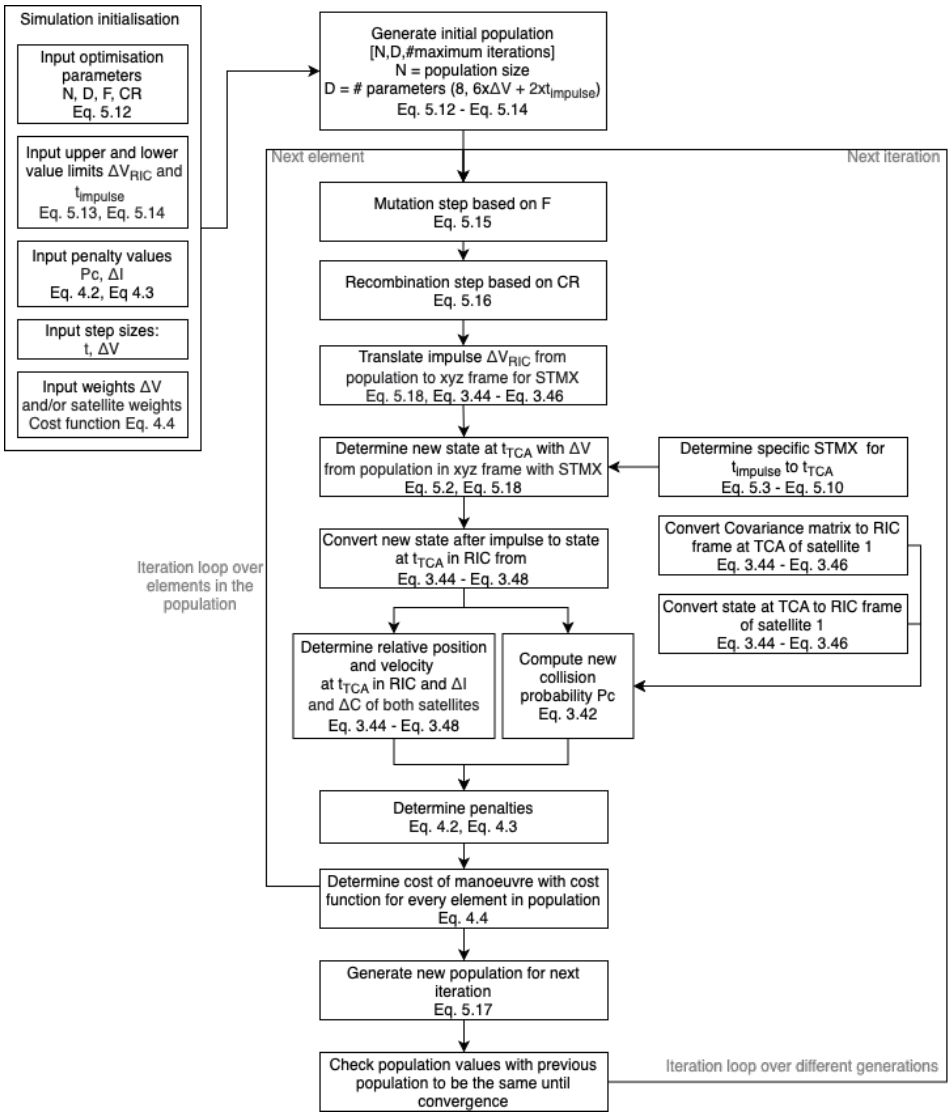

Figure 5.7: Full iteration loop from initialization until convergence including formulas

6

Verification and Validation

Following the setup of the code and the pieces of analytical computations, the validity of these pieces of code need to be checked. This will be done in this chapter.

First the conversion to RIC frame and relative position and velocity calculations will be checked. This will then be followed by the initialization and the calculations with the state transition matrix. The next formula that will be checked is the collision probability, which is followed by the verification of the optimization algorithm.

Once all these different aspects of the code have been verified, these formulas and pieces of code can be used to obtain the final solutions.

6.1. RIC conversion and relative distance

As the collision messages are given in the radial, in-track and cross-track frame and as the constraints for the station keeping box are also needed in this frame, a simple conversion needs to be done from Cartesian frame to the RIC frame. This step is then followed by a calculation on the relative distance and speed, based on the RIC frame of the primary satellite. Although STK is able to give the relative motion of the two satellites, a direct analytical computation in Matlab would speed up the process significantly.

The equations described in Section 3.3 will be checked against the relative motion function in STK and these results will then be evaluated with the RIC position and velocities that are given in the CDMs. 10 CDMs are used, which can be seen in Table 6.1. This table shows the RIC position and velocity as given by de CDM as well as the analytical result and the STK result. The values of the CDMs are given with one digit behind the comma, whereas it was chosen for the results of the analytical computation and the STK result to show the values with three digits behind the comma.

From this table it can be seen that the RIC relative position gives accurate results, which means that the analytical calculation as well as the STK calculation are both accurate to calculate the relative position. The preference however goes out to the analytical method of calculating these values, given the long computation time of STK.

Looking at the relative velocities a few things can be noticed. First of all, it can be seen that the relative velocity in cross-track direction is the same for both the analytical as the STK computation. For the in-track relative velocity it can be seen that the STK values are not always the exact same as given in the CDM, while this does seem to be the case for the analytically calculated values. For example, some of the CDM values are given without a digit behind the comma as seen in the first three cases, which is assumed to mean that this is a value rounded off to a zero behind the comma. Rounding off the analytical values would result in the exact same result as the CDM is giving, which is not the case for the STK results.

The radial velocity on the other hand also shows large deviations from the CDM values when looking at the STK values. Even though the differences are not that clear in the last three examples, the first seven examples show a clear difference with the rounded off values compared to the analytical results. The analytical results show similar results as the CDM.

Following the results as shown above it can be concluded that the analytical method for calculating the radial, in-track and cross-track relative position and velocity is more accurate for the problem at hand. This method will therefore be used in the code.

Table 6.1: Comparison of analytical and STK results with the given values of the RIC position and velocity of CDMs

	R [m]	I [m]	C [m]	$\dot{R}$ [m/s]	$\dot{I}$ [m/s]	$\dot{C}$ [m/s]
CDM	96.4	415.4	170.7	4.2	-2175	5321.2
Analytical	96.433	415.367	170.677	4.238	-2174.990	5321.213
STK	96.433	415.367	170.677	4.693	-2175.095	5321.213
CDM	97	330.7	135.2	4.3	-2175	5321.2
Analytical	96.976	330.703	135.162	4.332	-2174.990	5321.213
STK	96.976	330.703	135.162	4.694	-2175.096	5321.213
CDM	167.2	-725.4	629.8	-1.2	-6488	-7511.3
Analytical	167.173	-725.429	629.812	-1.239	-6487.995	-7511.304
STK	167.173	-725.429	629.812	-2.035	-6488.178	-7511.304
CDM	106.7	88	-252	26.6	-13464.4	-4805.4
Analytical	106.661	88.020	-251.969	26.611	-13464.400	-4805.373
STK	106.661	88.020	-251.969	26.708	-13464.517	-4805.373
CDM	83.2	188.9	623.9	-27.5	-13847.3	4292.4
Analytical	83.159	188.942	623.908	-27.492	-13847.303	4292.426
STK	83.159	188.942	623.908	-27.285	-13847.394	4292.426
CDM	57.5	309.1	804.3	-24.9	-13190.7	5121.8
Analytical	57.523	309.142	804.273	-24.947	-13190.667	5121.844
STK	57.523	309.142	804.273	-24.608	-13190.730	5121.844
CDM	-168	-80.5	-483.2	-1.6	-14783	2472.3
Analytical	-168.015	-80.528	-483.228	-1.632	-14783.039	2472.302
STK	-168.015	-80.528	-483.228	-1.720	-14782.855	2472.302
CDM	-167.1	-50.9	-294.4	-1.7	-14783	2472.3
Analytical	-167.053	-50.899	-294.417	-1.657	-14783.045	2472.299
STK	-167.053	-50.899	-294.417	-1.713	-14782.862	2472.299
CDM	78	-88.4	-189.1	0.1	-12401.4	5560.4
Analytical	78.001	-88.395	-189.119	0.148	-12401.357	5560.354
STK	78.001	-88.395	-189.119	0.056	-12401.438	5560.354
CDM	73.9	-105.1	-226.1	0.2	-12401.4	5560.4
Analytical	73.945	-105.086	-226.055	0.166	-12401.351	5560.355
STK	73.945	-105.086	-226.055	0.057	-12401.428	5560.355

Table 6.2: Error between propagated relative positions and velocities for a ΔV of 5 m/s ±5 orbits before TCA

		Δx = 5m, Δv = 5m/s		Δx = 1m, Δv = 1m/s		Δx = 1m, Δv = 0.1m/s	
	Propagated	STMX	Error [%]	STMX	Error [%]	STMX	Error [%]
R [m]	-2817.41	7449.76	-364.42	11075.40	-493.11	11291.01	-500.76
I [m]	-317053.18	-210706.41	-33.54	-311294.81	-1.82	-317097.70	0.01
C [m]	-304963.17	-199851.66	-34.47	-299204.02	-1.89	-304936.98	-0.01
$\dot{R}$ [m/s]	495.69	329.33	-33.56	487.64	-1.62	496.77	0.22
$\dot{I}$ [m/s]	-2192.41	-2186.62	-0.26	-2181.95	-0.48	-2181.66	-0.49
$\dot{C}$ [m/s]	5305.62	5311.97	0.12	5315.47	0.19	5315.68	0.19

Table 6.3: Error between propagated relative positions and velocities for a ΔV of 1 m/s ±5 orbits before TCA

		Δx = 5m, Δv = 5m/s		Δx = 1m, Δv = 1m/s		Δx = 1m, Δv = 0.1m/s	
	Propagated	STMX	Error [%]	STMX	Error [%]	STMX	Error [%]
R [m]	1848.71	1567.10	-15.23	2292.23	23.99	2335.35	26.32
I [m]	-63047.17	-41808.99	-33.69	-61926.67	-1.78	-63087.25	0.06
C [m]	-60814.01	-39833.79	-34.50	-59704.26	-1.82	-60850.85	0.06
$\dot{R}$ [m/s]	102.64	69.26	-32.52	100.92	-1.68	102.74	0.10
$\dot{I}$ [m/s]	-2176.69	-2177.32	0.03	-2176.38	-0.01	-2176.32	-0.02
$\dot{C}$ [m/s]	5319.76	5319.36	-0.01	5320.06	0.01	5320.11	0.01

6.2. State Transition Matrix

Given the way the state transition matrix method linearizes the dynamics of the problem as was described in Section 5.1.1, an error will result from this simplification. This error needs to be assessed in order to see if this implementation is realistic and gives a good approximation of the results.

As all the input and output of the calculations is done in the radial, in-track and cross-track frame of the primary satellite, the error will also be assessed in this frame. Two analyses will be done to see the results of the use of the state transition matrix, where the first analysis is done to assess what delta step needs to be used to get the most accurate results for the state transition matrices. The second analysis is then done to assess the error in the results of the state transition matrix compared to the propagated values. This will also at the same time give an idea of the sensitivity of the state transition matrix. This sensitivity analysis is therefore combined and will not be re-iterated in Chapter 7.

6.2.1. State Transition Matrix Delta Evaluation

Given the delta in position and velocity that need to be chosen to find the state transition matrices as described above, it can be expected that a certain step would perform better or less than another delta step. With the total manoeuvre ΔV expected to be far below 5 m/s, three ΔV velocities are simulated to evaluate the delta that needs to be chosen with which the state transition matrices are determined, being 5 m/s, 1 m/s and 0.5 m/s. The actual manoeuvre magnitude is expected to be in the order of the latter value. Additionally, it is not expected that the manoeuvre will take place more than 5 orbits before TCA (one orbit estimated to be around 6000s), which is why this value is chosen as the maximum output error. Altogether, this means that the delta step chosen here is based on the most maximum of situations with are expected to have the largest errors, as a larger propagation time as well as disturbance from the manoeuvre ΔV would lead to a larger error.

Table 6.2 shows the comparison of the results for a manoeuvre of 5m/s of the propagated and analytically computed RIC relative positions and velocity, as well as the results based on the propagated values of the state transition matrix (indicated with STMX). Looking at the error over the different deltas chosen, it can be seen that the overall error percentages go down with the decrease in delta steps. The smallest error is seen for a delta step of 1 m for the position and 0.1 m/s for the velocity. The only error that seems to increase is that of the radial direction.

Table 6.3 shows the same analysis as done in Table 6.2, but then with a ΔV of 1 m/s. The same trend in the error can be seen as in Table 6.2, where again the radial direction seems to have the largest and growing error. Overall it can also be seen that the error in the radial direction is smaller than in the first example with a ΔV of 5 m/s. This indicates already that a larger value for ΔV will result in larger errors, but this will be discussed

Table 6.4: Error between propagated relative positions and velocities for a ΔV of 0.5 m/s ±5 orbits before TCA

		Δx = 5m, Δv = 5m/s		Δx = 1m, Δv = 1m/s		Δx = 1m, Δv = 0.1m/s	
	Propagated	STMX	Error [%]	STMX	Error [%]	STMX	Error [%]
R [m]	1118.32	831.77	-25.62	1194.33	6.80	1215.89	8.72
I [m]	-31312.00	-20696.81	-33.90	-30755.65	-1.78	-31335.94	0.08
C [m]	-30317.25	-19831.56	-34.59	-29766.79	-1.82	-30340.09	0.08
$\dot{R}$ [m/s]	53.45	36.75	-31.24	52.58	-1.63	53.49	0.07
$\dot{I}$ [m/s]	-2175.73	-2176.15	0.02	-2175.69	0.00	-2175.66	0.00
$\dot{C}$ [m/s]	5320.59	5320.29	-0.01	5320.64	0.00	5320.66	0.00

Table 6.5: Error between propagated and estimated radial, in-track and cross-track state based on 0.5 m/s and 0.1 m/s ΔV at ± 5 orbits before TCA

	0.5m/s			0.1m/s		
	Propagated	STMX	Error [%]	Propagated	STMX	Error [%]
R [m]	1118.32	1215.89	8.72	324.12	320.32	1.17
I [m]	-31312.00	-31335.94	0.08	-5929.42	-5934.89	-0.09
C [m]	-30317.25	-30340.09	0.08	-5926.14	-5931.48	-0.09
$\dot{R}$ [m/s]	53.45	53.49	0.07	14.08	14.09	-0.07
$\dot{I}$ [m/s]	-2175.73	-2175.66	0.00	-2175.12	-2175.12	0.00
$\dot{C}$ [m/s]	5320.59	5320.66	0.00	5321.11	5321.10	0.00

in more detail in Section 6.2.2. Again the smallest error is seen for the delta step of 1 m for the position and 0.1 m/s for the velocity.

The last table, Table 6.4, shows the same comparison as the two tables above, but with a ΔV of 0.5 m/s in all directions. Again, the same can be observed as in the two tables above, where the last delta step shows the smallest error. Also the radial direction seems to have the largest error, but is significantly lower compared to the error as found in the previous two tables with lower ΔV. From this it can again be already seen that the smaller the ΔV, the more accurate the state transition matrix is able to estimate the position of the satellite.

Also lower values for the delta step were analyzed, but it was seen that smaller steps would not make the error smaller and could even lead to a somewhat larger error. Given the tables and results shown above, it can be seen that the largest delta step shows the largest error and the smallest error is seen for a delta step of 1 m for the position and 0.1 m/s for the velocity. This delta step is therefore chosen to compute the state transition matrices with.

6.2.2. State Transition Matrix Error Evaluation

Based on the conclusion of the previous section that the delta step for the determination of the state transition matrices can be set to 1 m for the position and 0.1 m/s for the velocity, an analysis can be done on the accuracy of the estimated values over varied times of manoeuvre. These results will be shown below. Three times of manoeuvre were chosen for this analysis, being 5, 3 and 1 orbits before TCA. For these three manoeuvre times a ΔV magnitude of 0.5 m/s and 0.1 m/s will be compared, as these are the values that are more likely to result from the optimization. Additionally, the manoeuvre is expected to be performed at earliest 12 hours before TCA, as the last screening is finished up to 12 hours before the manoeuvre needs to be determined [23].

Table 6.5 shows the comparison of the results from a propagated relative state with a ΔV of 0.5 m/s and 0.1 m/s at about 5 orbits before TCA. As was also seen in the previous results, the error in the radial position dominates the total error that is seen from the estimation with the state transition matrix. The smaller value of ΔV also seems to be of significant influence on the accuracy, which is what was expected. Apart from the lesser accuracy in the radial position, the other values show that the state transition matrix estimates the state with an error below the 0.1%.

Table 6.6 shows the same analysis with a manoeuvre ΔV of 0.5 m/s and 0.1 m/s from a manoeuver time of 3 orbits before TCA. The same conclusions as above can be made, where a larger error is seen in the radial position for both manoeuvre magnitudes. It is also observed again that the remaining relative positions and velocities show accurate results with the largest error being 0.15%. The error between the 0.5 m/s ΔV at 5 orbits before TCA and 3 orbits before TCA becomes smaller, where the error for a ΔV of 0.1 m/s between 5 orbits and 3 orbits keeps the same order of magnitude (but might seem to get a little higher because of the

Table 6.6: Error between propagated and estimated radial, in-track and cross-track state based on 0.5 m/s and 0.1 m/s ΔV at ± 3 orbits before TCA

	0.5m/s			0.1m/s		
	Propagated	STMX	Error [%]	Propagated	STMX	Error [%]
R [m]	663.73	687.54	3.59	218.27	214.65	1.66
I [m]	-18366.80	-18388.32	0.12	-3340.50	-3345.37	-0.15
C [m]	-17778.65	-17798.12	0.11	-3418.38	-3423.08	-0.14
$\dot{R}$ [m/s]	33.74	33.77	0.09	10.14	10.14	0.00
$\dot{I}$ [m/s]	-2175.40	-2175.38	0.00	-2175.07	-2175.07	0.00
$\dot{C}$ [m/s]	5321.27	5321.29	0.00	5321.23	5321.23	0.00

Table 6.7: Error between propagated and estimated radial, in-track and cross-track state based on 0.5 m/s and 0.1 m/s ΔV at ± 1 orbit before TCA

	0.5m/s			0.1m/s		
	Propagated	STMX	Error	Propagated	STMX	Error
R [m]	244.65	241.30	-1.37	127.06	125.41	1.30
I [m]	-5772.68	-5784.92	0.21	-822.00	-824.69	-0.33
C [m]	-5723.77	-5734.98	0.20	-1007.85	-1010.45	-0.26
$\dot{R}$ [m/s]	14.34	0.14	0.02	6.26	6.26	0.00
$\dot{I}$ [m/s]	-2175.10	-2175.10	0.00	-2175.01	-2175.01	0.00
$\dot{C}$ [m/s]	5321.78	5321.77	0.00	5321.33	5321.33	0.00

smallest value of the relative position).

The last analysis done is that of a manoeuver of 0.5 m/s and 0.1 m/s at 1 orbit before TCA. As mentioned above, here again the radial position error is larger than the other errors. The magnitude of this error is decreased significantly though, where the maximum error is 1.37%. This shows that the state estimation at a short time before TCA can be done accurately with the state transition matrix.

The manoeuver time before TCA is expected to be below 3 orbits, where an accurate result was already seen at 3 orbits before TCA. Also taking into account that these ΔVs are also expected to be the magnitude that results from the optimization, it can therefore be concluded that the state transition matrix shows a result that is accurate enough for position estimation. By doing the position determination through an estimation with the state transition matrix, a large amount of simulation time can be saved. As MATLAB can do matrix multiplications fast and as no additional propagation is needed anymore except for the initialization of the simulation and computation of the state transition matrices with the delta steps, a large part of the propagation work of STK can thus be omitted.

The effect of the error in the estimated positions also needs to be analyzed in terms of effect on the collision probability, but this will be discussed in the sensitivity analysis in Section 7.1.

6.3. Collision Probability Formula

As mentioned before in Section 3.2.3, the collision probability formula can be simplified to a 2D problem, where the assumption is made that the collision area is a square to allow for an ever more simplified version of the formula. Using Equation 3.43, the resulting collision probability can be checked against the probability that is given in the CDMs.

With the coordinates in the CDMs given in the ITRF frame, these can be imported in STK in the fixed frame. After input in the fixed frame the propagation can be done in inertial reference frame, from which then the relative distances and velocities can be derived. This relative state can then be used as an input to compute the collision probability.

Table 6.8 shows some results of the analytical computation from the derived formula and the collision probabilities as provided in the CDMs. As this thesis deals with the collision between two satellites, this will also be the focus of the verification of the formulas. The collision probabilities between satellites and debris are however also given, to give a complete picture of the derived formula. It also needs to be noted here that it is assumed that the CDM gives the true value of the collision probability. The maximum allowed error assumed for the purpose of this thesis is one order of magnitude smaller than the actual collision probability itself (given that there are multiple ways of calculating the collision probability). This has to do with the

Table 6.8: Comparison and error between given collision probabilities and computed collision probabilities

From Formula	CDM	Error	Type
$1.772 \cdot 10^{-6}$	$1.770 \cdot 10^{-6}$	$2.439 \cdot 10^{-9}$	Sat - Sat
$1.161 \cdot 10^{-6}$	$1.160 \cdot 10^{-6}$	$7.418 \cdot 10^{-10}$	Sat - Sat
$5.981 \cdot 10^{-6}$	$5.870 \cdot 10^{-6}$	$1.114 \cdot 10^{-7}$	Sat - Sat
$1.653 \cdot 10^{-6}$	$1.630 \cdot 10^{-6}$	$2.313 \cdot 10^{-8}$	Sat - Sat
$8.349 \cdot 10^{-6}$	$8.400 \cdot 10^{-6}$	$-5.102 \cdot 10^{-8}$	Sat - Sat
$2.820 \cdot 10^{-17}$	$5.350 \cdot 10^{-19}$	$2.767 \cdot 10^{-17}$	Sat - Deb
$3.976 \cdot 10^{-15}$	$4.950 \cdot 10^{-16}$	$3.481 \cdot 10^{-15}$	Sat - Deb
$2.342 \cdot 10^{-4}$	$2.499 \cdot 10^{-4}$	$-1.572 \cdot 10^{-5}$	Sat - Deb
$4.249 \cdot 10^{-4}$	$5.724 \cdot 10^{-4}$	$-1.475 \cdot 10^{-4}$	Sat - Deb
0	0	-	Sat - Deb

threshold of the collision probability, where a probability from $1 \cdot 10^{-6}$ or higher will be investigated for further action. If the calculated probability would have a larger error than the order of magnitude of the value itself, it would mean that it could stay below the threshold even though it needs to be investigated for further action. This also means that a positive error (where the formula gives a higher value than that of the CDM) is also preferable, as this gives a more conservative value to do calculations with.

Starting with the satellite - satellite conjunctions, it can be seen that the error is negligible compared to the value given by the CDM. It can also clearly be seen that the order of magnitude of the errors are lower than the allowed error mentioned above. Once the collision probability would have an error that results in a value in different order of magnitudes, the threshold for action becomes more questionable. From the other satellite - satellite conjunction warnings that are not shown in this list the same order of error is observed, from which can therefore be concluded that the formula gives accurate results for this research.

For the satellite - debris conjunction warnings different results can be observed compared to the satellite - satellite results. It needs to be noted though that the warnings with a value smaller than $1 \cdot 10^{-6}$ are not considered to be of 'danger' to the satellite, meaning that there is no need for a further decision on a collision avoidance manoeuvre (as was mentioned in Chapter 3). The first two satellite - debris warnings were therefore not of importance to see if further action needs to be taken. Additionally, as Matlab has a precision up to 16 digits[1], meaning that these values are passing this precision and could therefore have a large error.

Then looking at the two collision probabilities following that have a value in the range of $1 \cdot 10^{-4}$, it can already be seen that these errors are lower than the two values mentioned above. An error of magnitude $1 \cdot 10^{-5}$ on a value of around $2 \cdot 10^{-4}$ is still accepted, as this is one order of magnitude lower than the actual value.

The last value shows a zero collision probability. This is something that is seen more often, which happens when the error function reaches its limits as can be seen in Figure 6.1. As can be seen in the figure, when a value of 2.0 or -2.0 or higher is used as input for the error function, the result will always go to 1.0 or -1.0 respectively. This results in a collision probability as two exact same values will be subtracted from each other, as can be recalled in Equation 3.43. This value of 2.0 and higher, or -2.0 and lower, is reached when the values of the covariance matrix in the B-plane are small. As can be seen in Equation 3.43, when the C_B values are small, the value from which the error function is calculated is automatically high and in this case higher than 2.0 or lower than -2.0.

As this is a result of the simplification of the code and as this result is seen in all the CDMs which give a probability of 0, this result is therefore also the accurate result.

Keeping in mind that the collision probability formula will be used in this thesis to assess the risk between two satellites and as it was concluded that the formula works for these events, it can therefore be concluded that this collision probability formula is accurate enough to use in the code.

6.4. Optimization Algorithm

In order to test the DE optimization that was written in Matlab, multiple test functions were used to verify the convergence of the code[2]. Four functions were chosen to verify the convergence, being the Beale function,

[1] https://nl.mathworks.com/help/symbolic/increase-precision-of-numeric-calculations.html date last visited 28-01-2021
[2] https://en.wikipedia.org/wiki/Test_functions_for_optimization date last visited 01-06-2020

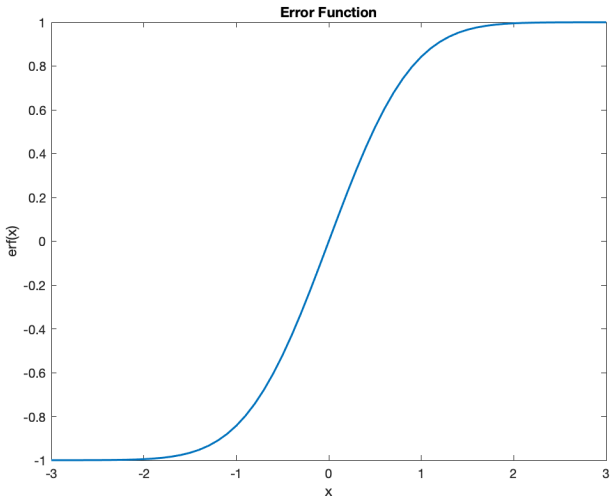

Figure 6.1: Error Function

Table 6.9: Optimization test functions

Function Name	Function
Beale function	$f(x,y) = (1.5 - x + xy)^2 + (2.25 - x + xy^2)^2 + (2.625 - x + xy^3)^2$
Levi N.13 function	$f(x,y) = \sin^2 3\pi x + (x-1)^2(1+\sin^2 3\pi y) + (y-1)^2(1+\sin^2 2\pi y)$
Himmelblau function	$f(x,y) = (x^2 + y - 11)^2 + (x + y^2 - 7)^2$
McCormick function	$f(x,y) = \sin(x+y) + (x-y)^2 - 1.5x + 2.5y + 1$

the Levi N. 13 function, the Himmelblau function and the McCormick function. All four functions were used to verify different aspects of the algorithm. All four functions will be described below, as well as the outcome of the optimization for these functions.

Table 6.9 shows the four test function expressions and Table 6.10 shows the corresponding minima and the search space. All four optimization functions were chosen because of different reasons. The Beale function was used as a first check to see if the code was working properly. For this function there is one minimum that can be found, made up of two function variables. The Levi N.13 function was chosen because of the sinusoids, where multiple local minima could be found instead of the global minimum. The Himmelblau function was then used to check if the code was able to find more than one minimum, as four minima exist. Last but not least the McCormick function was used to see if the code was also capable in finding a non-zero minimum.

The runs showed that for the Beale function no difficulties were found in finding the minimum. This was also achieved with a low number of iterations.

For the Levi N.13 function the same results were found, where the minimum was found with a low number

Table 6.10: Optimization test functions minima and ranges

Function Name	Minimum	Search Space
Beale function	$f(3, 0.5) = 0.0$	$[-4.5 \leq x, y \leq 4.5]$
Levi N.13 function	$f(1,1) = 0.0$	$[-10 \leq x, y \leq 10]$
Himmelblau function	$f(3.0, 2.0) = 0.0$	$[-5 \leq x, y \leq 5]$
	$f(-2.805118, 3.131312) = 0.0$	
	$f(-3.779310, -3.283186) = 0.0$	
	$f(3.584428, -1.8481262) = 0.0$	
McCormick function	$f(-0.54719, -1.54719) = -1.9133$	$[-1.5 \leq x \leq 4]$
		$[-3 \leq y \leq 4]$

of iterations. Also the correct minimum was found out of the possible local minima.

The Himmelblau function required a different approach, where the code needed to be run multiple times to find all minima. It was seen that certain values seem to be reached easier than other values, but overall it was seen that all four minima were found. The convergence speed was also more than was seen for the previous two functions.

The final function, the McCormick function, showed a little more difficulty with finding the minimum. Even though the global minimum that was found is close to the minimum as shown in Table 6.10, some minima that were found were out of the search boundaries. Focusing on the results within this search space, it was seen that the minimum that was found had was not the exact same value as given in Table 6.10. The values were however close and good enough for the estimation of the global minimum.

With these four functions it was therefore concluded that the optimization code works and can be used in the simulations. A more detailed discussion on the results can be found in Appendix D.

7

Sensitivity Analyses

This chapter will discuss the sensitivity of the collision probability parameters and formula, followed by the sensitivity analysis of the covariance matrix. As the sensitivity of the state transition matrix was already discussed in Chapter 6, it will not be analyzed in this chapter. These sensitivity analyses will give an indication of the variations in the results based on the input and propagation time for example.

7.1. Collision Probability

The main determining parameters in this code is the collision probability. There are two ways in which the sensitivity will be checked of this collision probability, being the sensitivity to offsets resulting from a linearized propagation (through the state transition matrix) and the sensitivity to position changes and velocity changes through ΔV. Both sensitivities will be analyzed in the same manner, where an offset in the relative position and/or velocity will be introduced and will show the change in collision probability.

The first sensitivity analysis that will be done is for the result of the state transition matrix. As was seen and discussed in the previous chapter on the verification and implementation of the state transition matrix, the maximum expected errors are mostly in the relative position and not much so in the relative velocity. More attention will therefore be given to the offsets in the relative position and less so on the relative velocity offsets.

As was be seen in Table 6.5 there is a large offset in the radial direction. It is however not expected that the ΔV impulse will reach 0.5 m/s at 5 orbits before TCA. The manoeuvre is expected to be between 1 and 3 orbits before TCA, which is why the focus will start with the offsets as seen in Table 6.6 and Table 6.7.

Starting with Table 6.6 the main error was seen in the relative position for a ΔV, which comprises of errors in the order of 20 m (absolute error) in radial, in-track and cross-track direction when the manoeuvre is done 3 orbits before TCA. This error slims down to errors of about (-) 4 m for a ΔV of 0.1 m/s. going over the errors in Table 6.7 it can be seen that the error in relative position is up to (-)10 m for a ΔV of 0.5 m/s and again goes down to about (-)2 m for a ΔV of 0.1 m/s. It needs to be noted here that the errors are mainly decreasing the relative position instead of increasing it, which could be beneficial in making it a more conservative estimation.

The sensitivity analysis of the collision probability formula will be done with increased relative position errors of 25 m and 10 m and increased relative velocities of 0.1 m/s and 1.0 m/s. Based on the values shown above and in the tables mentioned, the error seems to be negative most of time. The same analysis will therefore also be done with decreasing relative positions and velocities, which are expected to show an increased value of the collision probability because of the smaller relative distances. This might however be favored against increased relative positions and velocities, as it will give a more conservative value for the collision probability.

Table 7.1 shows the error evaluations for both position offsets and velocity offsets that make the relative state larger. Logically, this leads to the collision probability decreasing. Looking at the collision probabilities for an offset of 25 m it can be seen that the risks stay in the same order of magnitude, except for the second row. The original value as given in the CDM is however on the threshold itself (if assumed to be $1{\cdot}10^{-6}$), where a value in the high $1{\cdot}10^{-7}$ is not unexpected when looking at a decreasing relative distance. Even though this error is not desirable and as the errors are expected to be smaller and decreasing the relative distance, this

Table 7.1: Collision probability error evaluation from offsets that increase the relative position and velocity

CDM	From formula	RIC pos + 10 m	RIC pos + 25 m	RIC vel + 0.1 m/s	RIC vel + 1.0 m/s
$1.77 \cdot 10^{-6}$	$1.77 \cdot 10^{-6}$	$1.72 \cdot 10^{-6}$	$1.62 \cdot 10^{-6}$	$1.77 \cdot 10^{-6}$	$1.77 \cdot 10^{-6}$
$1.16 \cdot 10^{-6}$	$1.16 \cdot 10^{-6}$	$8.39 \cdot 10^{-7}$	$4.83 \cdot 10^{-7}$	$1.16 \cdot 10^{-6}$	$1.16 \cdot 10^{-6}$
$5.87 \cdot 10^{-6}$	$5.98 \cdot 10^{-6}$	$5.42 \cdot 10^{-6}$	$4.76 \cdot 10^{-6}$	$5.98 \cdot 10^{-6}$	$5.98 \cdot 10^{-6}$
$5.85 \cdot 10^{-6}$	$5.99 \cdot 10^{-6}$	$5.39 \cdot 10^{-6}$	$4.70 \cdot 10^{-6}$	$5.99 \cdot 10^{-6}$	$6.00 \cdot 10^{-6}$
$1.63 \cdot 10^{-6}$	$1.65 \cdot 10^{-6}$	$1.60 \cdot 10^{-6}$	$1.53 \cdot 10^{-6}$	$1.65 \cdot 10^{-6}$	$1.65 \cdot 10^{-6}$
$8.40 \cdot 10^{-6}$	$8.35 \cdot 10^{-6}$	$8.10 \cdot 10^{-6}$	$7.72 \cdot 10^{-6}$	$8.35 \cdot 10^{-6}$	$8.35 \cdot 10^{-6}$

Table 7.2: Collision probability error evaluation from offsets that decrease the relative position and velocity

CDM	From formula	RIC pos - 5 m	RIC pos - 10 m	RIC pos - 25 m
$1.77 \cdot 10^{-6}$	$1.77 \cdot 10^{-6}$	$1.80 \cdot 10^{-6}$	$1.82 \cdot 10^{-6}$	$1.89 \cdot 10^{-6}$
$1.16 \cdot 10^{-6}$	$1.16 \cdot 10^{-6}$	$1.35 \cdot 10^{-6}$	$1.55 \cdot 10^{-6}$	$2.28 \cdot 10^{-6}$
$5.87 \cdot 10^{-6}$	$5.98 \cdot 10^{-6}$	$6.31 \cdot 10^{-6}$	$6.67 \cdot 10^{-6}$	$8.06 \cdot 10^{-6}$
$5.85 \cdot 10^{-6}$	$5.99 \cdot 10^{-6}$	$6.35 \cdot 10^{-6}$	$6.75 \cdot 10^{-6}$	$8.08 \cdot 10^{-6}$
$1.63 \cdot 10^{-6}$	$1.65 \cdot 10^{-6}$	$1.68 \cdot 10^{-6}$	$1.71 \cdot 10^{-6}$	$1.82 \cdot 10^{-6}$
$8.40 \cdot 10^{-6}$	$8.35 \cdot 10^{-6}$	$8.48 \cdot 10^{-6}$	$8.61 \cdot 10^{-6}$	$8.99 \cdot 10^{-6}$

error is deemed as acceptable because of this boundary value. However, in case the ΔV exceeds the 0.5 m/s at about 3 orbits before TCA, an additional more accurate run might be needed to check the results.

Looking further at the error in the relative position with an offset of 10 m, again the second row is one order of magnitude higher than the CDM value. As explained above, the original value was already in the low $1 \cdot 10^{-6}$, meaning that an increase in relative position automatically results in a high $1 \cdot 10^{-7}$ value. The difference compared to an offset of +25 m is however much lower and gives a much more accurate result. The errors found here are also one order of magnitude smaller than the original collision probability value, meaning that the result is accurate enough to give an indication of the collision probability.

For the error in velocity however, a marginal difference can be seen with respect to the results from the self-computed collision probability. As those self-computed collision probabilities were concluded to be accurate enough, these errors in the velocity are also not seen as a problem for the accuracy.

Moving on to the decreased relative position due to a smaller value resulting from the linearized estimation, these results can be seen in Table 7.2. As mentioned before, with a decreasing relative position the collision probability is expected to be higher, which is also observed in this table. What is also seen in this table is that the results still are within the same order of magnitude, where the offset for -25 m is a little higher than -10 m for example (also expected). The values as are found for an error of -10 m to -5 m are expected to be most occurring, which are also one order of magnitude smaller than the CDM values and lean towards the more conservative side of the values.

Looking at all the results as shown above, it can be concluded that there is some offset in the collision probability for the results of the linearization of the propagation. However, depending on the magnitude of the manoeuvre ΔV, which is not expected to be higher than 0.5 m/s because of the minimization, and for the time of manoeuvre, which is not expected to be earlier than about 3 orbits before TCA, the errors that are seen are acceptable. It needs to be noted however that when the ΔV is expected or found to be higher than 0.5 m/s or the time of manoeuvre is expected to be earlier than 3 orbits before TCA, a run with higher precision needs to be done. Comparing the run time of 7hr compared to the few minutes it takes to run the linearized code, preference is given to a first computation with the linearized model.

7.2. Covariance Matrix

As the collision probability is largely dependent of the covariance matrix of the state of the satellite, research has been done on the validity and accuracy of this covariance matrix. This research will be shortly discussed here and used for the analysis of the covariance matrices that will be used for the scenarios that are used in this thesis.

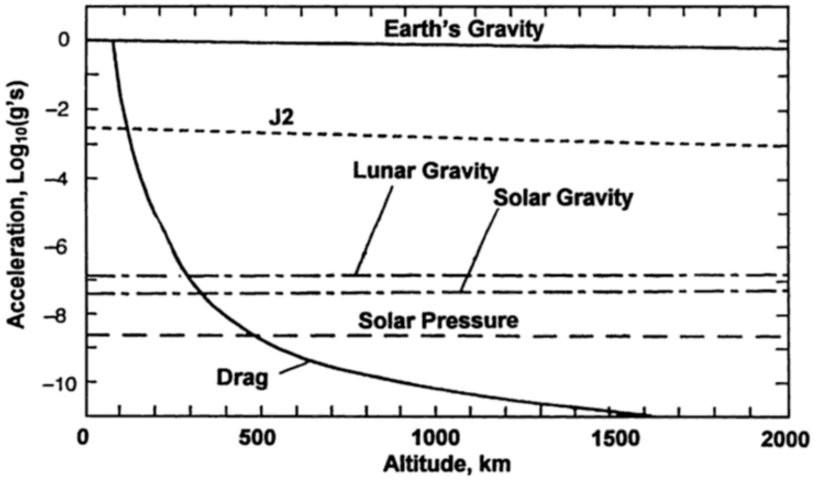

Figure 7.1: Accelerating influence of the Earth's gravity, J_2, lunar gravity, solar gravity, solar pressure and atmospheric drag [24]

The position determination as well as the covariance matrix setup depend on the use of different force models, combined with observations and estimated orbits [24]. This is then propagated forward to get an estimate of the state and covariance matrix at the time of closest approach. Given the uncertainty because of the level of accuracy of propagation, it could well be that the covariance matrix is not accurate enough while this is one of the most important input values for the calculation of the collision probability (as was discussed in Chapter 3). Five forces are the main determining part in orbit determination:

- Two-body motion
- Non-spherical Earth
- Atmospheric drag
- Third body effects
- Solar radiation pressure

Figure 7.1 shows the variability of these five forces in acceleration at different altitudes and how they vary over different altitudes. From this it can be readily be seen that the atmospheric drag force has a large variation over the different altitudes and can very quickly go from the most influential disturbance to least disturbance. So even though the drag might not be the largest disturbance at the altitude of the scenarios in this report, it can still be considered the most variable as atmospheric temperatures are difficult to estimate [24].

The first estimations of the state and state covariance were done using TLE and general perturbations, which was fast but not that precise. It was a more simplified model, without solar radiation pressure or third body effects included. This was then moved to a more precise method of calculating this, including special perturbations, which was slow but more precise. Although more accuracy is obtained this way, most of the atmospheric models are still empirical based. The latest model used for the CDMs is Jacchia-Bowman-HASDM-2009 (JBH09) [17], where the High Accuracy Satellite Drag Model (HASDM) was used to debias the Jacchia-Bowmann-2008 (JB08) model [24]. This HASDM showed improved epoch accuracy, covariance realism and ballistic coefficient consistency [25]. However, with this improved accuracy there are still biases and inaccuracies which need to be researched further.

For accurate collision avoidance, the covariance matrix needs to be an accurate representation of the uncertainty in the state. Given the way the collision probability is calculated there are two aspects to this accuracy:

- Does the error in the position volume follow and conform to a trivariate Gaussian distribution?
- If a trivariate Gaussian distribution is followed, does it have the correct orientation and dimension?

For the first point mentioned above a study was done to understand the Gaussian error volume on the collision risk assessment. This study showed that high collision probabilities of $1 \cdot 10^{-4}$ experience insignificant impact of the non-Gaussian effects and deviations [26]. It was then concluded in this study that the state uncertainties represented with the corresponding covariance matrix are in general small for high P_c cases and therefore will have low non-Gaussian deviations. This can be explained as that high collision probability

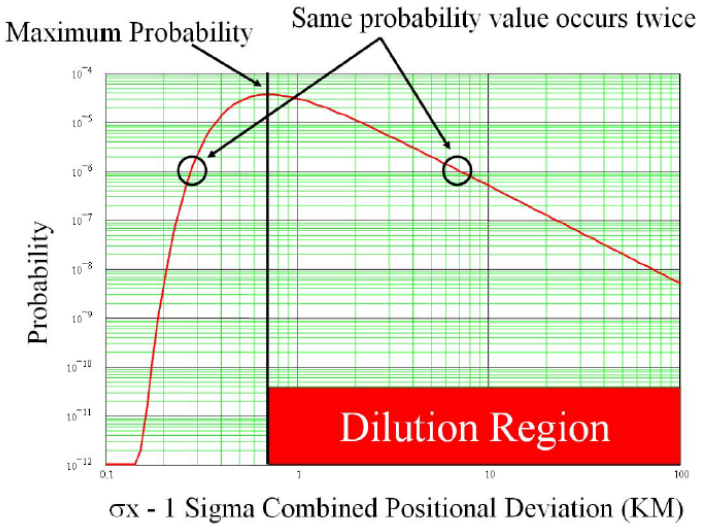

Figure 7.2: Dilution region for collision probability and standard deviation values [28]

cases might have an overlap in the covariance volume near the center of the covariance volume, which is then not affected by this non-Gaussian effect.

Continuing with the second point named above on the size and dimension of the covariance, this can be checked with a calculation of the squared Mahalanobis distance ($\epsilon \cdot C^{-1} \cdot \epsilon^T$, where ϵ contains the residuals and C is the combined covariance). This Mahalanobis distance shows how many standard deviations P is removed from the mean D, where in the case of a trivariate distribution the expected outcome is 3 [24]. However, as only the CDM is used as an information source, the residuals ϵ needed to compute the Mahalanobis distance cannot be obtained.

Another way in which the covariance can be checked is by looking at the dilution region, which considers the ratio between the miss distance and covariance size. If this ratio is larger than $\sqrt{2}$, the collision probability resides in the dilution region. In case a low collision probability is found, which is in the dilution region, no conclusion can be drawn. The reason for this is that because of a large uncertainty, it could well be that the distance of the two objects is closer than expressed in a collision probability. This can also be seen in Figure 7.2, where the robust region gives a more accurate result because of the lower covariance values and lower values of the residuals. On the right side of the figure the same collision probability can be found even though there is a large inaccuracy meaning large covariance and large residuals [27].

Another practice, which is used by CNES (Centre National d'Etudes Spatiales), is to scale the covariance matrices of both the primary and secondary satellite and create a heat map of the collision probabilities with these scaled covariances [29]. The factors range from 0.5 to 3.0 [27], creating an $n \times n$ grid of P_C values that will give insights in the potential errors in the covariance matrix. Through this method the small changes in covariance can be assessed beforehand, where the maximum P_C can be analyzed using these scale factors. This way it can also be seen if the maximum collision probability passes the threshold for an avoidance manoeuvre, even though this might be too conservative.

Another study looked at the predicted errors of the CDMs with the corresponding covariances [30]. The results from this study showed that the CDM covariances give a good and realistic indication of the inaccuracy of the orbits, but do however seem to be underestimating this inaccuracy. Additionally, a common scaling factor could not be found, as these scaling factors depend largely on the orbit and observations. For the CDMs that are used in this report, a common scaling factor is therefore also not expected to be found.

Given that the method with safety factors does not rely on additional orbit data (which is not available for this thesis), this method will be elaborated below to give an indication of the variability of the collision probabilities.

With the information given above on the realism and accuracy of the covariance matrices, it can be seen that without actual orbit data and CDM data only, finding a more precise covariance matrix is questionable. Additionally, with JSpOC providing the information in the CDMs from the High Accuracy Catalogue and them also being the party that provides the TLEs [23], finding more accurate results for the covariance matrices using TLEs is also not an option for the timespan and scope of this research. It is however advised for further

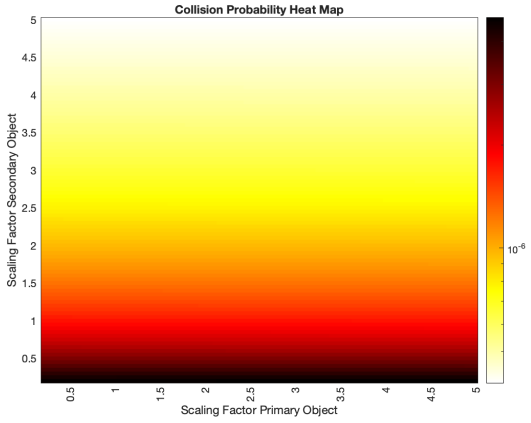

Figure 7.3: Scaling factor influence on collision probability of $1.77{\cdot}10^{-6}$

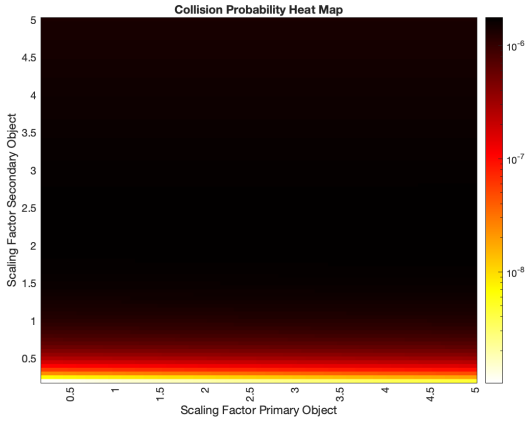

Figure 7.4: Scaling factor influence on collision probability of $1.16{\cdot}10^{-6}$

Table 7.3: Scaling factors and corresponding minimum and maximum collision probability

Example	Given P_c	Minimum P_c	SF_1	SF_2	Maximum P_c	SF_1	SF_2
Fig 7.3	$1.772{\cdot}10^{-6}$	$4.040{\cdot}10^{-7}$	5.0	5.0	$4.702{\cdot}10^{-6}$	5.0	0.2
Fig 7.4	$1.161 \cdot 10^{-6}$	$1.041{\cdot}10^{-9}$	0.2	0.2	$1.765{\cdot}10^{-6}$	5.0	2.2
Fig 7.5	$8.349{\cdot}10^{-6}$	$1.732{\cdot}10^{-6}$	5.0	5.0	$3.478{\cdot}10^{-5}$	0.2	0.2
Fig 7.6	$2.342{\cdot}10^{-4}$	$7.908{\cdot}10^{-9}$	0.2	0.2	$8.430{\cdot}10^{-4}$	0.2	3.4

research to look more into the accuracy of the covariance matrix data.

Four CDM covariance matrices are analyzed and discussed below. Figures 7.3, 7.4, 7.5 and 7.6 show what happens to the collision probability when a scaling factor ranging from 0.2 to 5 is applied to the covariance matrices. From all figures it can be seen that the collision probability is not much affected by the scaling factor of the secondary object. This can be explained by the covariance values of the primary object having much smaller values than that of the secondary object. This means that the covariance values of the secondary object will dominate the collision probability.

In Figure 7.3 it can be seen that the collision probability gets larger for a lower value of the covariance values of the secondary satellite. For this CDM the collision probability was $1.77{\cdot}10^{-6}$ and depending on what the threshold is, here using the example threshold of $1{\cdot}10^{-6}$, the collision probability will lower to a safe value when a scaling factor of about 2.0 or higher is used.

The opposite is found to be true for the CDM in Figure 7.4, where lower collision probabilities are found for lower values of the scaling factor. The collision probability that is given is $1.16{\cdot}10^{-6}$, where values larger than the above mentioned example threshold are found for higher values for the scaling factor.

The third figure shows more of a gradient in collision probability values then multiplied with a scaling factor. It needs to be noted here that although it looks like the collision probability is lower for a high scaling factor, it still passes the threshold of $1{\cdot}10^{-6}$ for a scaling factor of 5. Only if the threshold value were to be moved up to $1{\cdot}10^{-5}$ the scaling factor would not influence that decision.

The last figure that is shown here to analyze the scaling factor is Figure 7.6. This figure shows that there is a small region for low values of the scaling factor where the collision probability passes. It is also seen here that the scaling factor of the primary object does happen to make a small difference, compared to the examples given above. The reason for this could be because of the secondary object being a piece of debris, where previous secondary objects were satellites that are manoeuvrable.

From these examples it can be seen that it greatly depends on the values of the covariance of the secondary object compared to that of the primary object. Where the first three examples in Figure 7.3, 7.4 and 7.5 show a factor of up to $1 \cdot 10^5$ between the primary and secondary object covariance values, the last example shows a factor of up to $1 \cdot 10^5$. This smaller factor in covariance matrix difference would explain the slightly tilted gradient of the last example.

As mentioned before, depending on the threshold that is set for the collision probability after which action

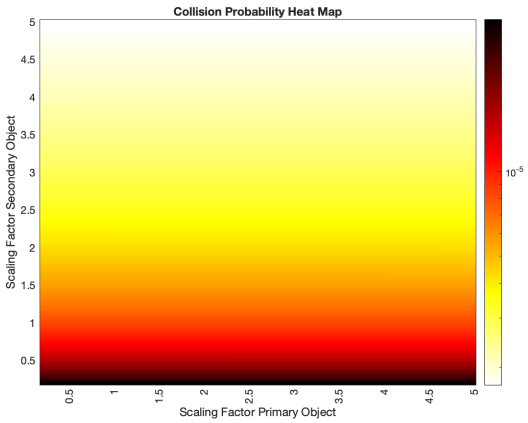

Figure 7.5: Scaling factor influence on collision probability of $8.35{\cdot}10^{-6}$

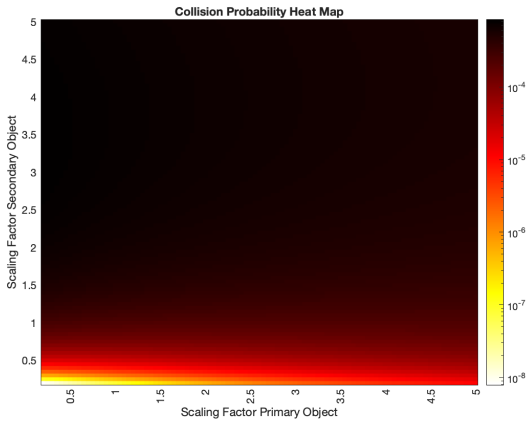

Figure 7.6: Scaling factor influence on collision probability of $2.43{\cdot}10^{-4}$

Table 7.4: Results for different ΔV weights in the cost function

Weight	ΔV_1	ΔV_2	t_1	t_2	ΔI_1	ΔI_2	ΔC_1	ΔC_2	Cost
$1 \cdot 10^2$	0.29	0	83802	0	0.1	0	0.3	0	29.4
$1 \cdot 10^3$	0.29	0	83802	0	0.1	0	0.3	0	290.4
$1 \cdot 10^4$	0	0.02	0	77744	0	575.2	0	0.8	776
$1 \cdot 10^5$	0	0.01	0	69717	0	519.8	0	0.8	1520.6
$1 \cdot 10^6$	0	0.01	0	69717	0	519.8	0	0.8	10520.6
$1 \cdot 10^7$	0	0.01	0	69717	0	519.8	0	0.8	100520.6

needs to be taken, some of these scaling factors have a value that will results in the collision probability either passing the higher threshold (e.g. $1{\cdot}10^{-5}$) or not being of importance at all after multiplication. The collision probabilities for the first and third example seem to stay in about the same order of magnitude, whereas the second and fourth example have a larger range. What is interesting to see is that also for these two examples, the scaling factor of the secondary object does not seem to be either the highest or lowest scaling factor.

7.3. Cost Function Initialization and CDM selection

As described in Chapter 4, the parameters and weights of the cost function still need to be initialized for the optimal result. This initialization is done by varying the weight of ΔV in the cost function, which therefore also tests the sensitivity of the weight of this ΔV. It is assumed and expected that the most important parameter in the cost function is the ΔV, for which therefore a higher weight needs to be added to have the most influence next to the collision probability. This analysis will be shown and explained below.

Using the advised parameter values for the optimization of $F = 0.5$ and $CR = 0.7$, a range of multiples of 10 are used to analyze the best weight to find the minimum ΔV from the optimization. With the minimum impulse of 0.001 m/s, a weight of at least 1000 is expected to be used to weight up against the displacement that is found from the manoeuvre (which are expected to be multiple meters).

Table 7.4 shows the otimization results for a range of $1 \cdot 10^2$ to $1 \cdot 10^7$ as weight for ΔV, for one CDM. This means that with every weight the simulation was done for the same CDM. With these weights, different solutions for the same CDM are found. This tabel shows that for the different weights a larger ΔV results when the weight is smaller. As the initial goal is to minimize ΔV, it is therefore expected that a higher weight is necessary to have the focus on the minimum ΔV.

From these results it can be seen that the first two weights cause the cost function to convert to the lowest displacement instead of the lowest ΔV. Even though this is desirable, the magnitude of ΔV has more priority to be minimized. This is what will result when increasing the weight to $1 \cdot 10^4$ and higher as can be seen in the table. Looking at the results for a weight of $1 \cdot 10^4$, it can be seen that the ΔV is not yet at its lowest, even though the timing is later than the time of manoeuvres for a higher weight. From $1 \cdot 10^5$ onward the influence of the weight can be clearly seen in the cost. As mentioned above, it is desirable to have a higher order of

Table 7.5: Initial results from minimizing the ΔV of the manoeuvre for three CDMs

	ΔV_{R1}	ΔV_{R2}	ΔV_{I1}	ΔV_{I2}	ΔV_{C1}	ΔV_{C2}	t_1	t_2	Cost
CDM1	0	0	0	0.01	0	0	0	69717	1520.6
CDM2	0	0	0.01	0.01	0	0	84691	71771	2513.8
CDM23	0	0	-0.01	0	0	0	83196	0	1078.4

magnitude for the value of ΔV as it needs to weight up against the displacement magnitude. In this case, this goal is reached with a value of $1 \cdot 10^5$ onward, which is why this weight is chosen for the determination of which CDMs will be used for the scenarios. A more detailed analysis of the results that were found above are done in Chapter 8. The base cost function including the ΔV weight looks as follows:

$$J = P_c + (1 \cdot 10^5 \Delta V_1 + \Delta I_1 + \Delta C_1) + (1 \cdot 10^5 \Delta V_1 + \Delta I_1 + \Delta C_1) \tag{7.1}$$

The next step is to analyze the CDMs using the weight for the impulse as determined above. From this analysis three CDMs can be chosen for the scenarios. Using the state transition matrix method as described in Section 5.1.1, all satellite-with-satellite conjunction messages (to availability) were ran with the code and the cost function as found above. With the minimum impulse bit of 0.01 m/s it was seen that most of the optimal manoeuvres would converge towards this value of ΔV.

To get a good understanding of the results of the code, all three CDMs chosen to have a different result in terms of ΔV usage. The CDM values as well as the geometry can be seen in Appendix E. Table 7.5 shows the preliminary results of these three CDMs.

Looking at the preliminary results it can be seen that the ΔV of the three CDMs differ in which of the two satellites needs to manoeuvre. The first CDM shows a manoeuvre for the secondary satellite and a ΔV that needs to be initiated in the in-track direction. The second CDM shows that both the primary and secondary satellite need to perform a manoeuvre in the in-track direction to get to the lowest cost at different times. For the third CDM it can be seen that the manoeuvre needs to be performed by the primary satellite in the negative in-track direction to get the lowest cost. Additionally, the first and second CDM are based on the same event. This will be useful in understanding the differences in the manoeuvre options that results from these two CDMs.

What was observed from all the simulations, is that the manoeuvre in all cases needs to be performed in the in-track direction. This is also seen in the three chosen CDMs in Table 7.5.

It also needs to be noted that upon running the optimization algorithm, multiple local minima were found. This means that the code might need to be ran multiple times to assess the actual lowest cost. This will also be shown and discussed in Chapter 8.

8

Results

Based on the cost function as well as the verification and sensitivity analysis of the different parameters and the code itself, the results can be generated. First the different scenarios will be described that are explored, where each scenario will provide information that can be used to formulate the answer to the research questions. Following this setup, the different scenarios will be ran, of which the results will be shown.

This chapter will only shows what the results are that can be observed. A more thorough explanaition of why the results look the way they look will be described in the next chapter, Chapter 9.

8.1. Scenarios and Setup

The results that will be generated are based on three CDMs, as this is the only available information on close approaches and conjunction events apart from the operators own calculations if available. As described before, this is also the only source for this thesis on the covariance values at the time of closest approach.

These three CDMs will be used to run three different scenarios, which will help in answering the research questions. As was seen in Chapter 2 there are two subquestions, of which one looks at the technical aspect of the manoeuvre in relation to a space traffic management and the other question looks at the operational aspect of the manoeuvre in relation to a space traffic management. Based on these two directions, the three scenarios chosen will be:

- Scenario 1: Input restrictions
  - ΔV limit
- Scenario 2: Output restrictions
  - Station keeping limits
- Scenario 3: Input/output weighing
  - Weighing per satellite based on constellation setup
  - Cost function parameter weights based on constellation setup or operator wishes

These scenarios can also be seen in the two directions as mentioned, where the first and second scenario are based on the technical side of the research and where the third scenario looks at the operational aspects if the optimization would be executed with preferences.

In order to be able to work on those scenarios, the code needed to be set up such that the final form is set, which was done in Section 7.3. Three CDMs were chosen based on the initial results, which were the CDM 1, CDM 2 and CDM 23. The parameters that are needed for the code can be seen in Appendix E. The initial results run with only a weighing factor for the ΔV can be seen in Table 8.1. This table shows the resulting ΔV per direction per CDM, as was found to be the lowest. In this case, all minima were found in the in-track direction and no ΔV in the radial and cross-track direction. Additionally, it shows the time of manoeuvre for the primary and the secondary satellite and the total cost as resulted from the cost function.

This chapter will show the results and give an overview of the result per scenario and per CDM. Chapter 9 will then discuss these results, which is then also a more elaborate view on these results.

Before continuing to the next section with the results, some additional information is needed to look at the results, which is shown in Table 8.2.1 and 8.3. The first table shows the orbit times of the primary and secondary satellite for the three different CDMs as well as the time of closest approach for that simulation.

Table 8.1: Initial results from minimizing the ΔV of the manoeuvre for three CDMs

	ΔV_{R1} [m/s]	ΔV_{R2} [m/s]	ΔV_{I1} [m/s]	ΔV_{I2} [m/s]	ΔV_{C1} [m/s]	ΔV_{C2} [m/s]	t_1 [s]	t_2 [s]	Cost [-]
CDM1	0	0	0	0.01	0	0	0	69717	1520.6
CDM2	0	0	0.01	0.01	0	0	84691	71771	2513.8
CDM23	0	0	-0.01	0	0	0	83196	0	1078.4

Table 8.2: Orbit times and time of closest approach for both satellite of the conjunction event

	cdm1	cdm2	cdm23
Orbit time sat 1 [s]	5730	5730	5730
Orbit time sat 2 [s]	5736	5736	5736
Time of closest approach [s]	86820	86820	85962

The orbit times indicate the amount of time it takes for the satellite to complete a full orbit. The time of closest approach is then the time in the simulation at which the satellites are at the closest range and have a probability of collision. Also the times of one to three orbits before TCA per CDM are shown in Table 8.3. This is then simply the subtraction of the time of one orbit from TCA per CDM. These values might be needed to assess the results that follow from the minimization, where it can be checked if the manoeuvre happens at full orbits before TCA or maybe at half orbits before TCA. As the first and second CDM are notifications for the same event, the orbit times are also the same.

These orbit times will be used in the figures in the following sections as well as in the discussion of the results in the next chapter.

8.2. Scenario 1

The first scenario, as mentioned above, assesses the manoeuvre that needs to be performed where a minimum ΔV needs to be achieved with a ΔV limit. It is assumed for this case that the manoeuvre can only take place from a little more than five orbits before TCA until 30 minutes before TCA. Additionally, the manoeuvre can be performed in the radial, in-track and cross-track direction. The cost function that is used has the following form:

$$J = P_c + (1 \cdot 10^5 \Delta V_1 + \Delta I_1 + \Delta C_1) + (1 \cdot 10^5 \Delta V_1 + \Delta I_1 + \Delta C_1) \tag{8.1}$$

where the weight of the ΔV is $1 \cdot 10^5$ as was found in Section 7.3.

The results of this scenario can be seen in Table 8.1. For this scenario it can be seen that the limit of ΔV is not of significance to the results, as the minimum is automatically found to be the minimum ΔV that is possible. It can therefore also be seen in the results that lowering the maximum value of ΔV has no influence on the results as the assumed minimum impulse bit was found, where for the first simulations a minimum of 0.5 m/s was used, after which a second minimum of 0.1 m/s was used.

8.2.1. CDM1

Table 8.4 and 8.5 show three different results that were found for the first CDM using the optimization. Table 8.4 shows the collision probability that is found after the manoeuvre with the corresponding total impulse magnitude as well as the displacement in each direction and time of manoeuvre. Table 8.5 then shows the manoeuvre magnitude in the different directions and the cost that is found from the cost function.

Table 8.3: Full orbit times from TCA in simulation time

	CDM1 - sat 1	CDM1 - sat 2	CDM2 - sat 1	CDM2 - sat 2	CDM23 - sat 1	CDM23 - sat 2
TCA [s]	86820	86820	86820	86820	85962	85962
TCA - 1 orbit [s]	81090	81084	81090	81084	80232	80226
TCA - 2 orbits [s]	75360	75348	75360	75348	74502	74490
TCA - 3 orbits [s]	69630	69612	69630	69612	68772	68754

Table 8.4: Simulation results for scenario 1, CDM1

Result #	Pc [-]	ΔV_1 [m/s]	ΔV_2 [m/s]	ΔI_1 [m]	ΔI_2 [m]	ΔC_1 [m]	ΔC_2 [m]	t_1 [s]	t_2 [s]
1	$9.985 \cdot 10^{-8}$	0	0.01	0	519.8	0	0.8	0	69717
2	$9.997 \cdot 10^{-8}$	0	0.01	0	547.1	0	0.9	0	67590
3	$9.991 \cdot 10^{-8}$	0	0.02	0	575.2	0	0.8	0	77774

Table 8.5: Detailed simulation results for scenario 1, CDM1

Result #	ΔV_{R1} [m/s]	ΔV_{R2} [m/s]	ΔV_{I1} [m/s]	ΔV_{I2} [m/s]	ΔV_{C1} [m/s]	ΔV_{C2} [m/s]	t_1 [s]	t_2 [s]	Cost [-]
1	0	0	0	0.01	0	0	0	69717	1520.6
2	0	0	0	0.01	0	0	0	67590	1548.0
3	0	0	0	0.02	0	0	0	77774	2576.0

As was also mentioned earlier, the code needed to be run multiple times as different results were found from convergence. It can be seen in Table 8.4 that the manoeuvre for this first CDM is in all cases done by the secondary satellite, where the lowest cost has a ΔV expense of 0.01 m/s. The highest value that is observed is 0.02 m/s. It can also be seen that the absolute displacement is mainly in the in-track direction, not coming close to the value of 35 km which was set for the threshold of the station keeping box. There is also a small movement in the cross-track direction.

Table 8.5 shows a more detailed view of the ΔV in the three directions as well as the cost. From this table it can be seen that all results found for this CDM have an impulse in the in-track direction. Additionally, it can also be seen that the timing of the manoeuvres is within the three orbits range for the first and third result, but that the second result is just outside this range.

Looking at the total cost, the influence of the higher ΔV can be seen, where the timing seems to have a smaller influence in the form of displacement.

The manoeuvres that resulted as seen in Table 8.4 and 8.5 can be seen in Figure 8.1 and 8.2. Figure 8.1 shows the first two found manoeuvres with a ΔV of 0.01 m/s in the in-track direction and Figure 8.2 shows the last found manoeuvre time for a ΔV of 0.02 m/s in the in-track direction, indicated with the blue stripe dotted line. The simulation time is cut of until the time of closest approach, meaning that TCA is the latest manoeuvre time that is indicated in these figures.

The upper part of the graphs show the relative distance at time of closest approach resulting from an impulse at a chosen time of manoeuvre between the two satellites in the local frame of the primary satellite (horizontal axis), is indicated with the blue, orange and yellow line. This is from simulation time t_0 until TCA (maximum simulation time). The second part of both graphs shows the collision probability that would result at a chosen manoeuvre time. Additionally, the vertical red striped lines indicate the full orbit time, which are comptued based on the time of close approach time, subtracting the full orbit times as were shown in Table .

In Figure 8.1 and 8.2 it can be seen that there is a dip in the collision probability, where the threshold is reached. The manoeuvre times are then also within these dips, where it can be seen that the manoeuvre times are either at the beginning or at the end of the dip, indicating that the optimization searches for the manoeuvres that are at the threshold to avoid a higher cost. Looking at the relative distances in RIC direction, this is also at manoeuvre times at which these distances are smaller compared to earlier manoeuvre times which will cost more.

Comparing these two figures, it can be seen that the displacements are also about twice the amount for an impulse of 0.02 m/s compared to an impulse of 0.01 m/s. This also comes back in the collision probability, where the amplitude is about twice as large for the impulse of 0.02 m/s compared to an impulse of 0.01 m/s. For the larger ΔV of 0.02 m/s, it can also be seen that the dip in collision probability moves back to a later time of manoeuvre, closer to the time of closest approach.

8.2.2. CDM2

Moving on to the second CDM, the optimized manoeuvre results can be seen in Table 8.6 and 8.7. Table 8.6 again shows the collision probability, ΔV magnitude, displacement and time of manoeuvre for both satellites resulting from the optimization. Table 8.7 gives a more detailed overview of that the ΔV is in the RIC directions as well as the cost that is related to these results.

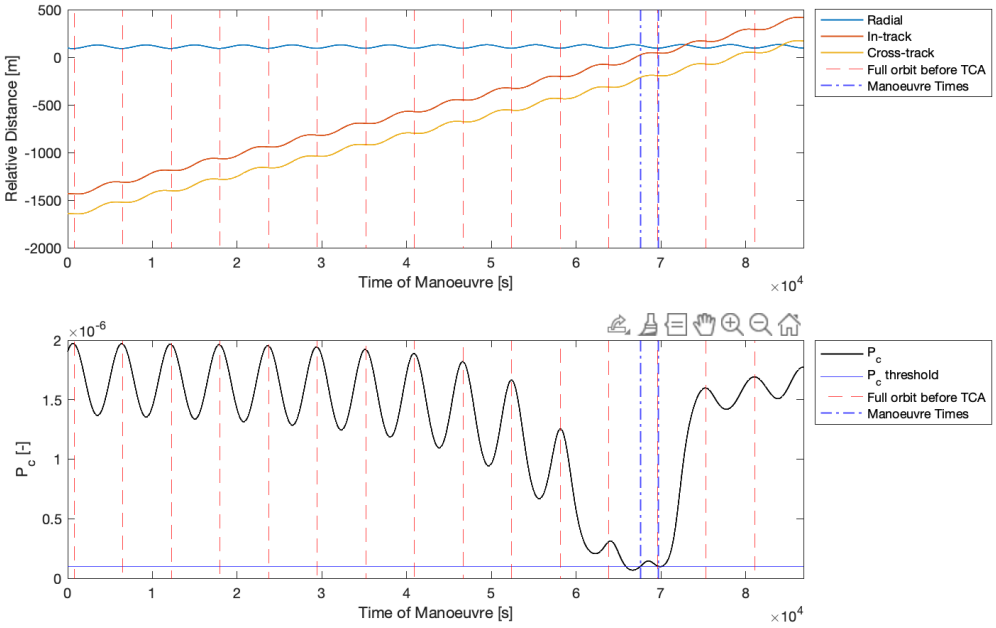

Figure 8.1: Relative RIC position and collision probabilities for a manoeuvre of ΔV_{I2} 0.01 m/s per simulation second for CDM 1

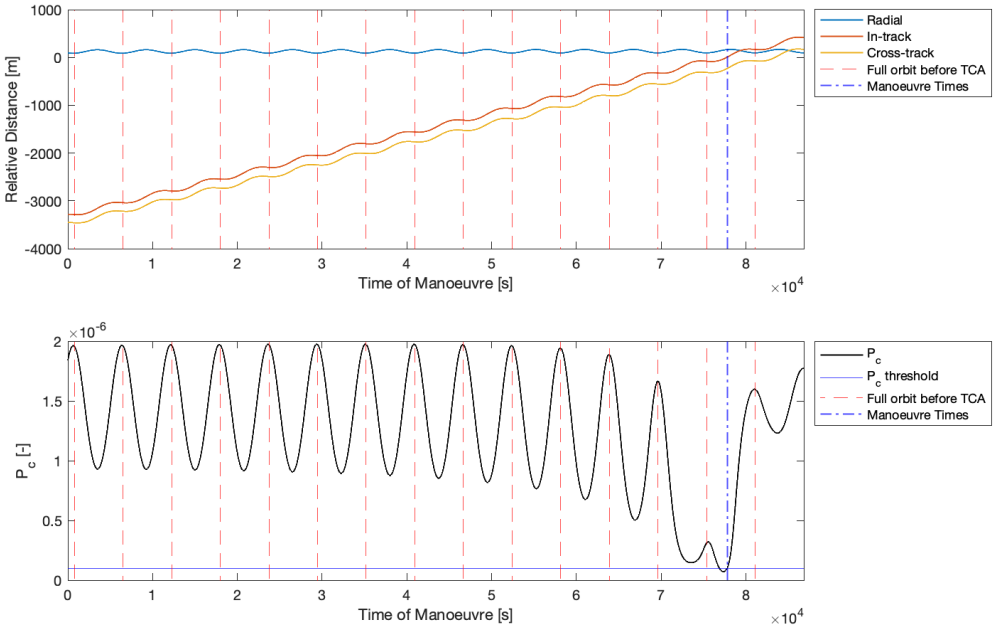

Figure 8.2: Relative RIC position and collision probabilities for a manoeuvre of ΔV_{I2} 0.02 m/s per simulation second for CDM 1

Table 8.6: Simulation results for scenario 1, CDM2

Result #	Pc [-]	ΔV_1 [m/s]	ΔV_2 [m/s]	ΔI_1 [m]	ΔI_2 [m]	ΔC_1 [m]	ΔC_2 [m]	t_1 [s]	t_2 [s]
1	$9.992 \cdot 10^{-8}$	0.01	0.01	36.9	476.2	0	0.7	84693	71769
2	$9.993 \cdot 10^{-8}$	0.01	0.01	37	476.1	0	0.7	84691	71771
3	$9.996 \cdot 10^{-8}$	0.01	0.02	53.6	500.6	0	0.8	84419	78316

Table 8.7: Detailed simulation results for scenario 1, CDM2

Result #	ΔV_{R1} [m/s]	ΔV_{R2} [m/s]	ΔV_{I1} [m/s]	ΔV_{I2} [m/s]	ΔV_{C1} [m/s]	ΔV_{C2} [m/s]	t_1 [s]	t_2 [s]	Cost [-]
1	0	0	0.01	0.01	0	0	84693	71769	2513.8
2	0	0	0.01	0.01	0	0	84691	71771	2513.8
3	0	0	0.01	0.02	0	0	84419	78316	3555.0

As mentioned before, multiple results are found. What can be seen here is that instead of one satellite moving, as was seen for the first CDM, both satellites need to move for the minimum cost. Again, the impulse magnitudes are at the minimum impulse bit of 0.01 m/s, where only for the third result an impulse magnitude of 0.02 m/s is seen for the secondary satellite only. It can also be seen that these results differ from CDM1, which is the earlier notification of CDM2 for the same conjunction event.

This table also shows that the manoeuvre results in a larger displacement for the secondary satellite compared to the primary satellite. This can be explained by the earlier manoeuvre time of the secondary satellite. The manoeuvre time of the primary satellite close to TCA (at 86820 seconds as was seen in Table 8.3), then results in a smaller displacement in the in-track direction. Again a small displacement in the cross-track direction is found.

Table 8.7 again shows a more detailed result overview for the ΔV in the different directions as well as the cost of the manoeuvres that resulted from the optimization. This table shows that all manoeuvres are done in the in-track direction, as was also found for the first CDM, except in this case this goes for both satellites. What can also be seen in this table, when looking at the cost, is that the first and the second result have the same cost. This also results from looking at the displacements in Table 8.6 when adding the displacement values. Again, a larger cost is seen for the third option, where the manoeuvre requires more ΔV.

The same graphs as shown above for the first CDM were made for this CDM, however, as the manoeuvre is done by two different satellites at different manoeuvre times, only the manoeuvre of one of the satellites can be shown on one plot. Figure 8.3 shows the manoeuvre of the primary satellite in the in-track direction. It can be seen here that the threshold of the collision probability is not met. The same goes for Figure 8.4, which shows the manoeuvre of the secondary satellite in the in-track direction. Again, the collision probability threshold is not met. Combining these two impulses however does seem to be passing the collision probability threshold, as is seen in the results.

Comparing the results of CDM1 with CDM2, it can be seen that the manoeuvre cost increased because of the double ΔV that needs to be expelled instead of the single satellite manoeuvre. It was also seen that the manoeuvre with only one satellite as in Figure 8.3 and 8.4 would not suffice in this CDM, compared to the result as seen in CDM1. The time of manoeuvre as well as the displacement are therefore also not similar.

8.2.3. CDM23

Continuing with the third CDM, the results can be seen in Table 8.8 and 8.8. Just as for the previous two CDMs, Table 8.8 shows the collision probability, manoeuvre magnitude and displacement for both satellites, as well as the manoeuvre time for both satellites. Table 8.8 then shows the manoeuvre magnitude in the different directions as well as the cost related to the manoeuvre as a result from the cost function of the optimization.

For this CDM again three different results are given, where two of the three have an impulse of the primary satellite and the third result given an impulse for the secondary satellite as can be seen in Table 8.8. It can also be seen here that the displacement of the satellite is in the in-track direction, where the magnitude is smaller in the first result compared to the second and third result. The manoeuvre time however for the first result is also closer to TCA than the second and third result.

Table 8.9 gives a more detailed overview of the result, where it can be seen that, as was also the case for the previous CDMs, the manoeuvre needs to be done in the in-track direction. As the absolute magnitude of

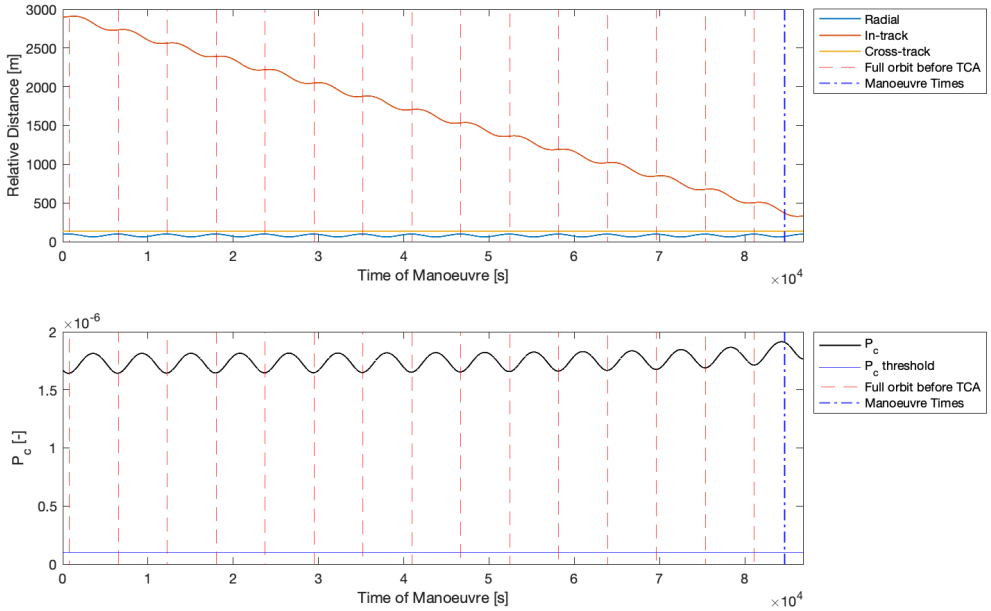

Figure 8.3: Relative RIC position and collision probabilities for a manoeuvre of ΔV_{I1} 0.01 m/s per simulation second for CDM 2

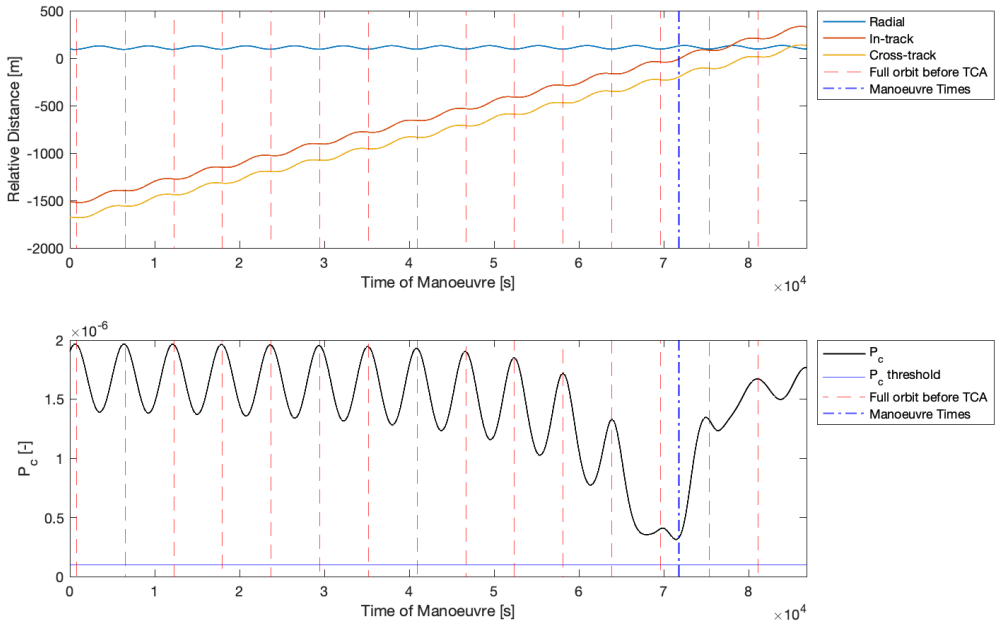

Figure 8.4: Relative RIC position and collision probabilities for a manoeuvre of ΔV_{I2} 0.01 m/s per simulation second for CDM 2

Table 8.8: Simulation results for scenario 1, CDM23

Result #	Pc [-]	ΔV_1 [m/s]	ΔV_2 [m/s]	ΔI_1 [m]	ΔI_2 [m]	ΔC_1 [m]	ΔC_2 [m]	t_1 [s]	t_2 [s]
1	$9.915 \cdot 10^{-8}$	0.01	0	78.4	0	0	0	83196	0
2	$9.998 \cdot 10^{-8}$	0.01	0	362.9	0	0.1	0	72659	0
3	$9.971 \cdot 10^{-8}$	0	0.01	0	440	0	0.4	0	71481

Table 8.9: Detailed simulation results for scenario 1, CDM23

Result #	ΔV_{R1} [m/s]	ΔV_{R2} [m/s]	ΔV_{I1} [m/s]	ΔV_{I2} [m/s]	ΔV_{C1} [m/s]	ΔV_{C2} [m/s]	t_1 [s]	t_2 [s]	Cost [-]
1	0	0	-0.01	0	0	0	83196	0	1078.4
2	0	0	-0.01	0	0	0	72659	0	1363.0
3	0	0	0	0.01	0	0	0	71481	1440.4

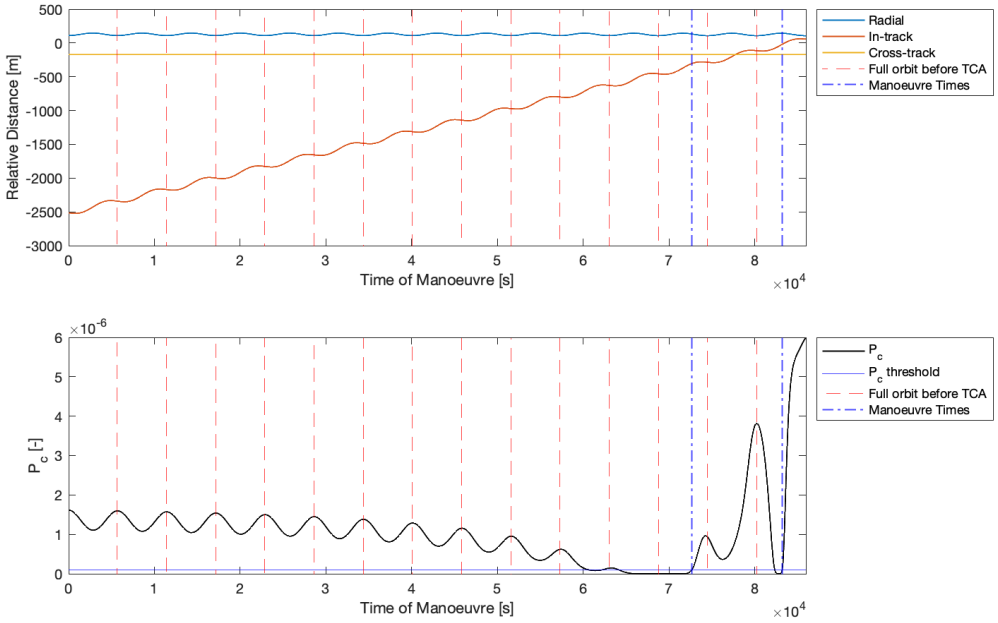

Figure 8.5: Relative RIC position and collision probabilities for a manoeuvre of ΔV_{I1} -0.01 m/s per simulation second for CDM 23

the ΔVs does not differ, it can also be seen that the costs are close to each other. The difference in the cost result because of the time of manoeuvre and the respective displacement that follows.

Figure 8.5 and 8.6 show the relative distances and collision probability for manoeuvre times from t_0 to TCA as was also done for the previous two CDMs. Figure 8.5 shows the manoeuvre times for a ΔV of -0.01 m/s in the in-track direction, where is can be see that there are three time periods where the collision probability threshold is reached. Here it is also seen again that the manoeuvre result is more towards the right end side of the period in which this threshold is reached.

Figure 8.6 shows the manoeuvre of the secondary satellite with a ΔV of 0.01 m/s. A comparable graph is seen for the collision probability as the first graph, where the result is that the manoeuvre happens at the right side of this period with the lower relative distance, resulting in a lower cost.

8.3. Scenario 2

In the second scenario the other technical aspect of the manoeuvre is assessed, being the displacement from the original location at TCA after a manoeuvre is performed at a certain instance of time. As there was a penalty for the displacement crossing the station keeping box boundary, which was set to 35 km, this distance is assessed using the outcome of what was found in the previous scenario. The displacement that is then allowed in this box, where it is assumed as was discussed in Chapter 4 that the satellite resides in the middle of this box at TCA, is 17.5 km.

Where the previous section showed the relative distances between the two satellites, this section will show the in-track and cross-track distance between the TCA location and the location of the satellite after manoeuvre.

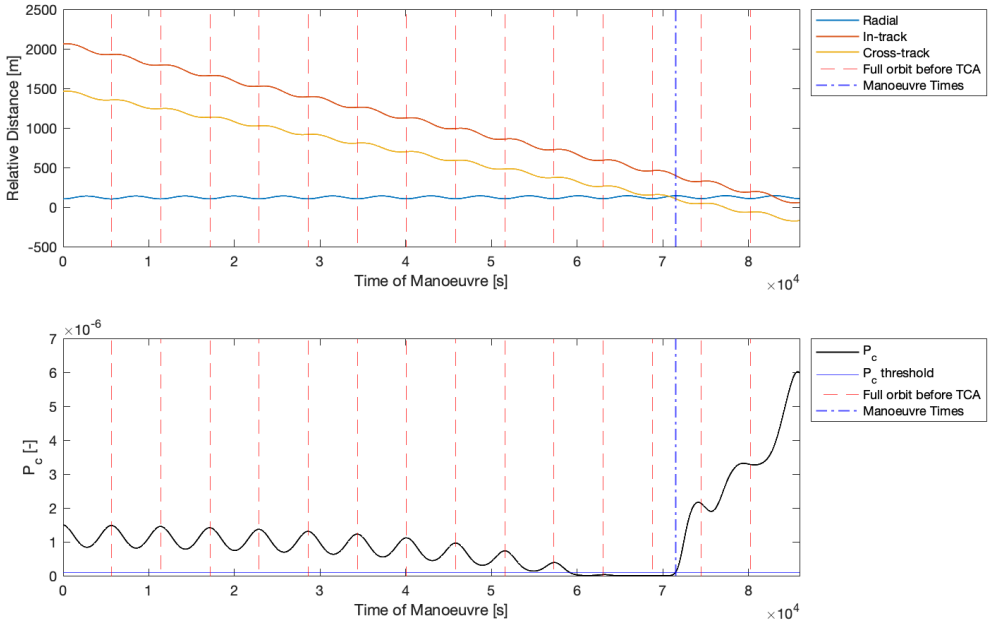

Figure 8.6: Relative RIC position and collision probabilities for a manoeuvre of ΔV_{I2} 0.01 m/s per simulation second for CDM 23

8.3.1. CDM1

For the first CDM, these results can be seen in Figure 8.7, where the displacement as well as the collision probability is seen for a ΔV of 0.01 m/s at all time steps.

From Figure 8.7 it can be seen that the absolute displacement in the in-track direction is significantly larger than the cross-track displacement. This can be expected though, as the manoeuvre is performed in the in-track direction and the minimization is done to limit the cross-track displacement.

In terms of the maximum displacement after which a penalty is added, which is 17.5 km, it can be seen that the manoeuvres with a ΔV of 0.01 m/s will not lead to a penalty throughout this simulation time. As the collision probability does not cross the threshold under which it needs to be, the elimination penalty of the collision probability is the one that will dominate the cost weighing. Additionally, the displacement in the cross-track direction does not get larger than 4 m.

Looking at the absolute values of the displacements over the complete simulation time, the values get lower the closer to TCA the manoeuvre is performed. This is something that can be expected, as the displacement can eventually be simplified to velocity times delta time. The earlier the manoeuvre is performed, the larger the displacement will then be.

Figure 8.8 shows the displacement for a ΔV of 0.1 m/s for comparison. This manoeuvre impulse is done for the same satellite in the same direction, being the secondary satellite and the in-track direction respectively. It can be seen that the displacement magnitude is also about 10 times bigger. With this higher value of the ΔV it can be seen that the penalty value for the displacement is reached at manoeuvre times up to 10 orbits before TCA. In this time where the threshold is passed, the penalty function for the displacement would come into play, as the collision probability passes the threshold below which it should be at every half orbit manoeuvre. The collision probability stays below this threshold for manoeuvres at every half orbit until TCA, meaning that the optimization converges to values that are close to TCA and where the collision probability passes the threshold.

The cost of this can be seen in Figure 8.9, where the figure on the left shows the cost at every time step and the figure on the right zooms in on the bottom part of the graph up to a cost of $1{\cdot}10^4$. Here it is seen that the dips of the collision probability result in a low cost, where penalty for the displacement is the main determining factor in the cost. The downward slant follows the penalty the lowering of the displacement for later manoeuvre times, where the quadratic penalty is observed starting close to 3000 seconds of the simulation. Looking back at the first graph in Figure 8.8, this is also where the 17.5 km threshold is passed and where the penalty function for the displacement ends.

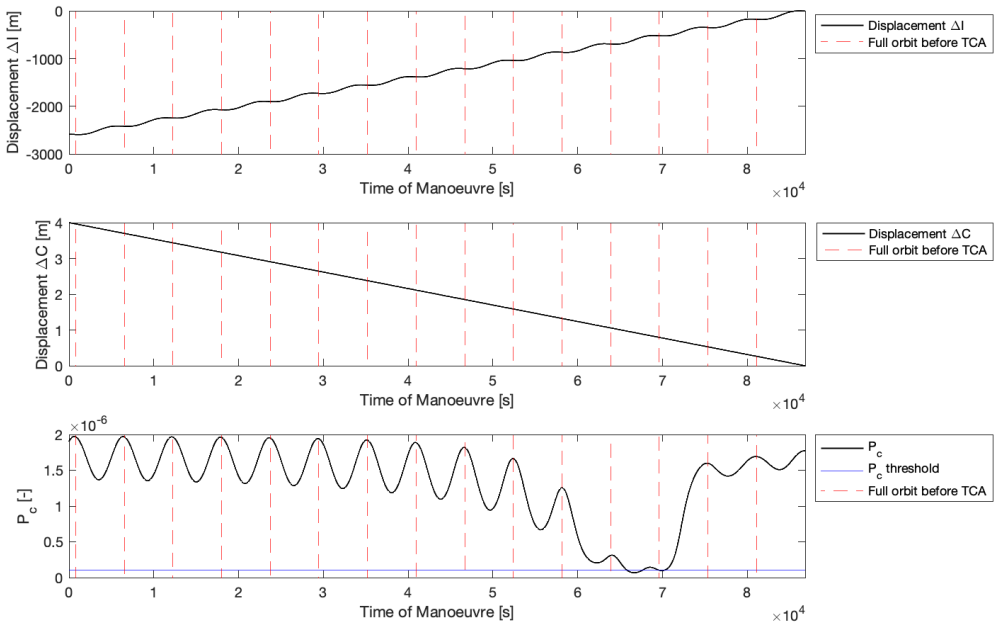

Figure 8.7: In-track and cross-track displacement and collision probabilities for a manoeuvre of ΔV_{I2} 0.01 m/s per simulation second for scenario 2, CDM1

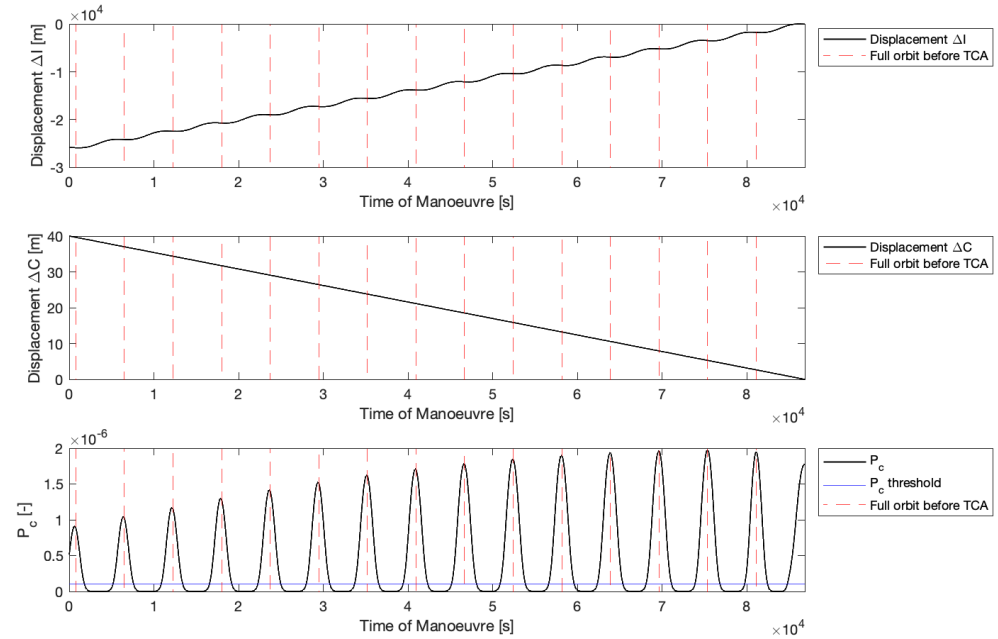

Figure 8.8: In-track and cross-track displacement and collision probabilities for a manoeuvre of ΔV_{I2} 0.1 m/s per simulation second for scenario 2, CDM1

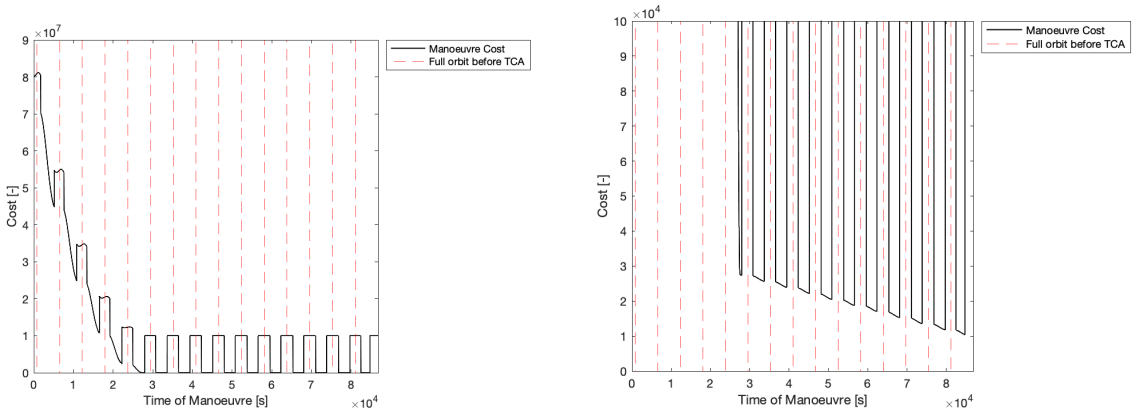

Figure 8.9: left: Cost for a manoeuvre of ΔV_{I2} 0.1 m/s per simulation second for scenario 2, CDM1 - right: Zoomed in cost up to $1{\cdot}10^4$ for all simulation seconds.

8.3.2. CDM2

The same analysis is done for the second CDM, which is the one where a manoeuvre for both satellites was seen as minimum. As mentioned in the previous scenario, the two ΔVs can only be shown separately as the optimum is a combination of two different manoeuvre times. Figure 8.10 shows the displacement in the in-track and cross-track direction of the primary satellite for a ΔV of 0.01 m/s. Similar as for the first CDM, the in-track displacement does not cross the threshold of 17.5 km and therefore no additional penalty is included in the cost. The collision probability on the other hand is also not crossing the threshold, meaning that the elimination penalty for the collision probability weighs more than the displacement if it were to pass the threshold of 17.5 km. Figure 8.11 shows the displacement in the in-track and cross-track direction for the secondary satellite, also with a ΔV of 0.01 m/s in the in-track direction. Just as for the primary satellite, the displacement does not reach 17.5 km, meaning that no additional penalty is taken into account and the collision probability also does not pass the threshold, which would outweigh the displacement in terms of cost.

Figure 8.12 and 8.13 show what were to happen to the displacements if the manoeuvres would have a ΔV of 0.1 m/s, ten times higher than the found minimum. The manoeuvre of the primary satellite (Figure 8.12) now passes the assumed station keeping boundary of 17.5 km. However, as the collision probability threshold is not met, this does not have an impact on the total cost as it will be outweighed by the elimination penalty of the collision probability. Something different is seen in Figure 8.13, where the displacement of the secondary satellite passes the 17.5 km and the collision probability is low enough at half orbit manoeuvres from the start of the simulation. This will then give the same cost development as was seen in Figure 8.9 and **??**

Again comparing the results of the first CDM with this CDM, it can be seen that the results differ. However, when looking at the ΔV_{I2} of 0.1 m/s, it can be seen that the collision probability threshold is passed for both CDMs (Figure 8.8 and 8.13. The cost is then however ten times larger than in the case of the minimum found for the first CDM and five times as large as the minimum found for the second CDM.

8.3.3. CDM23

The last CDM is also analyzed in the same way, where the displacement in the in-track and cross-track direction can be seen in Figure 8.14. The ΔV that was found for this CDM to be the minimum cost is 0.01 m/s in the negative in-track direction (meaning backward). Here again the magnitude of 0.01 m/s does not result in a higher penalty for the displacement. The cross-track displacement is lower than was seen in the previous cases.

Figure 8.15 shows an increased result, where the manoeuvre magnitude is increased to 0.1 m/s in the negative in-track direction. Here it can again be seen that the station keeping box penalty threshold is passed at 17.5 km up to about 10 orbits before TCA. The collision probability is not passing the threshold yet though as can be seen in the third graph of Figure 8.15. This threshold is only passed after about 3000 seconds of the simulation, which is different than what was seen above where this threshold was passed from the start of the simulation. This threshold is again passed at manoeuvres initiated every half orbit.

Figure 8.16 shows the development of the cost for the case in which a ΔV of -0.1 m/s in the in-track di-

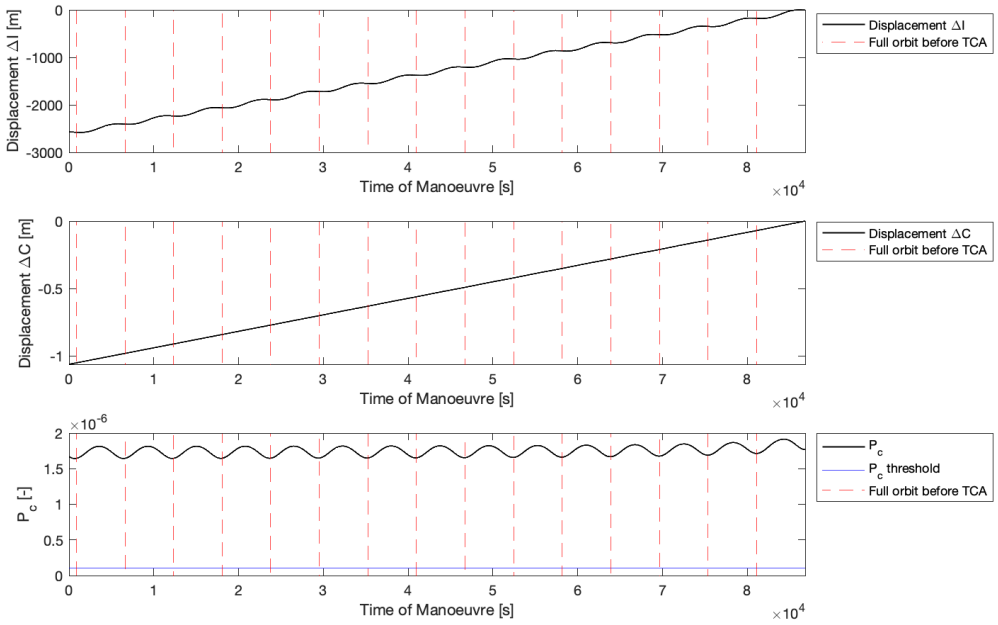

Figure 8.10: In-track and cross-track displacement and collision probabilities for a manoeuvre of ΔV_{I1} 0.01 m/s per simulation second for scenario 2, CDM2

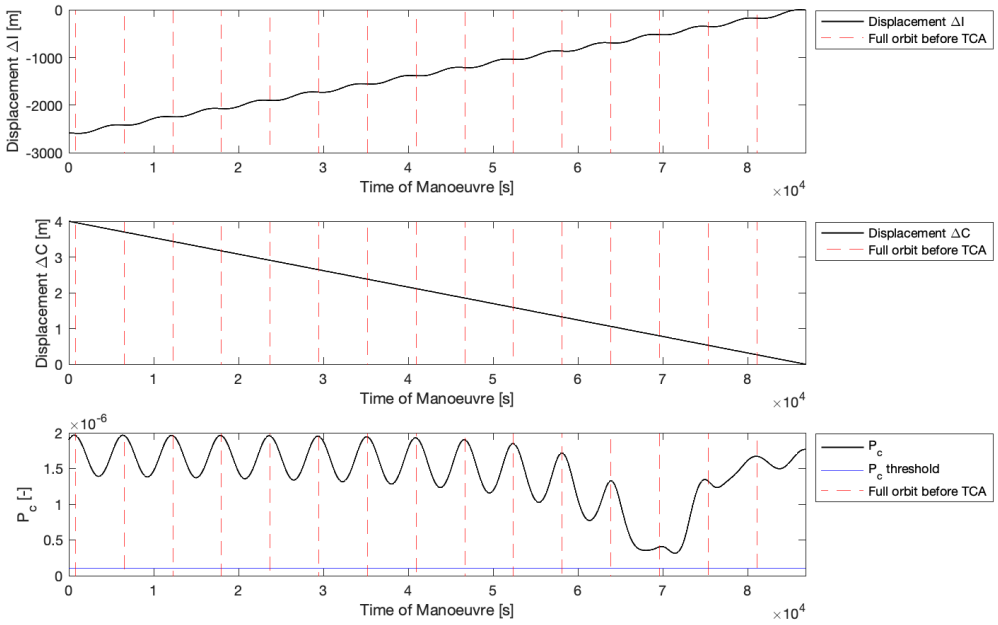

Figure 8.11: In-track and cross-track displacement and collision probabilities for a manoeuvre of ΔV_{I2} 0.01 m/s per simulation second for scenario 2, CDM2

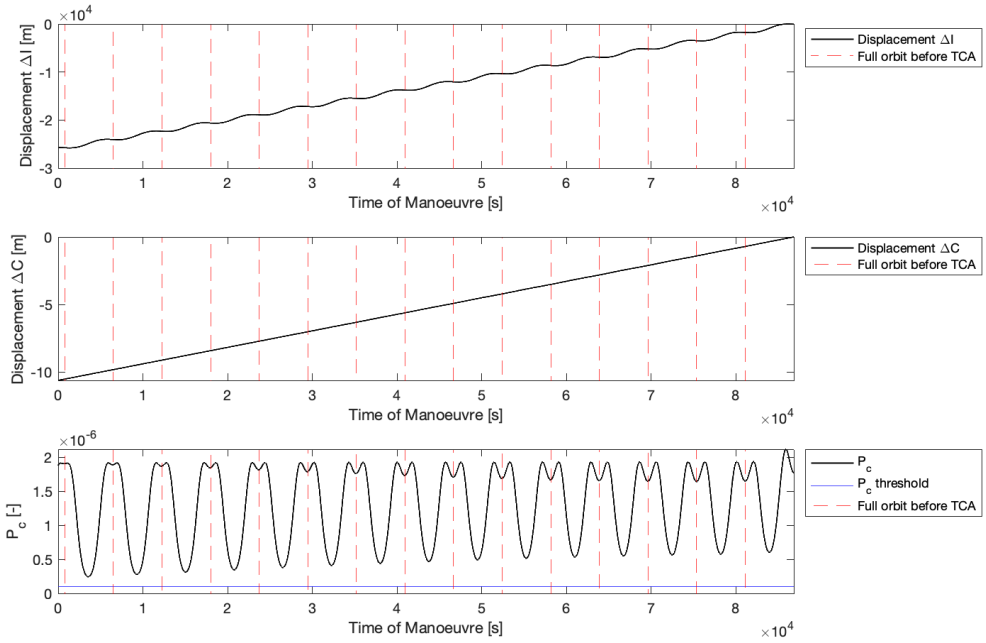

Figure 8.12: In-track and cross-track displacement and collision probabilities for a manoeuvre of ΔV_{I1} 0.1 m/s per simulation second for scenario 2, CDM2

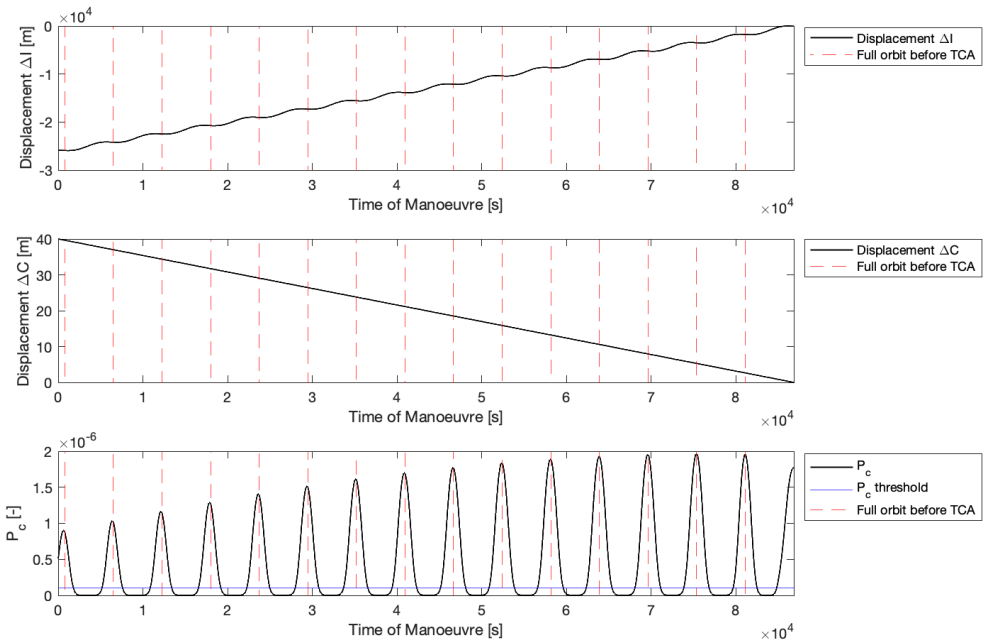

Figure 8.13: In-track and cross-track displacement and collision probabilities for a manoeuvre of ΔV_{I2} 0.1 m/s per simulation second for scenario 2, CDM2

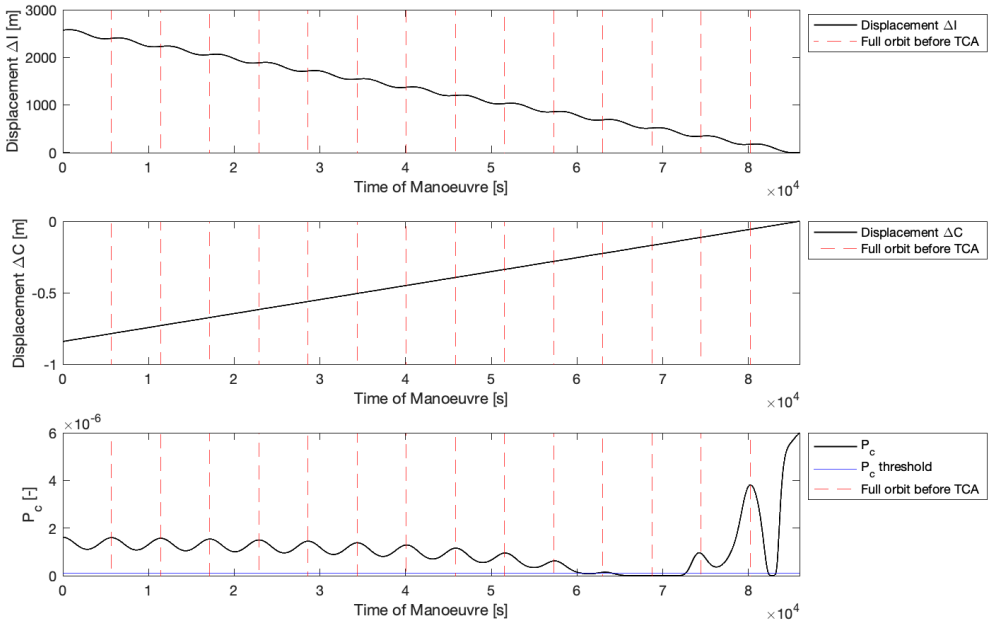

Figure 8.14: In-track and cross-track displacement and collision probabilities for a manoeuvre of ΔV_{I1} -0.01 m/s per simulation second for scenario 2, CDM23

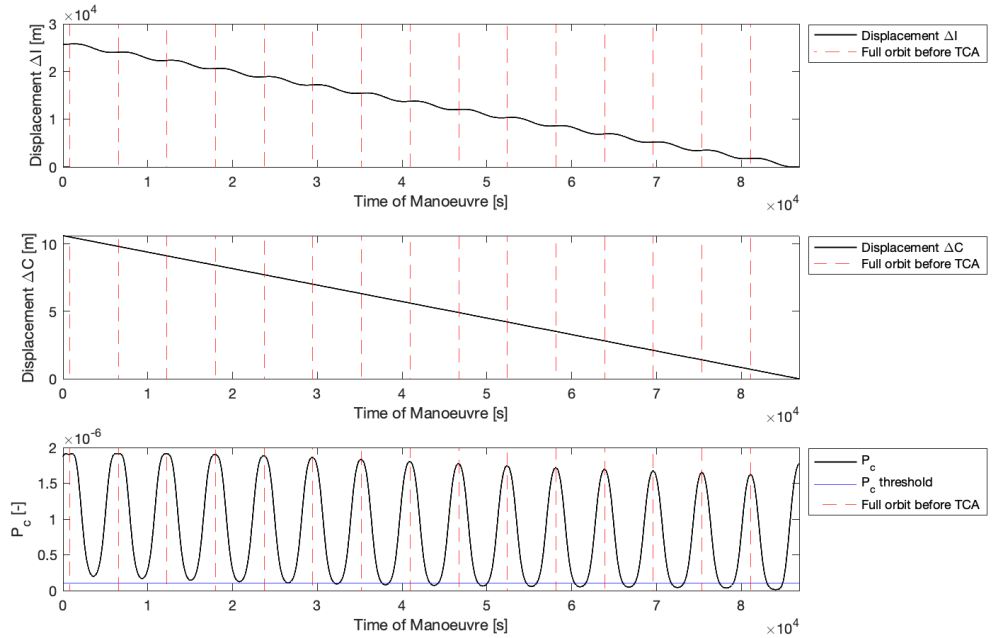

Figure 8.15: In-track and cross-track displacement and collision probabilities for a manoeuvre of ΔV_{I1} -0.1 m/s per simulation second for scenario 2, CDM23

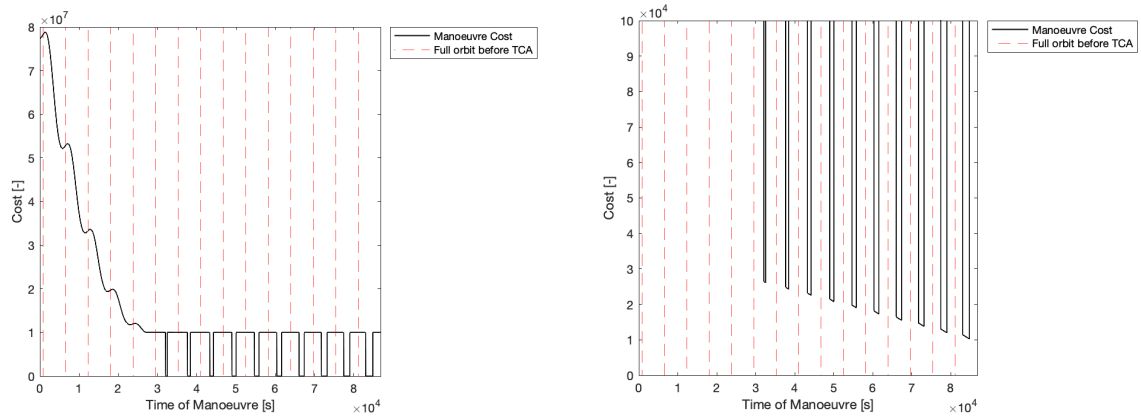

Figure 8.16: left: Cost for a manoeuvre of ΔV_{I1} -0.1 m/s per simulation second for scenario 2, CDM23 - right: Zoomed in cost up to $1{\cdot}10^4$ for all simulation seconds.

rection is performed, where the figure on the right is zoomed in on the lower part of the graph up to $1{\cdot}10^4$ for all simulation seconds. It can be seen here that from the beginning of the simulation up to about 3000 seconds of the simulation is an exponential curve with values ranging up to about $8{\cdot}10^7$. This is the result of a combined penalty, where the elimination penalty is the most prominent because of the collision probability not reaching the threshold and the added penalty is for the displacement being larger and resulting in an exponential penalty. After about 3000 seconds, the collision probability passes the threshold, leading to lower cost values. The zoomed in figure then also shows the somewhat linear decrease in displacement and therefore penalty when getting closer to the TCA.

8.4. Scenario 3

In the third scenario, the weight of the satellites can be changed to see if the manoeuvre can be divided between the two satellites or if the manoeuvre can be pushed to the other satellite. In the case of the first CDM, the manoeuvre is performed by the secondary satellite, where it can be analyzed if the manoeuvre can be split between the two or if the manoeuvre can be pushed to the primary satellite. The opposite holds for the third CDM, where the primary satellite needs to manoeuvre for the minimum cost. It can therefore be analyzed if the manoeuvre can be divided with the secondary satellite or maybe even pushed to the secondary satellite altogether. In the second CDM the minimum required both satellites to manoeuvre. By adding weights per satellite in this scenario it can be analyzed if one satellite can manoeuvre more or if the manoeuvre can be done by one of the two satellites.

As was also seen in Section 7.3, the weight of ΔV can be changed. In Table 7.4 showed the results of the cost as well as the displacements and resulting ΔV when the weight was increased.

$$J = P_c + w_1(1 \cdot 10^5 \Delta V_1 + \Delta I_1 + \Delta C_1) + w_2(1 \cdot 10^5 \Delta V_1 + \Delta I_1 + \Delta C_1) \tag{8.2}$$

The cost function with weights per satellite, including the ΔV weights is seen in Equation 8.2. Looking at this cost function, which needs to be minimized, it can be seen that if either one of the weight is increased, that the preference for movement goes to the satellite that had the least weight. The 3 CDMs will be analyzed with different weights for w_1 and w_2 (2, 5 and 10), where the weight is increased for the satellite that does not need to move according the results of the minimum cost.

It was found that all resulting manoeuvres with weight, just as found in scenario 1, need to be performed in the in-track direction. Therefore, it was chosen to only give these numbers and leave out the radial and cross-track ΔV. Additionally, again multiple results were found, where it was chosen to only show the most occurring results from the simulations.

8.4.1. CDM1

Table 8.10 and 8.11 show the manoeuvre results of the first CDM with increased weights. The weight of the second satellite is increased to move the manoeuvre to the primary satellite. It can be seen here that the weight of 2 for the secondary satellite does not change the result, compared to the result in Table 8.4. The

Table 8.10: Manoeuvre results for an increasing weight for w_2, scenario 3, CDM1 (1)

Weight Sat 1	Weight Sat 2	ΔV_{I1} [m/s]	ΔV_{I2} [m/s]	t_1 [s]	t_2 [s]	Cost [-]
1	2	0	0.01	0	69717	3041.2
1	5	-0.07	0	84325	0	7418
1	10	-0.07	0	84325	0	7418

Table 8.11: Manoeuvre results for an increasing weight for w_2, scenario 3, CDM1 (2)

Weight Sat 1	Weight Sat 2	Pc	ΔI_1	ΔI_2	ΔC_1	ΔC_2
1	2	$9.985 \cdot 10^{-8}$	0	519.8	0	0.8
1	5	$9.992 \cdot 10^{-8}$	417.8	0	0.2	0
1	10	$9.992 \cdot 10^{-8}$	417.8	0	0.2	0

weight of 5 however flips the manoeuvre to the primary satellite. It can also be seen that this manoeuvre magnitude is larger than the required magnitude if the secondary satellite were to manoeuvre, which is in this case 0.07 m/s compared to 0.01 m/s. The cost also increases with this increase in ΔV magnitude.

Continuing to Table 8.11, it can be seen that the displacement as a result of the manoeuvre is not that different from the result in scenario 1. The in-track displacement of the primary satellite, when the manoeuvre is done by the primary satellite, is even about 100 meters less than when the manoeuvre is performed by the secondary satellite. The ΔV expenditure however is the main driver of the total cost, which therefore results in the higher cost for this option of the primary satellite manoeuvring.

8.4.2. CDM2

Moving on the second CDM, where both satellites needed to manoeuvre for the minimum cost, the results with weights can be seen in Figure 8.12 and 8.13. Because both satellites needed to manoeuvre, the weight analysis was done for both satellites, where for both satellites the weights were increased. It was also observed here that multiple results with the same total cost were found. These are also given in the tables.

Looking at Table 8.12 it can be seen that the weight of 2 for the primary satellite barely changes the outcome of the minimization, except for the time of manoeuvre. With a weight of 5 and 10 for the primary satellite the manoeuvre is pushed to the second satellite, where an increase is seen in the ΔV that is needed to lower the collision probability to the threshold of $1 \cdot 10^{-7}$. It can also be seen here that there is no difference between a weight of 5 and 10, but that the weight of 2 for the primary satellite is not enough to push the manoeuvre completely to the secondary satellite.

For the weight of the secondary satellites it can be seen that the weight of 2 for the secondary satellite does not move the manoeuvre to the primary satellite. It does however change the result to be in the negative direction compared to the initial minimum that was found (Table 8.6). Also because of the weights, more results are found with the same total cost, which is seen here in the case of a weight of 2 and 5. With the weight of 10 the manoeuvre is performed by the primary satellite, where the magnitude also increases significantly to (absolute) 0.08 m/s.

Table 8.12: Manoeuvre results for an increasing weight for w_1 and w_2, scenario 3, CDM2 (1)

Weight Sat 1	Weight Sat 2	ΔV_{I1} [m/s]	ΔV_{I2} [m/s]	t_2 [s]	Cost [-]	Cost [-]
2	1	0.01	0.01	84798	71626	3547.4
5	1	0	0.05	0	83650	5534.1
10	1	0	0.05	0	83650	5534.1
1	2	-0.01	-0.01	72548	84026	3583.4
1	2	-0.01	-0.01	72536	84032	3583.4
1	5	-0.01	-0.01	72453	84060	6820.1
1	5	-0.01	-0.01	72439	84063	6820.1
1	10	-0.08	0	84495	0	8390.3

Table 8.13: Manoeuvre results for an increasing weight for w_1 and w_2, scenario 3, CDM2 (2)

Weight Sat 1	Weight Sat 2	Pc	ΔI_1	ΔI_2	ΔC_1	ΔC_2
2	1	$9.998 \cdot 10^{-8}$	31.1	484.5	0	0.7
5	1	$9.999 \cdot 10^{-8}$	0	533.4	0	0.7
10	1	$9.999 \cdot 10^{-8}$	0	533.4	0	0.7
1	2	$9.994 \cdot 10^{-8}$	421.8	80.6	0.2	0.1
1	2	$9.996 \cdot 10^{-8}$	422.6	80.2	0.2	0.1
1	5	$9.998 \cdot 10^{-8}$	428.4	78.2	0.2	0.1
1	5	$1.00 \cdot 10^{-7}$	429.4	78	0.2	0.1
1	10	$9.984 \cdot 10^{-8}$	390.1	0	0.2	0

Table 8.14: Manoeuvre results for an increasing weight for w_1, scenario 3, CDM23 (1)

Weight Sat 1	Weight Sat 2	ΔV_{I1} [m/s]	ΔV_{I2} [m/s]	t_1 [s]	t_2 [s]	Cost [-]
2	1	0	0.01	0	71481	1440.4
5	1	0	0.01	0	71481	1440.4
10	1	0	0.01	0	71481	1440.4

Continuing with Table 8.13 it can be seen that for the weight of 2 on the primary satellite causes the displacement to be a little more shifted to the secondary satellite compared to the result found in Table 8.6. Moving the manoeuvre to lower the collision probability to the secondary satellite then results in a somewhat larger displacement in the in-track direction. However, comparing this displacement with the expenditure of ΔV, it can be seen that the minimization moves towards the lower magnitude of combined total ΔV. The displacement in the cross-track direction is again, as was found before, close to negligible.

The added weight to the secondary satellite on the other hand shows that an absolute magnitude of 0.01 m/s moves the total displacement towards the primary satellite, where also a displacement of about 80 m is found for the secondary satellite. Moving on to the weight of 5, it can again be seen that the weight moves even more towards the primary satellite, although still both satellites have a ΔV for the minimum cost. With a weight of 10 for the secondary satellite the manoeuvre is completely done by the primary satellite and even though the magnitude is much larger than the previous found, the displacement of the primary satellite is lower. This is then the result of the main focus on minimizing the total ΔV expenditure.

Again comparing CDM1 and CDM2 it can be seen that for the highest weight for the secondary satellite the manoeuvre magnitude is becoming more similar. The higher weight for the primary satellite does not make the manoeuvre similar to the first CDM. Increasing the weights in the first CDM also does not seem to push it to a transition zone where both satellites need to manoeuvre.

8.4.3. CDM23

Going on with the last CDM, the results can be seen in Table 8.14 and 8.15. In Table 8.14 it can be seen that the weight on the primary satellite causes the manoeuvres to be moved to the secondary satellite, while the initial minimum that was found resulted in a manoeuvre of the primary satellite. It can also be seen here that the magnitude of the weight does not influence the result and the minimum cost, as the same results are found for all the added weights to the primary satellite.

Moving with Table 8.15, it can be seen that the resulting displacement logically stays the same for the different weights as well. The displacement in the cross-track direction is again close to negligible.

Table 8.15: Manoeuvre results for an increasing weight for w_1, scenario 3, CDM23 (2)

Weight sat 1	weight sat 2	Pc	ΔI_1	ΔI_2	ΔC_1	ΔC_2
2	1	$9.971 \cdot 10^{-8}$	0	440	0	0.4
5	1	$9.971 \cdot 10^{-8}$	0	440	0	0.4
10	1	$9.971 \cdot 10^{-8}$	0	440	0	0.4

Table 8.16: Manoeuvre results for an increasing weight for w_1 and w_2, scenario 3, CDM1 (3)

Weight sat 1	weight sat 2	ΔV_{I1} [m/s]	ΔV_{I2} [m/s]	t_1 [s]	t_2 [s]	Cost [-]
0.9	0.1	0	0.02	0	77774	257.6
0.75	0.25	0	0.01	0	69717	380.15
0.5	0.5	0	0.01	0	69717	760.3
0.25	0.75	-0.01	-0.01	71686	84856	1141.025
0.1	0.9	-0.07	0	84325	0	741.8

Table 8.17: Manoeuvre results for an increasing weight for w_1 and w_2, scenario 3, CDM1 (4)

Weight sat 1	weight sat 2	Pc	ΔI_1	ΔI_2	ΔC_1	ΔC_2
0.9	0.1	$9.991 \cdot 10^{-8}$	0	575.2	0	0.8
0.75	0.25	$9.985 \cdot 10^{-8}$	0	519.8	0	0.8
0.5	0.5	$9.99 \cdot 10^{-8}$	0	519.8	0	0.8
0.25	0.75	$1.00 \cdot 10^{-7}$	478.7	28.3	0.2	0.1
0.1	0.9	$9.992 \cdot 10^{-8}$	417.8	0	0.2	0

8.4.4. Alternative Weighing

Another way of dividing the weight of the satellites is by making the weights such that they are fractions and together add up to a value of 1.0. This was also done for the three CDMs, of which the results will be shown below. The weight distributions shown in these results are 0.9:0.1, 0.75:0.25, 0.5:0.5 and vice versa.

These results for the first CDM can be seen in Table 8.16 and 8.17. It can be seen that for the first distribution of 0.9:0.1 that the manoeuvre magnitude is double of what was found in scenario 1, where the displacement that results in the in-track direction is also larger than was found for the minimum in scenario 1. For the weight distribution of 0.75:0.25 it can be seen that the result is back to the minimum that was found in scenario 1, which also goes for the 0.5:0.5 results. This shows that this weight distribution also shifts the manoeuvre to the secondary satellite with a lower weight, where in the case of the 0.9:0.1 weight it looks like more emphasis is put on the manoeuvre magnitude and on time manoeuvre. Continuing with the 0.25:0.75 weight, it can be seen that the manoeuvre is shifting towards the primary satellite, where in this case a manoeuvre need to be performed by both satellites. This shift is also reflected in the displacement of the satellites, as the in-track displacement of the secondary satellite is smaller than it was for the first three weight distributions, but where it has not moved to the primary satellite completely. The last result found for the weight of 0.1:0.9, shows the same result again as in scenario 3 for this CDM, where the manoeuvre is shifted completely to the primary satellite, where also the displacement is then logically completely done by the primary satellite.

Moving on to the second CDM, of which the results can be seen in Table 8.18 and 8.19, comparable development of the results is seen. The first result with the higher weight on the primary satellite showed the same result as was found above for the higher weight on the primary satellite for the same CDM. This manoeuvre then also shows the similar displacement in the in-track direction of the secondary satellite. The next two weights for this CDM show a shift towards the manoeuvre magnitude and displacement of the primary satellite.

Looking at the weight distribution of 0.75:0.25 and comparing it with the next weight of 0.5:0.5, it can be seen that the magnitude is the same (as was also found for the minimum magnitude in scenario 1 for the second CDM), but that the manoeuvre time of the 0.75:0.25 weight is not the same as was found in scenario 1 but the weight of 0.5:0.5 is. This is then also reflected in the displacements that are found, where a shift from the displacement in the in-track direction of the secondary satellite shifts towards a displacement in the in-track direction of the primary satellite as the weight shifts towards the secondary satellite. This shift is then continued for the weight of 0.25:0.75, where still both satellites need to manoeuvre, but where the displacement is larger for the primary satellite. The last result that is found for the weight of 0.1:0.9 is then again the same as was found for the higher weight of the secondary satellite in scenario 3, with the displacement completely shifted towards the primary satellite.

The results of the last CDM with these weight distributions can be seen in Table 8.20 and 8.21. These results show that for the first two weight distributions the manoeuvre is done by the secondary satellite and for the last 3 weight distributions the manoeuvre is done by the primary satellite. Comparing this to the

Table 8.18: Manoeuvre results for an increasing weight for w_1 and w_2, scenario 3, CDM2 (3)

Weight sat 1	weight sat 2	ΔV_{I1} [m/s]	ΔV_{I2} [m/s]	t_1 [s]	t_2 [s]	Cost [-]
0.9	0.1	0	0.05	0	83650	553.41
0.75	0.25	0.01	0.01	84842	71518	1144.325
0.5	0.5	0.01	0.01	84691	71771	1256.9
0.25	0.75	-0.01	-0.01	72490	84050	1165.75
0.1	0.9	-0.08	0	84495	0	839.03

Table 8.19: Manoeuvre results for an increasing weight for w_1 and w_2, scenario 3, CDM2 (4)

Weight sat 1	weight sat 2	Pc	ΔI_1	ΔI_2	ΔC_1	ΔC_2
0.9	0.1	$9.999 \cdot 10^{-8}$	0	533.4	0	0.7
0.75	0.25	$9.994 \cdot 10^{-8}$	28.8	490.2	0	0.7
0.5	0.5	$9.993 \cdot 10^{-8}$	37	476.1	0	0.7
0.25	0.75	$9.998 \cdot 10^{-8}$	425.8	78.9	0.2	0.1
0.1	0.9	$9.984 \cdot 10^{-8}$	390.1	0	0.2	0

Table 8.20: Manoeuvre results for an increasing weight for w_1 and w_2, scenario 3, CDM23 (3)

Weight sat 1	weight sat 2	ΔV_{I1} [m/s]	ΔV_{I2} [m/s]	t_1 [s]	t_2 [s]	Cost [-]
0.9	0.1	0	0.01	0	71481	144.04
0.75	0.25	0	0.01	0	71481	360.1
0.5	0.5	-0.01	0	83196	0	539.2
0.25	0.75	-0.01	0	83196	0	269.6
0.1	0.9	-0.01	0	83196	0	107.84

Table 8.21: Manoeuvre results for an increasing weight for w_1 and w_2, scenario 3, CDM23 (4)

Weight sat 1	weight sat 2	Pc	ΔI_1	ΔI_2	ΔC_1	ΔC_2
0.9	0.1	$9.97 \cdot 10^{-8}$	0	440	0	0.4
0.75	0.25	$9.97 \cdot 10^{-8}$	0	440	0	0.4
0.5	0.5	$9.92 \cdot 10^{-8}$	78.4	0	0	0
0.25	0.75	$9.92 \cdot 10^{-8}$	78.4	0	0	0
0.1	0.9	$9.92 \cdot 10^{-8}$	78.4	0	0	0

results found for the previous two CDMs, there is no shift from one satellite to the other. The minimum as found in scenario 1 for this CDM is then also the result as is seen with weights of 0.5:0.5. The results found for these weights are then also the same results as were found above for this CDM, where a higher weight on the primary satellite shows a manoeuvre of the secondary satellite and the higher weight on the secondary satellite shows a manoeuvre of the primary satellite.

8.5. Final Remarks

Looking at these results altogether, a few summarizing remarks can be made regarding these results.

The first thing that is observed is that the minimum that is found in most cases just passes the collision probability threshold and has a minimum ΔV which is in this case the impulse bit that was assumed to be the minimum. As a result of this minimum impulse, the displacements that follow are also far below the station keeping box limit as was set with penalties.

The impulses that need to be performed are all found to be at the minimum if performed in the in-track direction. This goes for the general minima that were found, as well as for the minima that were found using the weights to add preference to one of the satellites. It is therefore that the displacements that are found are also dominating in the in-track direction. The cross-track displacement that follows is then left to a minimum, which is in some cases close to negligible.

For all the manoeuvres that were found, the timing of the manoeuvre showed also to be possible within about three orbits before TCA up to about half an orbit before TCA. It needs to be noted though that this is the case for the CDMs shown here, and that it is possible that different minima and manoeuvre times are found for other CDMs. For a more general conclusion it would therefore be needed to do more analyses, next to improving the information that is in these CDMs (will be discussed more in Chapter 11).

It was also found that it is possible to have a case in which both satellites need to manoeuvre for the minimum cost solution. Comparing this result to the case in which the manoeuvre is then shifted to one of the two satellites using weights, it was shown that the ΔV that is needed to perform this manoeuvre through one satellite only, is larger than was found for the minimum. The displacements in this case were still kept to a minimum, where it is also seen that the cumulative displacement has the same order of magnitude for one satellite as for the manoeuvre of both satellites for these CDMs.

It becomes clear that the results show to be case sensitive, meaning that it is difficult to make an early estimate of the manoeuvre that needs to be performed. This is seen from the different results found above, as well as the differences in the results of CDM1 and CDM2, which are reporting the same conjunction event.

What can be seen in all three cases though, is that the manoeuvre is performed in the in-track direction and that therefore the displacement is also in the in-track direction. Additionally, the manoeuvre can be performed close to TCA (close in this case being less than three orbits before TCA). However, when these manoeuvres need to be performed and at what exact time and magnitude, as well as direction (positive or negative in-track direction), are difficult to predict. Not only for the minimum result, but it was also seen that the manoeuvre 'windows' that result in an acceptable collision probability are not overlapping, making it difficult to give a more general solution.

9 Discussion

This chapter will discuss the results that were found in the previous chapter. It will follow the same order in which the results were found. Based on the sensitivity analysis of the covariance matrix for the different conjunction events, these discussed scaling factors will also shortly be discussed here and compared to the results that were found.

It was observed from the results of the first scenario that the manoeuvre mainly appears to happen in the in-track direction, where also the minimum impulse bit is seen as the manoeuvre magnitude. Additionally, it was found that the minimum manoeuvre magnitude could be achieved within about three orbits before TCA. From the second scenario it was seen that the displacements are mainly occuring in the in-track direction, where the outcome values do not reach the set boundary limit to activate the penalty function. The cross-track displacement does not appear to have a large value, which is also something that was not desired as was discussed earlier for the cost function. Last but not least it was found that the added weights to the cost function were able to determine tha manoeuvre magnitude as well as the satellite that needs to perform the manoeuvre in the third scenario.

9.1. Scenario 1

The first scenario investigated the effect of the ΔV limits on the optimized collision avoidance manoeuvre and the effects of this ΔV in terms of displacement and collision probability. The results that were found in Section 8.2 for the first CDM showed a manoeuvre of the secondary satellite in the in-track direction at about three orbits before TCA. With the setup of the cost function to minimize the expelled ΔV as much as possible and with that the cross-track displacement, this is also seen in the results. The minimum impulse bit magnitude is found for the ΔV expense. This is also in line with what was found in literature, where a single in-track velocity increment to avoid the collision consumes less fuel [11]. The difference with respect to this study, is that in this research the simulation is done with two satellites that are manoeuvrable, whereas the study analyses satellite - debris conjunctions. These parameters named above with the thresholds that are set define the input and output that are needed to answer the first research question on what input and output parameters are needed and what the effect of the constellation is on the manoeuvre optimization.

All minima found in the results are done in the in-track direction, which causes the cross-track displacement to be as small as possible. Additionally, if the manoeuvre would be done in the radial direction, the displacement in the cross-track direction becomes much larger as can be seen in Figure 9.1. The in-track displacement is lower for a radial manoeuvre than is found for the manoeuvre in the in-track direction, but as the magnitude of the cross-track direction needs to be kept as low as possible and the magnitude of the in-track displacement needs to stay within bounds, the preference goes out to keeping the cross-track displacement as small as possible. Even though the displacements are larger in the in-track direction, the collision probability does not reach the set threshold, meaning that a larger ΔV is needed if the manoeuvre needs to be performed in the radial direction. This gives an indication of the effect of the manoeuvre on the constallation satellites, which refers back to the first research question.

The next thing that can be observed from the results is that the relative distance does not need to be significantly larger than it is at TCA. The behavior of the relative distances is also what can be expected, where the manoeuvre in the in-track direction causes the in-track and cross-track distance to increase. A change in

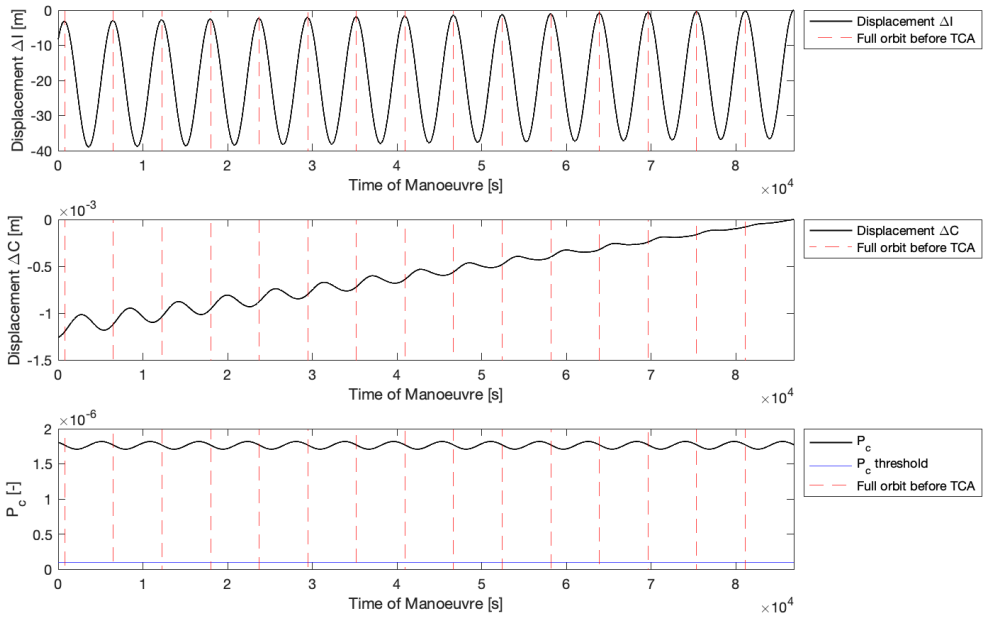

Figure 9.1: In-track and cross-track displacement and collision probabilities for a manoeuvre of ΔV_{R2} = 0.01 m/s per simulation second for scenario 1, CDM1

velocity in the in-track and cross-track plane will always change the relative distance and velocity, in this case the more time between TCA and the manoeuvre the larger the relative distance. It is then also expected that the earlier the manoeuvre is performed, the larger the relative distance becomes. As there is a larger Δt before TCA multiplied with the change in velocity, a distance increasing with Δt results. This is also observed in Figure 9.2, where the range at TCA is shown as a result of an impulse of 0.01 m/s in the in-track direction of the primary satellite.

What is also observed is orbital periodic motion of the satellite in the collision probability. This has to do with the position in the orbit at which the manoeuvre is performed, which is the same reason for the wave-like motion of the relative distances. As can be seen in Figure 8.1, the collision probability is higher when the manoeuvre is performed at full orbits compared to when the manoeuvre is performed at half orbits. This is also expected, as a manoeuvre in the in-track direction at half orbit positions causes the orbit to get larger at TCA. At the full orbit positions however, the range at TCA does not increase that much when the orbit reaches the same position in the orbit again.

Going back to the shape of the collision probability again, it can be seen that there is a dip in the collision probability if performed between the simulation time period just before 6000 seconds and just after 7000 seconds. Looking at the relative distances and the range, it does not seem that this is a direct cause of this dip. Diving into the code and formulas, it was found that this dip happens in the collision probability formula. This collision probability calculation is started with the transformation to the B-plane, as was explained in Section 3.2.2, by using a transformation matrix that is made up from the unit vectors of the relative position and relative velocity of the two satellites at TCA.

The values in this transformation matrix are shown in the top figure of Figure 9.3, which is the first CDM simulation with a manoeuvre magnitude of 0.01 m/s of the secondary satellite in the in-track direction (as was found from the minimization in scenario 1). Looking carefully at the similarities between the values of this transformation and the collision probability results, it can be seen that this dip starts where the $X_B(2)$ and $Y_B(2)$ trend cross each other. Similarly, the dip ends where the trends of $X_B(1)$ and $Y_B(1)$ cross. This indicates that the geometry between the two satellite changes at TCA with respect to each other, as the unit vectors determine these values of the transformation matrix. The green trend will be discussed below.

The same is seen for the results with a magnitude of 0.02 m/s of the secondary satellite in the in-track direction manoeuvre, which is shown in Figure 9.4. Here the same is observed, where the dip starts just after 7000 simulation seconds and ends at just before 8000 seconds. Looking at the values of the transformation

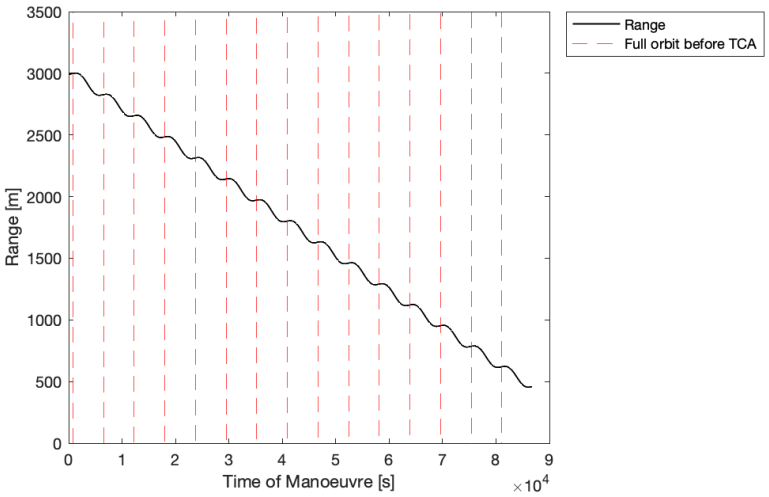

Figure 9.2: Range at TCA between primary and secondary satellite for a manoeuvre of $\Delta V_{I2} = 0.01$ m/s per simulation second for scenario 1, CDM1

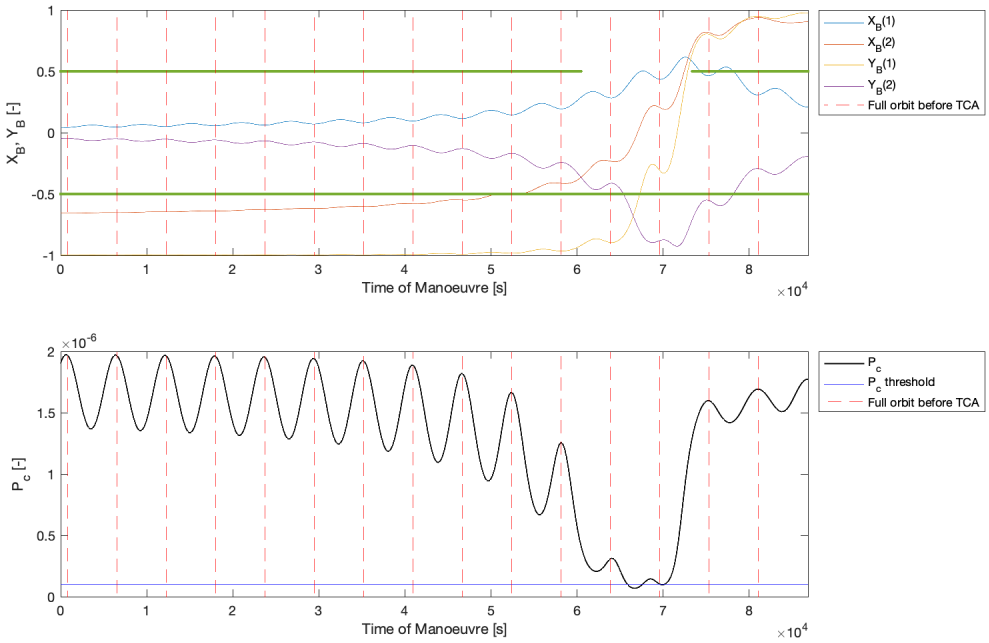

Figure 9.3: X_B and Y_B vector values for $\Delta V_{I2} = 0.01$ m/s per simulation second for scenario 1, CDM1

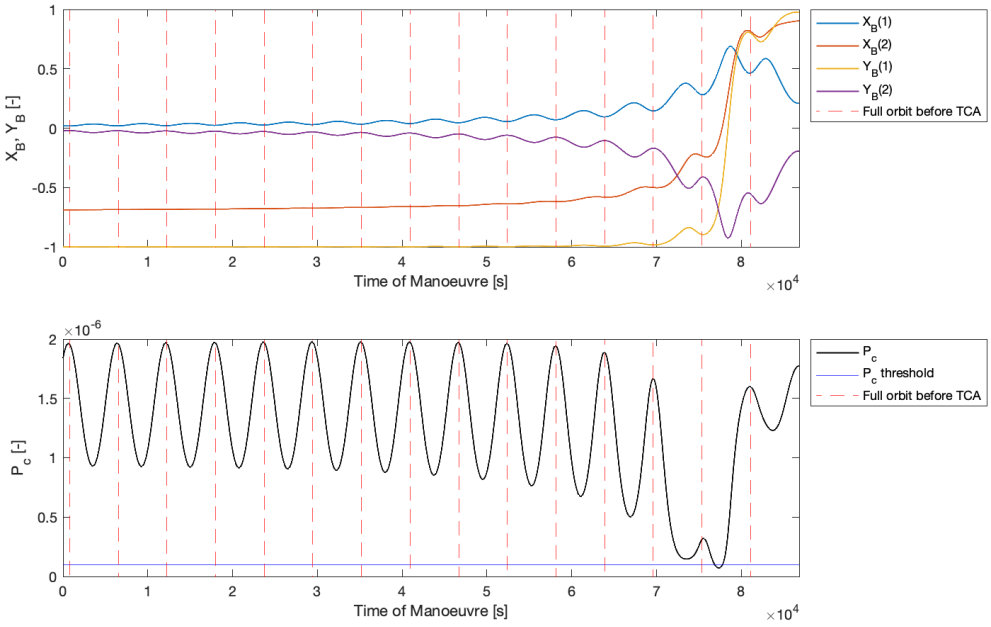

Figure 9.4: X_B and Y_B vector values for ΔV_{12} = 0.02 m/s per simulation second for scenario 1, CDM1

matrix (and with that the unit vector values in the B-plane), this is also when the trends of $X_B(2)$ and $Y_B(2)$ cross, where the dip starts, and the crossing of the $X_B(1)$ and $Y_B(1)$ trends again show that the collision probability restores.

When looking at the way the eigenvalues of the covariance matrix behave in terms of which eigenvalue is larger (as was described in Section 3.2.2, it can be seen that there is a change during the period where the collision probability seems to have a dip. Moving on to the green trend in Figure 9.3, this shows the switch in which value belongs to which axis. When the eigenvalues of $C_{B,X}$ are larger than the eigenvalues of $C_{B,Y}$, the value in the graph is 0.5. In the case this is the opposite, the value in the graph is -0.5. Where first a constant back and forth change is seen in which axis belongs to which value (green line both 0.5 and -0.5), the manoeuvre period where the dip is seen does not show this back and forth movement (only -0.5). In fact, it is seen that during this period of the dip, there is no movement in which eigenvalue belongs to which axis.

Figure 9.5 shows the eigenvalues of the covariance matrix in the B-plane, also including the switch of axes (instead of absolute 0.5, here a value of absolute $1{\cdot}10^{10}$ is used). Here it can be seen that indeed there is a constant switching in the eigenvalues, where the switching stops around the simulation period where a manoeuvre will cause the collision probability to have a dip. It can be seen here that the eigenvalue $C_B(1,1)$ is lower than $C_B(2,2)$. It needs to be noted here that the values on the off-diagonal are zero values.

As the transformation of the covariance values in three dimensions to the B-plane is done through the transformation matrix as mentioned above, this again indicates that this dip is caused by the geometry of the problem. This will be recommended in Chapter 11 for further research.

Continuing with the second CDM, which showed a manoeuvre for both satellites to keep the ΔV budget to a minimum, the same graphs as above can be seen in Figure 9.6 and 9.7. Figure 9.6 shows the manoeuvre results of the primary satellite with a magnitude of 0.01 m/s and Figure 9.7 shows the manoeuvre results of the secondary satellite with a magnitude of 0.01 m/s as well.

In Figure 9.6 it can be seen that there is no dip in the collision probability. Using the same analogy as above, where the X_B and Y_B trend are analyzed, it can also be seen that these trends do not cross each other, which appears to cause the drop in collision probability.

Looking at the manoeuvre of the secondary satellite again with a magnitude of 0.01 m/s, the results in Figure 9.7 are found. This figure again shows the dip in the collision probability, where also the crossing of the X_B and Y_B trends is observed at the manoeuvre times where the dip occurs.

Another thing that is seen here is that the collision probability in these two figures have the opposite phase with respect to the full orbit locations. In the first figure, Figure 9.6, it can be seen that the minima of

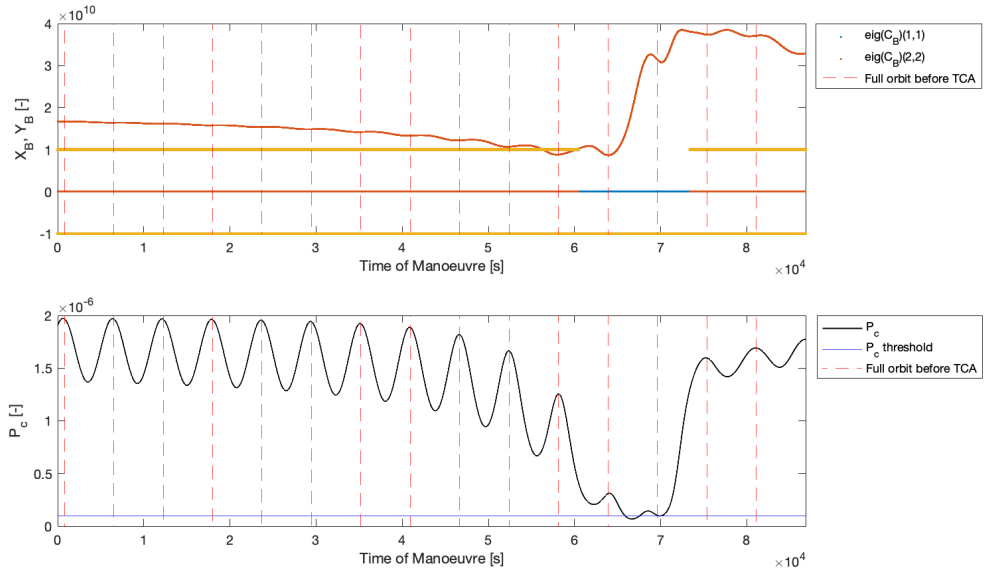

Figure 9.5: eig($C_B(1,1)$) and eig($C_B(2,2)$) values for ΔV_{I2} = 0.01 m/s per simulation second for scenario 1, CDM1, including switch of axes

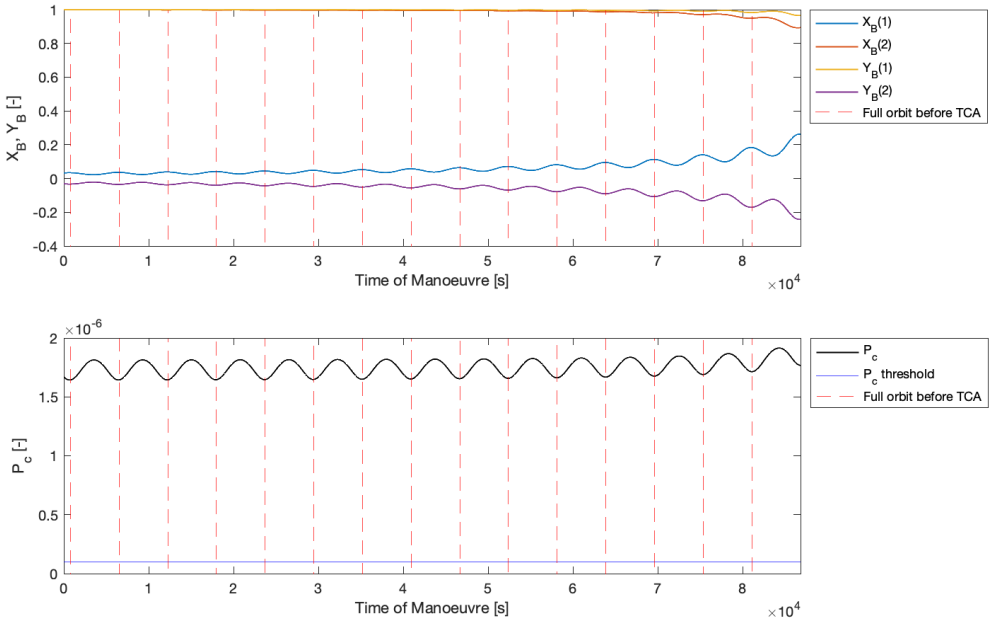

Figure 9.6: X_B and Y_B vector values for ΔV_{I1} = 0.01 m/s per simulation second for scenario 1, CDM2

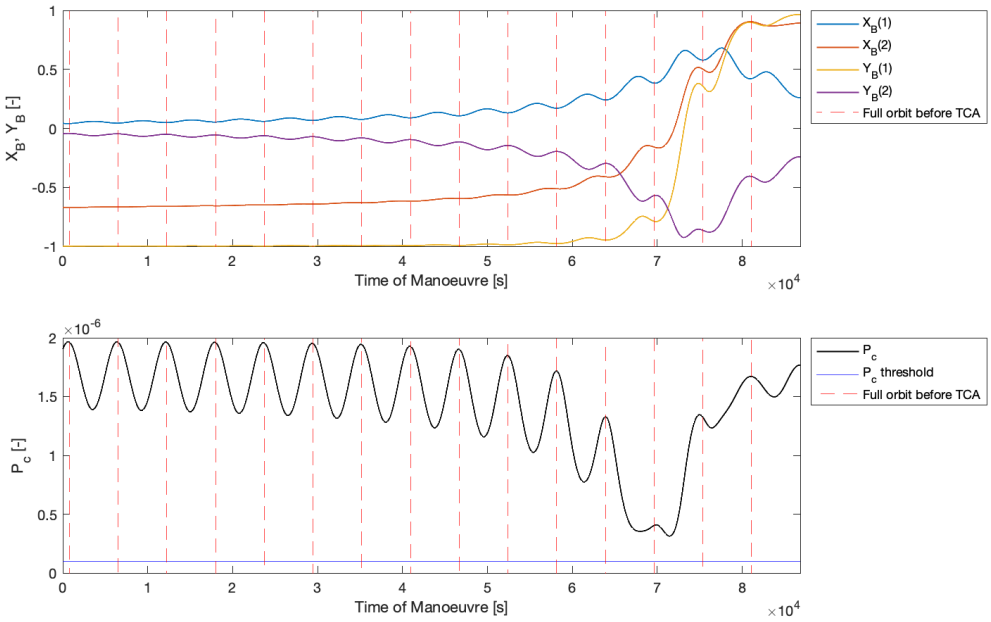

Figure 9.7: X_B and Y_B vector values for ΔV_{I2} = 0.01 m/s per simulation second for scenario 1, CDM2

the collision probability is found when the manoeuvre is performed every full orbit before TCA. In the second figure, Figure 9.7 it can be seen that the minima of the collision probability are found when the manoeuvre is performed every half orbit before TCA. This can be explained by the way in which the problem is set up, where all the computations are done relative to the primary satellite. Where the primary satellite manoeuvres in Figure 9.6, the secondary satellite manoeuvres in Figure 9.7. When the secondary satellite manoeuvres, the primary satellite does not change the TCA location and therefore the reference point does not change. When the primary satellite manoeuvres however, the reference satellite changes position, where the lowest collision probability is seen every orbit instead of every half orbit for a manoeuvre of the secondary satellite.

For the third CDM the results can be seen in Figure 9.8 and 9.9, where Figure 9.8 shows the manoeuvre results for a ΔV of -0.01 m/s of the primary satellite and Figure 9.9 shows the manoeuvre results for a ΔV of 0.01 m/s of the secondary satellite. Here the same behavior is observed as above, where the collision probability shows a dip at the manoeuvre times where the X_B and Y_B values cross.

Referring back to research question one, it can be seen from the results of scenario 1 that the optimization is driven by the input and output parameters as well as some of the thresholds that were set before the simulation. The results that were seen following these boundaries and thresholds point out that the maximum allowed ΔV as well as the maximum allowed station keeping magnitude do not influence the minimization as much as the minimum allowed values. In case of the ΔV it was seen that the minimum impulse bit is the main driving parameter for the ΔV in the minimization, where in the case of the displacement the set boudary is also not met. For the collision probability however, the theshold is a driving parameter, which is seen throughout the results.

The limits that are set by the operators in case of ΔV are then of large influence to the optimization, where the effect of the optimization itself shows that the operator has to take into the effect of a displacement as well as ΔV expense if the manoeuvre is performed.

9.2. Scenario 2

The seconds scenario was set up to investigate the limits in the station keeping dimensions. It was however found from the results that the minimized values do not overstep this station keeping box in-track dimension. This has to do with multiple reasons, where the first reason is that the found ΔV is the minimum from what it can be, which is 0.01 m/s as assumed in the code. The second reason is that the manoeuvre is done within the last three orbits before TCA, which means that the displacement is small when there is little time between manoeuvre and TCA. The last reason, is that the minimization looks at the lowest values and therefore only

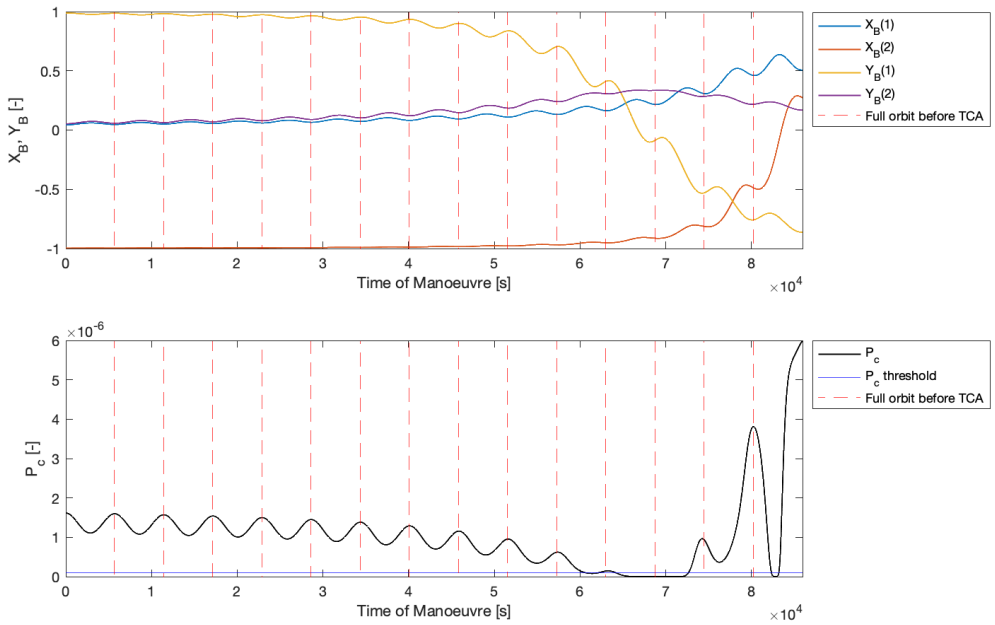

Figure 9.8: X_B and Y_B vector values for ΔV_{I1} = -0.01 m/s per simulation second for scenario 1, CDM23

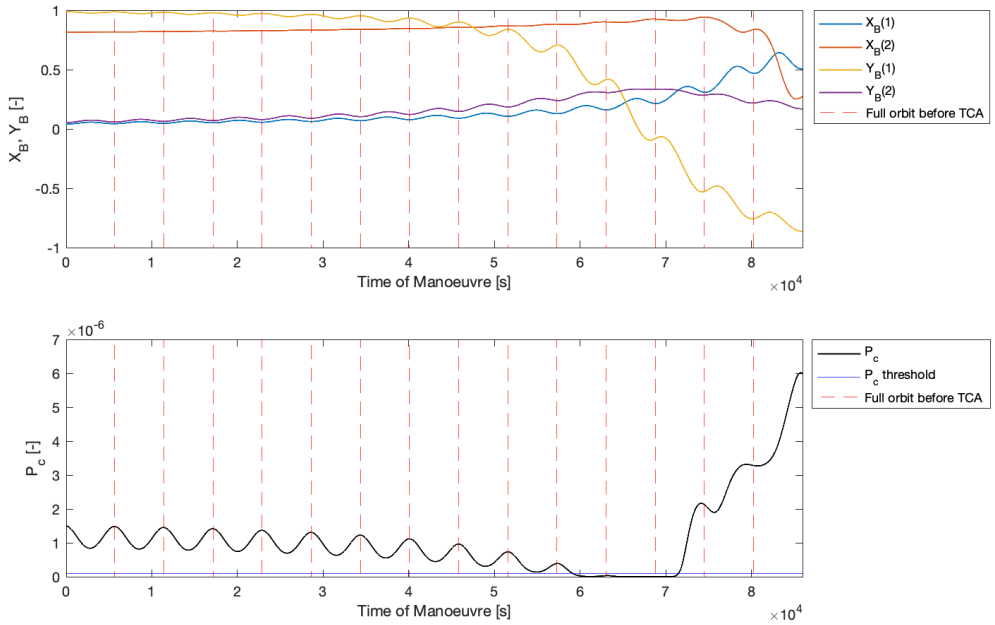

Figure 9.9: X_B and Y_B vector values for ΔV_{I2} = 0.01 m/s per simulation second for scenario 1, CDM2

the lower bound results are found. From this it can also be directly seen that the minimum ΔV results in the lowest displacement in the in-track and cross-track direction. This indicates that the effect of the boundary value of the station keeping box does not influence the result of the optimization for these CDMs. Even though it is still needed to take this into account in case the displacement does overstep this boundary, the effect of the optmized result will have a minimum effect on the constellation as was questioned in the first research question.

Another observation that can be made here when looking at the displacements that follow from the manoeuvres, is that it does not directly relate to the collision probability. Where the displacement in the in-track direction shows a wave-like trend, the displacement in the cross-track direction shows a straight line. Comparing this to the shape of the collision probability trend that is seen, a sinusoidal shape is observed with a sudden dip.

The slanted wave-like motion of the displacement in the in-track direction, can be explained with two different aspects, of which the first was already discussed, being the linear decrease in displacement towards TCA. The second aspect can be related to the location in the orbit where the manoeuvre is performed. When the manoeuvre is performed close to the full orbit positions, the resulting displacement plateaus as the manoeuvre is performed close to the TCA location. This manoeuvre close to TCA results in the displacement being larger at the other side of the orbit, resulting in the steeper part of the wave-like motion of the graph. If the manoeuvre would then be performed around the half orbit location, the displacement is larger at the TCA position. It needs to be noted here that this counts for the secondary satellite as the primary satellite is the reference point of view. For the manoeuvre of the primary satellite this is the other way around.

The cross-track direction manoeuvre geometry differs from the in-track direction manoeuvre geometry, as a manoeuvre in the in-track direction changes the apogee and perigee height (therefore also eccentricity). This is not the case for the cross-track direction manoeuvre, which changes the inclination of the orbit, which is not influenced that much by the location at which the manoeuvre is performed. Because of this reason, the cross-track displacement is a more linear trend than that of the displacement in the in-track direction.

So even though the requirement is still needed for the station keeping box for the early anaylzed manoeuvre times, the minimum that is found does not have a large influence on the constellation as the displacement is kept within bounds. It needs to be noted though that the displacement is something that needs to be taken into account for operations, meaning that it will have an effect, but this effect is kept to a minimum, which provides information to answer the first research question.

9.3. Scenario 3

In scenario 3, different weights were added to the cost function. Initially, the weight of ΔV was determined in Chapter 7, which is also a form of adding weights to the cost function. Here it was found that a higher weight of ΔV showed a lower value for the manoeuvre magnitude. This was to be expected, as the cost function is minimized, where a higher ΔV value is able to weigh up against the other values in the cost function. The results for the lower weights of ΔV show that the displacement is however much lower, even less than a meter. From this it can also be seen that it is therefore possible to focus on smaller displacement magnitudes, compared to the lower ΔV values that are focused on in all the scenarios. This way of using weights in the cost function greatly influences the use of resources with respect to the optimization that is needed, providing information to answer the second research question. If an optimization is needed in terms of ΔV this can be done separately from the optimization in terms of the displacement, which can also me minimized using the correct weights.

In the second step weights were added to the two satellites separately, where the weights can resemble a number of things based on the interpretation and implementation of the operator. However, the different interpretations of these weights all come down to the preference of one satellite over the other satellite. In this case, as the goal is to minimize the manoeuvre expenses, the satellite with the higher weight has a higher priority of not performing a manoeuvre and the satellite with the lower weight is then pushed to performed the manoeuvre. This is also what is observed in the results.

From these results a few things can be seen, of which the first is that by increasing the weight of one satellite, the manoeuvre is indeed pushed towards the other satellite. This push to the other satellite however shows that this costs more ΔV than was needed for the optimized minimum in the first two CDMs. It needs to be noted here that in case the manoeuvre can only be performed by the primary satellite as for the last CDM, the minimum cost manoeuvre that was found was indeed the one as shown for the move of the weight to the other satellite. this was also the case for the first CDM, when only allowing the primary satellite to

Table 9.1: Scaling factor per satellite for maximum collision probability

	cdm1	cdm2	cdm23
Satellite 1	5	5	5
Satellite 2	0.2	0.2	0.3
Collision Probability	$4.70 \cdot 10^{-6}$	$4.65 \cdot 10^{-6}$	$9.81 \cdot 10^{-6}$

manoeuvre.

Moving on to the second way in which the weights are distributed, similar result as mentioned above were found. It becomes clear that a manoeuvre performed by both satellites as in the second CDM is cheaper in terms of ΔV than when one satellite needs to make the manoeuvre. Comparing this in terms of the displacement it can be seen that the cumulative displacement is not larger compared to when the manoeuvre is done by one satellite. Both ways of weight distribution are therefore possible, where comparable results can be found.

Both ways of weight assignment show that a distribution in manoeuvre load can be achieved. This is largely dependent of the initial minimum of the manoeuvre though, as can be seen in the results from the distribution for the three CDMs.

For the first CDM it was seen that the minimum manoeuvre was performed by the secondary satellite only. Adding the weights on the satellites, it was seen that this manoeuvre was slowly shifted towards the primary satellite and with the largest weight completely done by the primary satellite. During this shift, it was seen that also an option appeared in which both satellites had to perform a manoeuvre impulse.

In the case of the second CDM, the minimum manoeuvre was performed by both satellites, where the weights shifted the manoeuvre from one satellite to the other. Using the weights in this case therefore made it possible to see what other minima exist in case one satellite cannot or is not allowed to manoeuvre.

For the last case where for the minimum manoeuvre the primary satellite has to manoeuvre, it was shown that the weights only cause a shift from one satellite to the other. There was no transition zone observed, where the manoeuvre is also distributed over both satellites. It is therefore that this shift is case sensitive.

Altogether, the inclusion of weights for the different cost function parameters show a way in which the operator would be able to shift the manoeuvre from one satellite to the other if needed. It will also provide the option to look at other manoeuvre possibilities and compare the use of manoeuvre resources. This gives insight in how the operator would interact with the optimized manoeuvre as well as the use of resources, which is investigated with the second research question.

9.4. Scaling Factor Influence

As was mentioned before in Section 7.2, a scaling factor can be added to assess the precision of the covariance matrix and with that the collision probability. Using these scaling factors, the manoeuvres were also minimized, as will be shown and discussed below. The scaling factors for which the maximum collision probability was found are shown in Table 9.1.

It can be seen in this table that the maximum values of the collision probability are still in the same order of magnitude as the original collision probabilities. These scaling factors were added to the code to find the minimum solution. Only the first scenario will be analyzed to get an indication of the results compared to the minimum as found in Chapter 8. Only the results of the manoeuvre direction in the in-track direction (as this is again the only manoeuvre direction that was found for the minimum) and displacement in both the in-track and cross-track direction, as well as the time of manoeuvre, resulting collision probability and cost of the manoeuvre are shown.

Table 9.2 shows the summarized results of the first CDM, using the scaling factors as mentioned in Table 9.1. As was also done in the results, multiple minima were found, in this case two. The first of the two minima show a manoeuvre that needs to be performed by the primary satellite in the negative in-track direction. The magnitude of this manoeuvre is the minimum as was set for the minimization, which is also the minimum impulse bit. The second minimum that was found needs to be performed by the secondary satellite in the positive in-track direction.

Comparing these results to the results as were found for the first scenario without scaling factor, it can be seen that the total cost is lower in the case a scaling factor is added. This is because of the displacement being less than the case without scaling factors. The magnitude of the manoeuvre ΔV is the same, indicating that for

Table 9.2: Results for the manoeuvre that needs to be performed in CDM1 when scaling factors are included

ΔV_{I1} [m/s]	ΔV_{I2} [m/s]	ΔI_1 [m]	ΔI_2 [m]	ΔC_1 [m]	ΔC_2 [m]	t_1 [s]	t_2 [s]	Cost [-]	Pc
-0.01	0	355.9	0	0.2	0	73711	0	1356.1	$9.99 \cdot 10^{-8}$
0	0.01	0	427.8	0	0.7	0	72496	1428.5	$9.97 \cdot 10^{-8}$

Table 9.3: Results for the manoeuvre that needs to be performed in CDM2 when scaling factors are included

ΔV_{I1} [m/s]	ΔV_{I2} [m/s]	ΔI_1 [m]	ΔI_2 [m]	ΔC_1 [m]	ΔC_2 [m]	t_1 [s]	t_2 [s]	Cost [-]	Pc
-0.01	0	315.6	0	0.1	0	77276	0	1315.7	$1.00 \cdot 10^{-7}$
0	0.01	0	369.1	0	0.6	0	73446	1369.7	$9.97 \cdot 10^{-8}$

this CDM the magnitude of manoeuvre as well as the cost are not subject to large differences. The manoeuvre performing satellite is however the primary satellite instead of the secondary satellite as was found in scenario 1 without scaling factor. The time of manoeuvre is also later than was found in the case of no scaling factor. It needs to be noted here that in case this same manoeuvre would be performed in case of no scaling factors, the collision probability threshold would not have been reached, meaning that there is still a risk of collision with a P_C higher than $1 \cdot 10^{-7}$.

For the second CDM the results can be seen in Table 9.3. It can be seen that in the case scaling factors are used, the manoeuvre is completely shifted to one satellite for the minimum cost. As this CDM is the follow up CDM of the first one, it becomes a bit more clear here that the resulting minima are similar. The time of manoeuvre is still different, resulting in a different displacement of the satellites, but the same manoeuvre magnitude of the same satellite is seen. This was not the case when no scaling factors were used. The cost that are found here are also lower, which is because the total ΔV that is found is half of what it is in case both satellites need to manoeuvre. Again two minima were found, where the first minimum shows a manoeuvre performed by the primary satellite and the second minimum shows a manoeuvre that needs to be performed by the secondary satellite.

The displacements found here for both minima are smaller than were found without scaling factors. In the situation that these scaling factors were to be used, this solution would then be somewhat 'cheaper' in terms of total cost than when no scaling factors are used.

Continuing with the last CDM, it can be seen that the manoeuvre is still performed by the same satellite. The magnitude as well as the direction of the ΔV is also the same. The timing of the manoeuvre is comparable, but a little later in the case with scaling factors. What is also observed is that the displacement in the in-track direction of the manoeuvring satellite is also smaller than was found without scaling factor. The cost that is found for this case with scaling factor is therefore also smaller. If this manoeuvre were to be performed at the time as found in Table 9.4 without scaling factor, this manoeuvre would not lead to a results that is accepted, as the collision probability threshold is not met.

It can be seen that the results found here with scaling factor have an overall lower cost than the cases without scaling factor. It is also seen that the scaling factors can influence the minimum significantly, in terms of total ΔV usage as well as the manoeuvre performing satellite and with that the resulting displacement. What was also seen is that the manoeuvre found with scaling factor, might not lead to a good enough manoeuvre in case of no scaling factor. This means that if this manoeuvre is performed as is found above, the collision probability does not reach the threshold in the case without scaling factor.

9.5. Final Remarks

From the discussed results above, it was seen that the the outcome of the minima in terms of direction is what was to be expected. However, these results are based on the CDMs that were analysed in the scenarios. This

Table 9.4: Results for the manoeuvre that needs to be performed in CDM23 when scaling factors are included

ΔV_{I1} [m/s]	ΔV_{I2} [m/s]	ΔI_1 [m]	ΔI_2 [m]	ΔC_1 [m]	ΔC_2 [m]	t_1 [s]	t_2 [s]	Cost [-]	Pc
-0.01	0	50.7	0	0	0	83605	0	1050.7	$9.89 \cdot 10^{-8}$

means that for different CDMs, there is a chance that these results will differ from the results that are shown above. It was found from previous studies that a manoeuvre in the in-track direction has the lowest use of ΔV, where it can also be observed that this minimum ΔV does not result in a large displacement with respect to the boundaries that were for the station keeping box.

It was seen that the relative distance as well as the range between the two satellites is not the main influencing factor in the time of manoeuvre. This together with the time of manoeuvre do not seem to be the driving variables that lower the collision probability. However, it was seen that it is connected to the covariance matrix and with that the unit vectors that result from the relative positions, indicating therefore that it is connected to the geometry of the problem. More research is needed to provide a clear answer on the behaviour of the collision probability, together with increasing the accuracy of the covariance data of both satellites.

As was also mentioned for some of the results, the scenarios provide direct answers to the research questions. This will be done in the next chapter, which will combine the results and discussion and provide a more elaborate answer to the research questions.

10 Conclusion

Following the results and the discussion of the results, this chapter will provide the conclusion.

First a summary will be given of the results that were found. After the results have been summarized, the subquestions will be answered. This will be done in the same order in which the questions were set up, with the corresponding additional questions under the subquestions. Following the answers of the subquestions, the main question can be answered.

10.1. Research Summary

From the introduction it was seen that the number of objects in space is growing, followed by an even steeper growth because of the current technological advancements. With this growth, the need for a generalized Space Traffic Management is rising.

Next from the newly launched mission with scientific purposes, communications constellations have the majority of the newly launched satellites. With these newly launched satellites, space is becoming more and more populated, where re-entry of these satellites is being worked on to become more regulated. However, as this re-entry process takes up a significant amount of time, the risk of collision increases as more satellites reside in space.

It was seen from incidents in the past that satellite collisions have a massive effect on the space environment, where the debris can reside in space for up to 20 years. This means that these debris clouds have a large influence on the collision risk of the satellites, where a cascading effect might even result without proper guidelines and regulations. To this end, the mitigation of these collision risks where possible, is key in securing a future in spaceflight.

With the current conjunction data messages that warn the operators of a collision risk, no manoeuvre advice is given. The decision to manoeuvre is left to the operators, where it could happen that no manoeuvre is performed and a collision results. To this end, the aim of this research is to investigate collision avoidance between constellations of different operators, with an eye on the ability to support Space Traffic Management by providing impartial manoeuvre advice. This is done by performing an optimization using the Differential Evolution method, where the minimum manoeuvre from a technical perspective is tried to be obtained.

The first step in setting up the optimization is to define the key parameters on which these manoeuvres need to be based and what these parameters influence in their turn. Here the distinction was made between parameters that have influence on the operations and parameters that have an influence on the lifetime of the satellite. The lifetime is seen as more impactful for the constellations than the temporary disturbance in operations, deeming the lifetime influence the determining factor in the decision for the parameters. Three groups of parameters were evaluated on the impact on the operations and lifetime, being station keeping, collision prediction and collision avoidance. From this evaluation it was decided that the station keeping box parameters in the in-track and cross-track directions, the collision probability and collision avoidance manoeuvre ΔV in radial, in-track and cross-track are of influence on the lifetime of the satellite and need to be included in the manoeuvre optimization. These parameters were then combined in a cost function, which needed to be minimized.

In the cost function, the collision probability is a hard limit value and is in this research not allowed to be larger than $1{\cdot}10^{-7}$. The amount of ΔV that is allowed to be used depends on the wishes of the operator, but

is also a hard limit in the cost function as this amount is then not allowed to be passed. The station keeping box on the other had was not a hard limit in the cost function, where a penalty function was added in case the threshold was passed. This penalty function was added for the in-track boundary, set to absolute 17.5 km in the in-track displacement of the satellite, where the displacement of the satellite in the cross-track direction needed to be minimized because of the larger impact a cross-track displacement has on the orbit.

Following the linearization of the propagation of the satellite orbits, the first step in the code is to generate the baseline scenario and values. After this step, the initialization of the minimization can be done, which generated a list of random variables as the baseline population. This baseline population is made up of ΔVs in different magnitudes and directions, as well as the time of manoeuvre. With these baseline population values, the displacement in the in-track direction and the cross-track direction is computed. Together with these displacement calculations, the collision probability is determined. These calculations are then followed by the mutation and recombination step, which are based on randomized in probability. Only after the recombination step the new displacement values and the collision probability is computed again. Following these computations the selection follows, where the computed values for the displacement and collision probability are substituted in the cost function. From the comparison of the cost of the previous values and the new values, the lowest of the two values is chosen. These values are then used again in the mutation step and the recombination step in a new iteration step until convergence is reached.

With the code complete and working, the results were generated. Three scenarios were set up that were tested with three CDMs. The first scenario looked at a ΔV limit, the second scenario looked at limitations in the station keeping parameters and the third scenario looked at the addition of weights to the two satellites in order to move the manoeuvre from one satellite to the other if priority or preference is given to one of the two satellites a well as weights for the parameters of the cost function. The three CDMs that were chosen also showed different results for the baseline minimization (limiting the ΔV as much as possible). The first CDM showed a manoeuvre of the secondary satellite only. For the second CDM both satellites needed to move for the minimization of the ΔV and for the minimization of the last CDM the primary satellite needed to manoeuvre.

For the initialization scenario, where the focus was on keeping the ΔV as low as possible, it was found that all manoeuvres for these three CDMs needed to be performed in the in-track direction. This then also leads to a displacement in the in-track direction. The amount of displacement however is far from the limits that were set for the station keeping box. Additionally, the time of manoeuvre was found to be within the range of three orbits before TCA until half an orbit before TCA.

From the first scenario where the amount of ΔV was limited to 0.1 m/s, no different results were seen compared to the initialization scenario. For all CDMs the ΔV that was found was also the minimum impulse bit that had been set, where it was also seen that the direction of manoeuvre is the in-track direction for all results. For the second CDM where both satellites need to manoeuvre, both satellites need perform a manoeuvre of 0.01 m/s in the in-track direction. With this manoeuvre in the in-track direction the magnitude of the displacement was found to be up to about 575 m, which is far from the 17.5 km that was set for the station keeping box. The displacement in the cross-track direction was found to be less than 1 m for all CDMs.

Moving on to the second scenario, where the station keeping box limits were investigated with different values, the same results could be used of the first scenario. This was also to be expected, as the displacement limits were far from passing threshold for the minimum manoeuvre in the given simulation time. As was also seen before, the in-track displacement is large compared to the displacement in the cross-track direction. This is also expected for a manoeuvre in the in-track direction. Only when the manoeuvre magnitude is increased by a factor 10 to 0.1 m/s, a displacement is observed that is larger than the threshold for simulation times earlier than 10 orbits before TCA. It was also seen that this manoeuvre magnitude results in more manoeuvre windows where the collision probability is on the right side of the threshold.

Going to the final scenario where weights are added to the satellites, it was seen that weights are able to influence the preferred manoeuvring satellite. For the full weights that are a factor multiplied with the cost of one of the satellites, it can be seen for the first and third CDM that the manoeuvre is shifted to the other satellite compared to what was found for the first two scenarios. The results of the second CDM showed that a transition is made, where not only the manoeuvre magnitude changes when looking at the extreme weights, but also a transition is seen for the displacement magnitudes. This transition was also seen for the first CDM, where adding weights to the secondary satellite in fractions showed a distribution where both satellites needed to manoeuvre. These same results were also seen for the second and third CDM, where a transition occurred for the second CDM and a direct shift of manoeuvring satellite was seen for the third

CDM. It needs to be noted here that all resulting manoeuvres are in the in-track direction, with a displacement also in the in-track direction. Additionally, the manoeuvre times were seen to be within about three orbits before TCA.

Overall it was found that the minimum manoeuvre cost for these three CDMs resulted in a ΔV that is the minimum impulse bit (assumed for these cases), with a collision probability that is just lower than $1{\cdot}10^{-7}$. This manoeuvre was also only performed in the in-track direction, where the displacement is also mainly seen in the in-track direction and far below the thresholds set for the station keeping box. Additionally, the manoeuvres that were found all need to be performed between three orbits before TCA up to half an orbit before TCA.

It was also seen that it is not always the case that one satellite needs to manoeuvre to obtain the minimum cost, but that a manoeuvre done by both satellites is also found to have a minimum ΔV expenditure. If this manoeuvre would be shifted to one satellite, the manoeuvre magnitude would be larger than the added magnitude of both satellites. Together with this, it was found that if the manoeuvre is pushed to the other satellite, also a larger manoeuvre magnitude is found to meet the collision probability threshold. Not only this, the follow up CDMs showed different results. It was thus shown that the minimization of the manoeuvre to lower the collision probability is case sensitive and depends on the CDM.

10.2. Research Questions

Answering the research questions will be done in steps, where first the subquestions are answered before the main research question is answered. All these answers combined will then give an answer to the main research question. After the questions have been answered a look will be taken at the research objective and if this is met.

10.2.1. Research Subquestions

The first research question was formulated as follows:

How does a collision avoidance manoeuvre optimization influence a predicted conjunction event between two satellites of different constellation satellites?

Following this research question the following subquestions were answered:

1. *What are the input and output parameters of a constellation focused collision avoidance manoeuvre optimization?*
   From literature it was found that multiple parameters are important to the constellation design, as well as collision detection and avoidance calculations. A distinction was made between the parameters that have an impact on the operations of the constellation and the parameters that have an impact on the lifetime of the satellite. With this analysis it was concluded that the parameters that influence the lifetime of the satellite are more important than the parameters that only influence the operations. The parameters that influence the lifetime of the satellite are the collision probability, the station keeping limits in the in-track and cross-track direction and the manoeuvre ΔV magnitude in the radial, in-track and cross-track direction.
   Looking at these parameters, the input that needs to be determined for a manoeuvre is the ΔV magnitude as well as the direction and timing of the manoeuvre. As the optimization looks for the minimum cost, only the boundary values of the ΔV magnitude (and direction) and manoeuvre time boundaries need to be used as input before starting the simulation. Because of the boundary values of the station keeping box and the limit of the collision probability, these boundary and limit values also need to be inserted as input for the minimization.
   Following convergence of the code, the output of the minimization is the minimum cost in terms of ΔV and displacement within the station keeping box (while the collision probability is also smaller than the allowed value). The output parameters are hence the ΔV in the three directions, the displacement in the in-track and cross-track direction and the manoeuvre timing.

2. *What requirements for the collision avoidance manoeuvre optimization would be needed from a constellation operator perspective?*
   Based on the influence of certain parameters on the lifetime of the satellites, these parameters are also those that have requirements. For the total ΔV it was seen that a low value has a limited impact on

other regular manoeuvres that need to be performed, such as station keeping itself, because of the limited use of the resources. Additionally, the minimum impulse bit that can be generated and direction in which this manoeuvre can be performed are requirements that can be set by the operator based on the specifications of the satellites.
Also, the manoeuvre timing window is something that might be a requirement by the operator, which can also be limited within certain boundaries. For some operators it might be required to perform the manoeuvre at latest one orbit before TCA because of data updates, or between certain orbits because of the operational windows.
With the manoeuvre magnitude and manoeuvre window, there is the station keeping box in which the satellite is allowed to manoeuvre. These station keeping boundaries are satellite dependent, meaning that this is also a requirement that needs to be set by the operators. Even though this station keeping boundary was not crossed in the scenarios that were run in the simulations, based on the situation as well as the boundary values this boundary could be met in a different situation.
Last but not least there is the collision probability. Even though it is assumed in this thesis that the collision probability needs to be brought to a value below $1{\cdot}10^{-7}$ for a close approach to be negligible, it differs per operator what the requirements are in this value and at what threshold a manoeuvre needs to be performed. This is therefore also a value that is required by the operator.

3. *What is the influence of the constellations on an optimized collision avoidance manoeuvre?*
With the determined parameters and requirements that can be set by the operators, the influence of the constellation on a collision avoidance manoeuvre is seen in the limitations and boundary conditions. Even though the station keeping boundaries were not met in the scenarios that were simulated, these boundary values could influence the cost depending on the case. It is however not expected that this limit is reached because of the minimization of the manoeuvre ΔV. The biggest influence on the collision avoidance manoeuvre is therefore the limitations in the ΔV. As was seen in the results, the minimum impulse bit allowed for the manoeuver was met in every scenario. It is therefore not the limitation in the maximum allowed ΔV, but more so in the minimum capable ΔV of the satellite thruster. It needs to be noted though that this depends on the case, but as the aim is to minimize the cost of primarily the ΔV, a maximum is not expected to be reached in the results.
The influence of the constellation on the manoeuvre can therefore be related to the limits and boundaries that are set in the optimization and directly come from the constellation and satellite design. For the resulting manoeuvre it is therefore possible that a lower minimum can be found, if the satellite specifications would allow for lower ΔV specifications. Other than that, the influence is not much of a problem as the boundaries are not met and the minimization searches for the lowest possible results.

4. *What is the impact of an optimized collision avoidance manoeuvre on the constellations?*
The other way around, looking at what the effect of the manoeuvre is on the constellation two things can be seen here. The first is that the manoeuvre ΔV means that some of this budget is used. Because of the minimization of this value, the expenditure is kept as low as possible, while at the same time passing the collision probability requirement. What is not taken into account here but also needs to be accounted for, is the manoeuvre back to the operational orbit. This usage of ΔV is needed if the aim is lower the collision probability to an acceptable level, where the risk of losing the satellite due to a collision might be more impactful on the operations than on the reduced lifetime (just as was traded off in the parameter determination).
The second thing that is seen is that there is a displacement as a result of the manoeuvre. This displacement is in most cases not desired, as the satellite needs to stay in its orbit for the optimal operations. However, similar to the above-mentioned trade off in ΔV usage, a pause in operations has less influence on the total operations than losing the satellite and it not being operational anymore. As was again seen in the results, this displacement is kept to a minimum and does not reach the boundaries that were set for the station keeping box, where it can be said that (following the goal of this station keeping box) the displacement that is found is allowed and does not have a large influence on the constellation.
Altogether, it can therefore be said that the impact of the collision avoidance manoeuvre has an impact on the operations during the manoeuvre. However, as the minimum is searched for using the minimization, the impact is kept as low as possible.

The answer to the first research question can then be summarized in four steps, starting with the input and output parameters.

From the input and output parameters, the conjunction event and minimization of the collision avoidance manoeuvre could be brought back to the collision probability, the manoeuvre magnitude, manoeuvre timing and the displacement of the satellite in the in-track and cross-track direction. With these four aspects the conjunction event can be influenced.

The amount of ΔV that is used, together with the timing and allowed displacement in the station keeping box, can be based on requirements from the operators. Even though the collision probability threshold can also be set by the operators, it common is that a collision probability threshold of $1 \cdot 10^{-7}$ is seen as an acceptable risk. Additionally, as was seen in the results, the minimization showed that boundaries in terms of ΔV and station keeping box were far from crossed.

The influence of the constellation on the manoeuvre optimization is translated from the requirements of the operator to the boundaries and limits that are set. These boundaries and limits are inserted as input values in the minimization, where the manoeuvre is optimized and searched for within these bounds. As the minimization searches for the lowest cost, these bounds are oftentimes not met, as was seen in the results. However, as this is case specific, the boundaries and limits are still important to take into account.

The other way around, the influence of the manoeuvre on the constellation satellites is that there is some ΔV taken out of the budget for the collision avoidance manoeuvre and that a displacement results, with a disturbance in the operational orbit. This ΔV taken out of the budget is however needed to prevent the loss of the satellite due to a collision, which also goes for the resulting displacement. Both the ΔV expenditure and the displacement are kept to a minimum as a result of the minimization.

Moving on to the second research question, which was formulated as:

How would the optimization of the collision avoidance manoeuvre between two satellites of different constellations support the development of a Space Traffic Management system?

the subquestions were answered as follows:

1. *How does the optimization of the collision avoidance manoeuvre impact the use of resources?*
   Given the minimization that is done, the results that were found were lowest to pass the criteria of the collision probability and stay within the bounds of the constellation and satellite requirements. It was seen that the ΔVs that were found are all the minimum impulse bit that is set upon starting the simulations. Letting the minimization focus on the minimum ΔV that can be found, it was therefore seen that the use of resources in terms of fuel is lowest that is possible.
   However, when looking at the third scenario where weights were added to the satellites in order to focus the manoeuvre on either one or both of the satellites, the total ΔV expenditure could be higher than the minimum that was found. In some cases, the amount of ΔV that needs to be used is 5-8 times higher than the minimum. In this case more resources are needed, where it therefore depends on the situation as well as the preference of manoeuvring satellite. If the decision is to have the least use of resources, the minimum as was found in scenario 1 and 2 need to be followed. If the decision is however that the resources of one satellite in particular needs to be minimized, it can be decided to shift the manoeuvre to either both or the other satellite completely, in its turn likely requiring more resources in terms of ΔV.

2. *How do the results of the optimization compare to traditional collision avoidance manoeuvres?*
   As was mentioned in Section 2, no collision avoidance advice is given with the CDMs. Traditional collision avoidance manoeuvre determination is therefore solely done by the operators, where politics might play a role. Additionally, as no manoeuvring advice is given, this method of optimization for both of the satellites gives an impartial advice based on the technical aspects and requirements of the operators only.
   Looking at the results of the optimization, it could be seen that in the case of the second CDM a manoeuvre performed by both satellites could save a large amount of ΔV in total. The current manoeuvring is mostly done by one of the two satellites, meaning that this way of optimizing might result in saving of total resources and show options that have not been considered by the operators themselves.
   In terms of the optimization itself, from an operator perspective the minimum use of resource is always something that is considered. In that sense this method of calculation is therefore not different. However, as optimization methods could differ from operator to operator, a common standardized initial calculation of the optimized collision avoidance manoeuvre could already give an idea for all operators what magnitudes are to be expected if the decision is made to manoeuvre.

3. *How would the advised collision avoidance manoeuvres from the optimization and the operators of the constellations interact?*
   As the final decision to manoeuvre still lies with the operators themselves, the results of the optimized collision avoidance simulations could give an indication of what magnitude of manoeuvre might be needed. Additionally, it gives insight in possibilities that might not have been considered, such as the manoeuvring of both satellites. Where mostly politics come into play regarding which operator is moving and which not, these advised manoeuvres are based on the technical aspects of the problem only.
   If the operators decide that it is still beneficial for one satellite to move more than the other, it was seen with the weights added in the third scenario that it is possible to shift the manoeuvre from one satellite to the other (it being partially or completely). With this it also becomes clear that guidelines regarding manoeuvring might be needed, where politics do not play such a big role anymore. Given the growing number of objects in space, it is not a matter of waiting to see if the satellite collides, but action needs to be taken to ensure the cascading effect does not happen.

Looking at the answers given above, it shows that the optimization of the collision avoidance manoeuvres can help the development of a space traffic management in two different ways.

In terms of minimizing the use of resources, which is a wish of most of the operators, this method of a centralized advised collision avoidance manoeuvre provides options which minimizes the use of resources when looking at the complete situation where both satellites are included. If the manoeuvre would be considered from the perspective of the operators separately, the resulting manoeuvre might have a higher amount of ΔV that needs to be expelled to meet the collision probability criteria.

The second way in which this method could help the development of a Space Traffic Management, is that it looks at the situation of both satellites instead of the perspective of one operator. This minimizes the need for an extensive political trade-off before a manoeuvre is decided on, as it gives impartial advice from a technical perspective. Where the manoeuvre planning and optimization is initially done by the operators themselves, using a centralized advice perspective provides a head start in manoeuvre trade-offs between operators. The final decision however still lies with the operators, where it is possible to have one specific satellite manoeuvre of the two by shifting the weight to the satellite that needs to be manoeuvred less. It is therefore not a forced advice, where interaction is still needed between operators and operators with the advised manoeuvres.

10.2.2. Research Question and Objective

Using the answers above that were given to the subquestions, the main research question can now be answered. The main research question was formulated as follows:

> **How could the result of an optimization based advice on collision avoidance manoeuvres for two satellites of different constellations in Low Earth Orbit be used to support the development of a Space Traffic Management?**

Looking at this question there are two perspectives in which this question can be answered, which was already mentioned earlier, being a technical perspective and an operational perspective.

From the technical perspective it was seen that the problem can be reduced to four main aspects of the problem, being the collision probability, manoeuvre magnitude, manoeuvre timing and the displacement resulting from the manoeuvre. The input that is needed for the manoeuvre are the restrictions in the manoeuvre magnitude, manoeuvre timing and the manoeuvre displacement boundary. On the other hand we have the output, which is then the minimized result in manoeuvre magnitude and displacement. Both of these results then also pass the collision probability criteria.

The influence of the constellation specifications on the manoeuvre is that there are boundary values and limiting values, imposed on the search space of the minimization. On the other hand, the effect of the manoeuvre itself on the constellation is that there is a disturbance in the operational orbit of the satellite as well as ΔV that is taken from the budget. However, as this is all minimized, the disturbance is kept to a minimum and is the least that is needed to prevent a collision.

From an operational perspective, it was seen that this minimization of the collision avoidance manoeuvre results in the lowest possible expenditure of ΔV, where other manoeuvre done by either the other satellite or in a different direction have a higher ΔV expenditure. The disturbance to operations is therefore also kept to a minimum.

Given that there is no manoeuvring advice given with the CDMs, the tendency to involve politics cannot be avoided. In terms of a centralized minimization, which takes both satellites into account and where a certain amount of weight can still be added based on different factors and wishes, this manoeuvre advice is from a technical perspective and is at the same time impartial. Hence, this manoeuvre advice will give insights and at the same time allows for wishes from operators in terms of manoeuvre action.

This result of an optimized collision avoidance manoeuvre could therefore support the development of a Space Traffic Management in a centralized way from a technical as well as an operational perspective. By providing insights in what the minimum manoeuvre magnitude options and corresponding displacement can be, taking both satellites into account as well as the boundaries and limiting values, a first step in the decision to manoeuvre is done. Additionally, this manoeuvre can still be influenced by the operators depending on the wishes of which satellite is preferred to manoeuvre. A Space Traffic Management will benefit from this, as less politics is involved and together with that the waste of resources is kept to a minimum, while at the same time encouraging a collision avoidance manoeuvre.

Going back to the research objective, which was formulated as below:

> *Provide impartial collision avoidance manoeuvre advice for two satellites of different Low Earth Orbit constellations in support of the development of a space traffic management, by presenting multiple manoeuvre options as a result of an optimized parameter cost function that takes into account constellation performance.*

it can be seen that impartial collision avoidance manoeuvre advice is provided, where multiple options can be given based on the specifications of the satellites and wishes of the operators. It was also seen that the constellation performance was taken into account in providing the results through a cost function that was minimized. It can therefore be concluded that the research objective was met.

11

Recommendations

Following the conclusion and the answers to the research questions, the parts which need further research or added research can be discussed. This chapter will provide an overview of the main simplifications that were made and the recommended research that needs to be done based on these simplifications. The last section will discuss further research that can be done following this research.

11.1. Further Research from Simplifications

Apart from the boundary values and limiting parameters, which were mostly assumed in this thesis, there are assumptions made regarding the setup of the problem and the code. These assumptions were done to make the research in this thesis easier or more time saving. However, with assumptions information gets lost or is not taken into account. The list below identifies the simplifications which can be improved to the full models or equations, for which more effort and research is needed.

- *Covariance matrix*
  For this research it was assumed that the covariance matrix does not change for different positions in TCA. This would of course not be the case when the propagation could be done after the manoeuvre has been performed. As the covariance matrix is an important parameter and has a large impact on the collision probability, it is needed to do further effort on obtaining the information needed for propagation of the satellite orbits. With the propagation of the satellite orbits, the covariance matrix can also be generated.
  Next to the propagation of the covariance matrix, there is the accuracy of the covariance matrix, which is also shortly discussed in Appendix E for the used CDMs throughout the research. It was found from studies that the covariance matrix in the CDMs is accurate enough for the estimates that need to be done, however, the covariance values could be more accurate. This has to do with the observations that are used to estimate the positions and with that the covariance matrix. The prediction of the orbit is then also something that could be improved, which is mainly based on empirical research. This means that the models that are used could be improved, leading to a more accurate covariance matrix and with that a more accurate collision probability.
- *Accuracy of the CDM information*
  Together with the covariance matrix values as mentioned above, more information is provided in the CDM which is subject to a certain level of inaccuracy [15]. It is therefore important to know how these values came about and if there is room for improvement of accuracy in these values. The most important parameters in the CDM needed for the calculation of the collision probability and the setup of the scenario (position, velocity, object radius, time and date of closest approach, covariance matrix values) are then expected to be of higher importance than the other values names in the CDM. However, there is more info in the CDM provided which is not used in this research. It could therefore also well be that there is more information which can lead to more accurate results of the minimization.
- *Simplification of the collision probability calculation*
  The formula that was used to compute the collision probability is a simplification, where the transformation to a 2D problem together with the assumption that the collision area in the B-plane is a rectangle instead of a sphere was done. Even though multiple sources mention that these simplifications can

be used without too much offset and are accurate enough, further effort could be put into the calculation of the collision probability in 3D and if this gives different results. Based on these results, combined with a more accurate estimation of the other parameters, such as the covariance matrix elements and the position and velocity, the collision probability could become more accurate.

- ΔV *manoeuvre impulse*
  In this research it is assumed that the manoeuvre is performed with an impulsive ΔV, which does not have a transition from one velocity to the other. This is however not what happens with an actual manoeuvre, where the propulsion always takes a certain amount of time. This transfer of one velocity to the other was not taken into account, which can (and will) make a difference in the timing of the manoeuvre as well as the resulting displacement.
- ΔV *in different directions/angles*
  Three directions were chosen to be possible for the manoeuvre, being the radial, in-track and cross-track direction. Current possibilities in manoeuvring however also include the option to manoeuvre at an angle. As this could also give a more minimized result, this can be included in the options of the code.

These are the points of further research which could potentially give more accurate and complete results. The next section will describe the further research that could be done to add to the current research.

11.2. Follow-up Research Recommendation

Following the research that has been done, there are additional research which could be done as a follow up. Some of the recommended follow up research is discussed below.

- *Manoeuvre timing*
  The results found in this research indicated that the manoeuvres cold be performed between about three orbits before TCA and TCA. However, as there might be CDMs which will show a manoeuvre that needs to be done even earlier, it could be debated if an earlier manoeuvre is justified. An earlier manoeuvre might also mean that the orbit data is not as accurate as when it would be based on data from a later time closer to TCA. This means that there will be a conflict (or paradox) in which decision needs to be made, it being either saving ΔV by manoeuvring earlier, or waiting until more accurate data is available and possibly not needing a manoeuvre.
- *Displacement accommodating station keeping*
  Another thing that can be implemented in the code is the option to have the displacement from the manoeuvre accommodate for a station keeping manoeuvre. This could however depend on multiple aspects, being the time of manoeuvre, the displacement that is needed and on the other hand the location of TCA, which could be conflicting with the desired station keeping operation. Using a minimization, the amount of ΔV can then be minimized, based on the station keeping wishes of the operator.
- *Manoeuvre methods*
  As was also mentioned above, the manoeuvre is assumed in this research to be an impulsive velocity change. With the market moving towards different ways of manoeuvring (electric propulsion for example), these different types of manoeuvring could be implemented if desired. This indicates that there is a transfer period, which not only needs to be taken into account in the use of 'ΔV' but also in the manoeuvre time and propagation of the satellite orbit.
- *Manoeuvre back*
  With the manoeuvre to avoid the satellite with which it has a close approach, the manoeuvre back is not taken into account here. This means that the use of ΔV might be larger, given that the satellite needs to move back to the operational position. However, it could be that this is not needed, which depends on the wishes of the operator. It might therefore be interesting to have an additional option in which is it possible to manoeuvre back to the original orbit, where taking this into account the minimization can be performed again. It could even be that this is weighed against a satellite that does not need to manoeuvre back.

Based on these recommendations for follow up research, this work could be expanded to have more options for the operators. This will then also give more leeway in advice for CDMs that are not similar to the ones that have been used in this research.

A

Space Traffic Management Introduction

In addition to the short introduction as provided in Chapter 1, this chapter will provide a more in depth discussion on what directions of space traffic management can be observed as well as how these have evolved over time.

A.1. Introduction to Orbital STM

Following the short introduction above, it becomes clear that unclear guidelines and rules are present to manage the space traffic as is. Some guidelines were set up[1], but are not enforced as rules with consequences. It has also become clear that the number of objects is increasing steadily, posing a big risk to the future accessibility and usability of space. To this end, it is important that more effort is put into setting up a Space Traffic Management on a (inter-)national level. But what does Space Traffic Management entail? And as this has been a constant and growing problem, previously maybe not as severe as the current situation, have there been previous efforts in setting up a form of Space Traffic Management?

Multiple attempts by different parties have been made at defining what a Space Traffic Management entails. Based on the components that are involved in such a management system, the following definition covers most, if not all, components that are involved:

> *"Space Traffic Management shall mean the planning, coordination, and on-orbit synchronization of activities to enhance the safety, stability, and sustainability of operations in the space environment."*[31]

It needs to be noted that this thesis is not aimed at finding a definition of Space Traffic Management. It is therefore that the definition as formulated above is used as definition of Space Traffic Management.

The field of Space Traffic Management can be split in three different branches:

- Ground infrastructure
- Suborbital
- Orbital

As the orbital branch is the point of focus, this is the branch that will be expanded as shown below.

The orbital branch of STM is maybe the largest of the three branches, as this is most of the space flight that is happening at the moment. It concerns all space objects that are orbiting Earth, but also objects that are not orbiting, but passing through our solar system. This regime of space flight can again be subdivided into three branches:

1. Space Situational Awareness (SSA)
   SSA covers all space objects that can be observed, which is then being tracked and stored in a catalogue. Apart from the objects that are tracked, there is also the branch of space weather, which tries to keep track of all natural interferences and events that are happening in our solar system.

[1] `https://www.unoosa.org/res/oosadoc/data/documents/2019/a/a7420_0_html/V1906077.pdf`

2. Orbital Slot Allocation
   As all spacecraft want to have their own orbit and frequency to communicate on, it is important to prevent signals from interference. Interference in this case can also mean physical interference of the orbits. Therefore, orbital slot allocation deals with assigning certain orbits and frequency to spacecraft. This is already a form of STM, which is currently of great importance to Geosynchronous Orbits (GEO) and with the predicted traffic also to Low Earth Orbits (LEO).
3. Space Debris Mitigation Guidelines
   The past few years have seen a growth in space debris. As collisions with space debris and the growth thereof are not beneficial to current and future space flight (even catastrophic), this needs to be minimized as much as possible. To this end, space debris mitigation guidelines were set up followed by post mission disposal (PMD) guidelines. Given the knowledge and the severity of the problem, these mitigation and disposal guidelines are not enforced and are merely an advice to the space fairing companies.

Each of the branches named above contains aspects that support and define the topic that is researched in this thesis, of which the most important are Space Situational Awareness and debris mitigation.

A.1.1. Space Situational Awareness

In order to be able to get an idea of what the situation is in space it is important to know what is floating and flying around the Earth. To this end, the European Space Agency managed to set up a Space Situational Awareness programme for European reference in 2009 [2]. This programme focuses on three main topics, being Space Weather (SWE), Near-Earth Objects (NEO) and Space Surveillance and Tracking (SST).

In terms of collision avoidance and knowing where the satellites are, SST is aimed at tracking the objects in space that are man-made as well as objects that resulted from collisions or impact. Not only is it useful to know where objects are in space, but these objects can also pose a threat to intact orbiting satellites. These objects range from debris to offline satellites or burned up rocket stages. As discussed before, the number of objects in space is increasing, therefore creating the need to be aware of what objects are where.

Next to the ESA SSA programme from Europe the U.S. Strategic Command (USSTRATCOM) Space Surveillance Network also tracks, detects and catalogues objects in space through a global ground-based network of sensors and tracking systems. Similar to ESA, the objects that are being tracked, range from debris to inactive satellites and used up rocket bodies, and are being updated in the Space Object Catalog. Another space surveillance system from the U.S. Air Force, called Space Fence, tracks artificial satellites and space debris in Earth Orbit. It is apparent that the U.S. is operational and further developed than that of Europe. Consequently, Europe does not have the technical capabilities yet to actively maintain a space object catalogue, which results in Europe being dependent of the U.S. data and their will to share it [32].

A.1.2. Debris Mitigation

Early studies done on the count of objects in space indicated that the population of debris is growing. Even though this debris is of little risk to unmanned spacecraft, this population is growing, together with the probability of collisions. To prevent a hazardous space environment for future generations' mitigation guidelines were set up, limiting the orbital lifetime after completion of the operation. Multiple space debris mitigation guideline handbooks have been set up by national as well as international spaceflight organizations, to push for efforts regarding space debris mitigation. Even though these handbooks are set up by different organizations, four components seem to be of fundamental importance [7]

1. Limitation of object releases during nominal operations
   All spacecraft, independent of orbital regimes, would be designed not to release debris while during nominal operations. In case release of orbital debris is unavoidable, it should be minimized in the amount, area and the orbital lifetime of this debris. If objects will be released in orbit during operations, these missions or programs should not be planned unless it can be verified that the risk to other operating spacecraft, orbital stages and orbital environment is acceptably low in the long-term.
2. Prevention of on-orbit break-ups
   These break-ups can happen during the missions, but can also be the result of accidental explosions and ruptures at the end-of-mission and intentional destruction, generating orbital debris that will take a long time to deorbit.

[2] `https://www.esa.int/Safety_Security/SSA_Programme_overview`

3. Removal guidelines for spacecraft and orbital stages after the end of mission or operation
   This component is made up of two main categories. The first category of post mission disposal is for the geosynchronous region, where spacecraft that have fulfilled their mission need to be manoeuvred far away from GEO to eliminate interference with spacecraft that are still in GEO orbit (to a disposal orbit). The second category is the passing of spacecraft through LEO to deorbit, where satellites that are posing a risk to operational satellites in LEO should be manoeuvred for a faster deorbit or direct re-entry. Connected to this guideline is also the maximum lifetime limit of 25 years, which was deemed reasonable and appropriate from studies and national guidelines.
4. Prevention of on-orbit collisions
   This is done by estimating and limiting the accidental collision probability with known objects. If the collision risk is not considered negligible, co-operation of launch windows as well as collision avoidance manoeuvres is needed to prevent loss of control and therefore preventing a post-mission disposal. Accidental collision limitation has two aspects [4], of which the first is to select a safe flight profile. This safe flight profile includes the mission altitude, the related background debris environment and the end of mission limitations to prevent from accidental collisions. The second aspect is to protect the satellite components from small micrometeorites and orbital debris impacts. This will ensure a successful post mission disposal operation.

Even though these guidelines are seen as important throughout the space sector, these guidelines are not forced, but merely encouraged to follow. Due to these guidelines not being forced, a large spread is observed in the compliance of these guidelines, in particular the 25-year limit on the disposal time of the satellite. An analysis of the global compliance of this rule showed that less than 50% actually achieves in staying within the 25 years [4]. Additionally, diverging results from future space environmental predictions is seen regarding the object count, making these guidelines subject to discussion on the validity of the proposed guidelines and their enforcement. Based on nominal future predictions, the 25-year rule would result in a 10% increase in the orbital object count in about 100 years.

An updated version of the Orbital Debris Mitigation Standard Practices was done in 2019 (the first version was set up in 2001), where the main update was an added limitation of “less than 100 objects-year” for debris releases during operations of spacecraft in LEO. This means that a mission with 10 identical mission related debris objects that would follow the operational lifetime, the orbital lifetime post mission must be shorter than 10 years. Another example is when there are 100 identical mission related debris objects following operations, each debris is expected to have a post mission lifetime of 1 year or less [4].

A.1.3. Space Object Evolution

It has been discussed earlier that the number of objects in space is growing. However, it has not been described yet what the current situation is in the space environment. This section will give a short overview of the objects that are currently in orbit and what some causes are of spikes in the object count and how these objects are then evolving. Based on the current market situation, where there is a peaking interest in the space sector particularly in Smallsat constellations, an evaluation is shown that describes the current space sector.

Looking at the evolution of the space market and space technologies it can be concluded that space is becoming more and more populated. Next to the man-made objects in space, it has been clear from the start of our space activity that there is more space debris in orbit than there are operational satellites. Initial research activities aimed at understanding the space environment started in the early 1960s, followed by constant tracking of space objects as well as advancing the space tracking technologies.

The latest space object count report that was set up by ESA showed the amount and classifications as can be seen in Figure 1.1. It needs to be noted that these objects are the catalogued objects, which means that the count is limited to the capabilities of the space surveillance system over time and might therefore be an under-representation of the actual count. Currently, objects smaller than 10cm are non-traceable, but are a danger to orbiting spacecraft as impact of these objects can be lethal to spacecraft.

From Figure A.1 it can be seen that the largest categories in the space object count are UI (Unidentified), RF (Rocket Fragmentation Debris), RB (Rocket Bodies), PF (Payload Fragmentation Debris) and PL (Payload). The largest share of the objects are the payloads (incidentally also the largest mass and area share of all objects in space) and the payload fragmentation debris, where both are gradually increasing over time. From the total number of objects in space, the largest amount is found in LEO [1]. Lowering of the object count can be a result of gradual atmospheric re-entry and orbital decay over time, resulting in the drops of object count

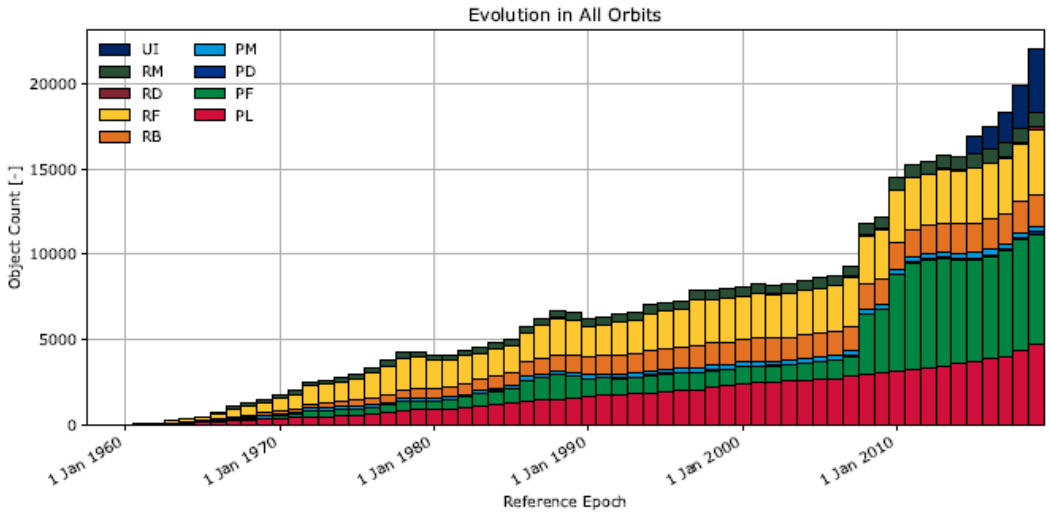

Figure A.1: Evolution of objects in space in all orbits [1], (PL: Payload, PF: Payload Fragmentation Debris, PD: Payload Debris, PM: Payload Mission Related Object, RB: Rocket Body, RF: Rocket Fragmentation Debris, RD: Rocket Debris, RM: Rocket Mission Related Object, UI: Unidentified)

[33].

Even though a clear increase in objects in space can be seen in Figure A.2, the amount of objects that is re-entering the atmosphere is declining, leading to an even larger increase in space objects. Not only does this mean that there is more traffic in space, it also increases the collision risk for the overall space environment.

A.2. Past On-Orbit Collision Events

As discussed before, the number of objects that are in orbit around the Earth is increasing. These objects are made up from orbital particles and man-made objects. With this increase in objects it is inevitable that objects will collide, even with the possibilities of conjunction detection and orbit determination of objects. The objects with possible conjunction risks are divided in two groups, being intact objects and debris. Following the earlier mentioned categories, payload fragmentation debris, rocket fragmentation debris and the unidentified objects fall under the debris category, and payload will fall under the intact objects term.

Up to mid-2013 three accidental hyper-velocity debris-intact collisions have occurred and one accidental hyper-velocity intact-intact collision, where from the debris-intact collision only few catalogued fragments were created. The intact-intact collision on the other hand, of which one satellite manoeuvrable, produced more than 2000 catalogued fragments. Keeping in mind that the increase in space objects is partly due to increased sensitivity of space surveillance sensors, approximately 50% of the 'old' catalogued objects were generated by two catastrophic events, one being intentional and one being unintentional [9].

It is concluded from research on the Iridium 33 and Cosmos 2251 event, that because of the little atmosphere that is seen at the altitude of the collision, most of the fragments that were created will remain in in orbit for several decades. The study found that one fifth of the fragments will have an orbital lifetime of 30 years, where fragments from Cosmos on average will have a longer lifetime because of the high area to mass ratio. The other 70% of the fragments will deorbit over the next 10 to 20 years, which is about the lifetime of the International Space Station (ISS), posing a small risk as the fragments will pass through the orbit of the ISS [5].

Long term evolution of a debris cloud shows that the fragments will first spread out in the ring of the orbit of the original satellite. Because of the non-spherical shape of the Earth, the orbit will slowly precess, causing the ring of debris to form a shell around the Earth at the altitude of the original satellite. Keeping this in mind, the Cosmos fragments will precess faster due to their higher speeds and lower inclinations and will be distributed around the Earth within 3 years. Both the Iridium and Cosmos fragments will however still pose a threat to the satellites that need to pass through this altitude [5].

Next to the unintentional collision as a result of crossing orbits because of a routine space activity, an intentional collision can occur by means of an anti-satellite weapon. These kinetic-energy ASAT weapons have the intention of destroying satellites, which is achieved by physically colliding with the satellite at high

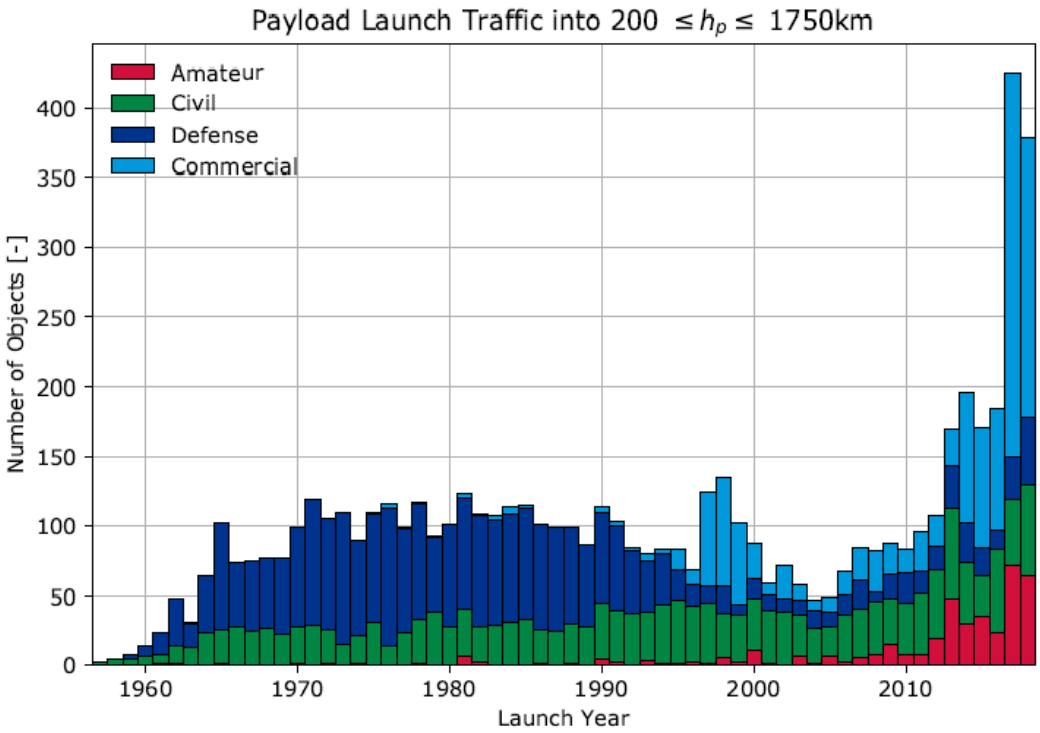

Figure A.2: Payload launch traffic throughout the years categorized by type of mission and/or funding [1]

speeds[34].

An analysis was done on the debris created by China's ASAT weapon test on the FY-1C satellite with the National Aeronautics and Space Administration (NASA) Standard Breakup Model. The estimated amount of debris that was generated is over 2 million particles in all size ranges. In the range of 1 cm to 10 cm an amount of 40,000 objects is estimated and a total of 1,500 objects were estimated to be larger than 10 cm. This is a large number of objects that would be added to the already existing objects in between the 800 km and 900 km altitude. The only previous test that was conducted using a kinetic-energy weapon was in 1985 conducted by the United States, targeting a satellite at 500 km altitude. Even though both tests created about the same amount of debris, the debris from the U.S. test would decay within a decade because of a lower altitude, while the debris from the Chinese test is expected to remain in orbit for multiple decades [34].

A more recent event in March 2019 involved the breakup of an Indian satellite at an altitude of 270 km, Microsat-R, on which they tested their first ASAT missile. Aiming to minimize the hazard of post-impact debris, test parameters were chosen carefully such that the debris would re-enter the atmosphere within 45 days. From this event 400 pieces were identified by NASA, where the North American Aerospace Defense Command (NORAD) published information on 83 newly registered objects, of which 69 of these fragments are at an altitude ranging from 400 to 2265 km [35].

A.3. Evolution of the Space Sector and Environment

The last few years have seen a tremendous growth in space activity, where this new space evolution is oftentimes referred to as NewSpace. More and more companies want to get knowledge based on satellite imagery or want to have their own specified satellites in space. This resulted in an increase in the commercial side of spaceflight. This not only included satellites, but also launch activity. More and more start-ups were founded to accommodate for the growing interest in launching satellites into space. Where previously satellites were only used for missions from space agencies or had specific scientific goals, private companies are now also gaining interest and are succeeding in setting up their space business.

A.3.1. General Space Market

Together with the increase in technological knowledge and connectivity around the world, rapid developments in the space sector have also been happening. Simultaneously with the last industrial evolution, also

known as 'Industry 4.0', the new space era is also evolving with these innovations and resulting in interaction between the private, political and societal aspects of the space industry. The results of this is smaller satellites, where desired with COTS part that are cheaper because they have been produced in larger amounts. But not only this, developments have been happening in five different categories in terms of space activity [6].

1. The first category in which change is apparent is that more and more companies want to have access to space. Accessibility to space has been made easier and cheaper in three different subcategories. Together with this, a new-found interest in making structures reusable can be observed, where SpaceX is a spectacular example of successfully reusing their rocket boosters.
2. The second category in which development is growing is the part where the need for more access to data from Earth observation.
3. Three main factors to accommodate for this growing sector are the low-cost manufacturing developments, more revisit orientated than legacy missions and the investments in data analytics and artificial intelligence. Next to Earth observation, communication satellites and services are also emerging in the form of large scale constellations. These constellations are driven by the possibility of global connectivity with low latency. This sector is however not only growing in terms of start-ups, but also the more established communication companies are joining this trend, like Boeing and OneWeb for example. Adding to the easier accessibility to space as well as more opportunities to gain insights by looking down from space, there is also a category that has increased operations and developments in itself regarding debris mitigation and end-of life disposal, in-orbit servicing (IOS) and in-space manufacturing.
4. The fourth category which is experiencing growth is the interest in space exploration. In the past, the main parties that would set up mission to the Moon, other planets and outer space were space agencies and scientific institutions.
5. The fifth and last category can be seen in the production and supply chain of materials and parts. Due to the growth in small satellite business, a different kind of supply chain and manufacturing is needed, where the legacy supply chains also need to adjust to accommodate for this emerging new market of satellites.

Altogether, from the eagerness to obtain more data to emerging businesses and new ways to use space, it can be concluded that space is about to get more and more crowded. It is not only a matter of future innovations in the space sector, but it also depends on policies and regulations. Even if it is early to predict what will exactly happen in terms of innovations in small satellite manufacturing or putting those satellites in space more easily, it can be seen that companies are starting to move toward space.

A.3.2. Constellation Market

Based on multiple forecasts and reports on the growing space industry, the general consensus is that the number of constellations will also increase over time [36], [37]. Given the technological advances as described the previous section, it becomes clear that the shift is towards smaller satellites in swarms. The constellations that are in development and in deployment are shown in Table A.1. Assuming that all these constellations will be launched and deployed, a total of nearly 20.5K new satellites will be launched in LEO, which is excluding the single satellite missions[38], and of which approximately 13.000 have been approved by the Federal Communications Commission (FCC)[37]. For comparison, throughout the history of the space age a total of around 8100 payloads have been put into Earth orbit, of which about a quarter is still active [36]. Even if most of the constellations that are listed in Table A.1 will not be launched, the amount of payloads in space will be more than doubled.

Following a report from PricewaterhouseCoopers (PWC), it can be seen that this increase will be quite significant in the coming few years in Figure A.3, where the amount of single-mission launches will start to minimize compared to the constellation launches [39]. Not only this, 80% of the Smallsat demand is expected to be driven by commercial markets in Earth Observation and communications constellations.

The operational lifetimes that are expected from these constellations in LEO is 5-10 years, after which the satellites are deorbited. This deorbiting can take considerable time, ranging from months to years, and will pass operational orbits where other satellites operate (or even the ISS) [36]. Depending on the need of these satellites that are deorbited, these satellites need to be replaced, again resulting in launches and traffic crossing different operational orbits and collision risks. The constellations that are being designed and planned for the coming decades are expected to comply with the debris mitigation guidelines, where the spacecraft needs to be removed from orbit within 25 years after operation. Many of these constellation satellites that are being planned even plan on deorbiting within 5 years after retirement [40].

Table A.1: Current Constellation Projects in Development and Deployment [38]

Current and Planned Constellation Projects	# of Satellites	Satellite Mass [kg]	Altitude [km]	Project Status
Amazon Kuiper	3,236	Unspecified	590-630	Development
Astrocast	80	3/6U CubeSats	500-600	Demonstration
Boeing V-Band	2,956	Unspecified	1,200	Development
Globalstar 2	24	700	1,410	In Operation
Hongyan	320	Unspecified	1,100	Demonstration
Hongyun	156	250	1,000	Demonstration
Iceye	18	80	587	Deployment
Iridium-NEXT	72	860	780	In Operation
Kepler	140	3U CubeSats	575	Development
LeoSat	108	1,000	1,432	Suspended Operations
OneWeb	648	147	1,200	Deployment
Planet	150	3U CubeSats	370-430	In Operation
SpaceX Starlink	4,425 (init.) (+7,518)	260	1,100-1,325 340 (add. Sats)	Deployment
Spire	175	3U CubeSats	385-650	In Operation
Swarm	150	0.25U CubeSats	300-550	Demonstration
Telesat LEO	117	Unspecified	1,000	Development
Theia	120	Unspecified	800	Development

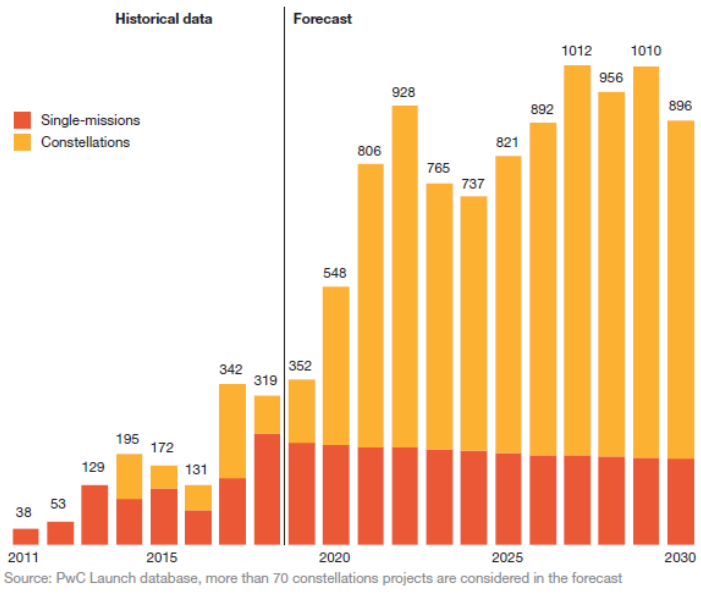

Figure A.3: Number of constellations and Smallsats (<500kg) for single missions forecast [39]

A.4. Effect of Constellation Traffic on the Future Space Environment

With the evolving space environment and business, it is observed that the number of constellations is growing. From a quick look at [41] it can be observed that 32 constellations have not been launched yet, of which 8 have information on the size of the constellation. Next to this, from the 30 constellations that announced to have 100 or more satellites, 6 have no launch announcement yet or have been cancelled. From the remaining 24 constellations, 21 constellations have one or more satellite in orbit and 3 already have more than 100 satellites in orbit. Additionally, 48 constellations and counting have been planned for 2019 up to 2022. Following a request from the FCC for Amazon to provide collision risks assessment of their Kuiper System satellites in case 5%, 10% or 15% of their constellation would fail, a total over the different shells resulted in 6.1%, 12.3% and 19.4% respectively. These numbers indicate a high risk in collisions in case deployment of the constellation fails [42].

Given the growing amount of spacecraft post mission disposal guidelines were set up, where the increasing number of constellations emphasize the need to follow these guidelines. Following the newly updated Orbital Debris Mitigation Standard Practices from 2019, three additional practices have therefore been added regarding large constellations [4]:

1. Reliability in the PMD should be at greater than 90%, where the goal needs to be at 99% or better
2. The reliability threshold of the PMD should be based on the orbital location, mass, collision probability and other relevant parameters
3. The preferred PMD option is the immediate removal

However, it was also noted that these guidelines are difficult to apply to all constellations, as not all constellations are set up in the same way [4]. For example, a failed spacecraft at an altitude of 900 km will not naturally decade for more than 1,000 years, while a spacecraft at an altitude of 700 km will naturally decade in about 50 years. This means that a higher PMD reliability would be needed for the spacecraft at the higher altitude. Additionally, collision probability is another factor that is impacting constellations at different altitudes, where a constellation at 850 km altitude has a collision probability of 10 times higher than a constellation at 1,300 km.

Another study was done on the response of the space environment on the deployment of large satellite constellations, combined with the PMD guideline compliance success factors of these large constellations [43]. The constellation that was introduced in the modelled space environment comprised of 1080 satellites with a 5-year design life, at an altitude of 1100km in 20 orbital planes with an inclination of 85°. It was assumed that all collision avoidance manoeuvres were performed successfully.

The trends of 50%, 80%, 90% and 100% compliance to the PMD guidelines were compared, of which the simulation results can be found in Figure A.4. Four different phases were seen from the results.

The first phase takes about 30 years and shows a steep increase in population, ranging from the launch of a constellation until the start of the re-entry phase. The second phase, taking about 20 years, shows about the same rate for the satellites that are being replaced compared to the re-entry rate of the satellites. This means that the number of objects stays about the same. This is followed by the third phase where the constellation starts to deorbit and therefore a decrease is seen in the number of objects (success rate higher than 50%), taking about 25 years. The last phase shows a gradual population growth, which depends on the interaction of the background population with the constellation satellites that were not able to deorbit[43].

Comparing the different disposal success rates, it was found that a clear increase happens in all cases. The interaction with the background population of the satellites that were not able to deorbit shows that the number of objects accumulates, where the 50% disposal rate showed a doubling of the number of objects in 30 years and a five-fold increase by the end of the projection period. Given the initial conditions for this analysis that only one constellation of 1080 satellites would be added, it must be noted that this underestimates the prediction as it is expected that more than one constellation will launch.

Based on the scenario without post mission guidelines, the number of objects larger than 10 cm in LEO will increase with about a factor 3 in the coming 100 years [44]. Even though a large part of the objects in space are explosion fragments, collision fragments will grow and be the main share of objects in space. On average, it is predicted that a total amount of 24 collisions will occur over the coming 100 years. From these 24 collisions, 14 are expected to happen between intact-fragment objects, 8.4 are expected to happen between intact-intact objects and 1.3 are expected to happen between fragment-fragment objects. Although intact-fragment seems to be the biggest share of the expected amount of collisions, the division between catastrophic and non-catastrophic seems to be the most important in terms of what needs to be expected in the coming 100 years.

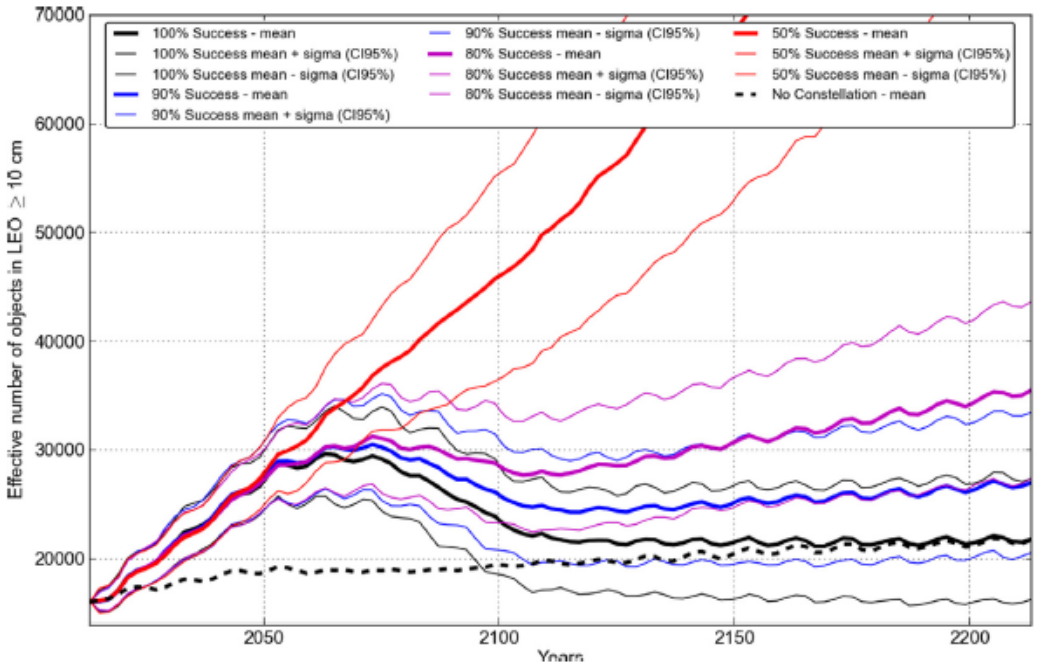

Figure A.4: Effect on object count prediction in LEO from PMD compliance rates in constellations [43]

In the event of a catastrophic collision, the target as well as the projectile are completely fragmented, while in a non-catastrophic collision results in only a small fraction of the target being chipped away, where a catastrophic collision has an impact of 40 J/g energy to mass ratio. Of the total expected collision between intact-intact and intact-fragment, the number of catastrophic collisions between intact objects is expected to be as high as 7.9 while intact-fragment goes to 4.5 from the 13.3 total catastrophic collisions that is predicted. From this it can be seen that the majority of catastrophic events are between intact-intact objects [44]. Together with the two objects being destroyed, two debris clouds will be formed instead of only one of the two being chipped.

Another simulation was done on the expected collision rate for the next few years. From this it was found that the collision risk has multiplied by 5.0 compared to 40 years ago, which closely matches the growth in objects in space. The expected collision probability up to 2030 is highest for one collision with a probability of 34.7%. The expected collision probability up to 2040 is highest for two collisions with a probability of 25.7% [9]. The collision probability among objects larger than 10 cm and intact bodies will increase in the coming decades, which is the reason why post mission disposal rules need to be implemented. However, even with the implementation of strict post-mission lifetime limitations the short-term situation will not improve. This is why an implementation of collision avoidance practices needs to happen among operators of manoeuvrable spacecraft, which could cut up to 30% of the average expected intact-intact collisions. Additionally, approximately 15% of the intact-fragment collisions can then be cut [9].

B

Constellation Design Parameters

This chapter will provide more information on the constellation design parameters. As these parameters are assumed to be set before the constellation is launched and are based on design, the influence of a manoeuvre will not disturb the design of the constellation. The parameters that are disturbed by a manoeuvre are discussed in Chapter 3.

Given that no set rules are available for the design of constellations, certain parameters are key to constellation design. One of the most important parameter for constellation design is the swath width. This parameter determines the coverage of the satellites of the constellation, which is the main driving reason to use a constellation over single satellite missions. An additional parameter that is of much importance is the eccentricity of the orbits of the satellites. As most constellations are chosen to have the lowest eccentricity close to zero as possible because of the added complexity and therefore costs of the constellation, this will not be one of the driving factors for this thesis.

Four primary parameters in constellation design will be discussed here, which are swath width, altitude, inclination and node spacing. In order to know which parameter to use for further calculations, it is important to get a deeper understanding of the influence of these parameters. It is therefore that an extensive analysis is done on what the effect of certain parameters is on the constellation.

B.1. Swath Width

This parameter is also called the maximum Earth central angle and is the key parameter in determining the coverage of the satellites of the constellation [13]. This coverage can be seen as a circle of coverage or a street of coverage, determining the spacing between the satellites.

The swath width is a function of two other parameters, being the altitude and the minimum elevation angle. The relation between the three parameters can be seen as follows. If the altitude increases, the area that is observed by the satellite also increases, therefore increasing the swath width. Depending on the minimum elevation of the satellite, it can also either observe a larger or smaller area. The lower the elevation, the more area is covered, hence the swath width is increased by increasing altitude and reducing the elevation angle. Figure B.1 shows three figures with the same swath width, but different altitudes. The first system, B.1(a), shows a swath width at an altitude of 525 km and minimum elevation angle of 5 degrees. The second system, B.1(b) shows the same swath width but with an altitude of 735 km and an elevation angle of 10 degrees. It can be seen from these two figures that there is an overlap in the coverage, which can not be seen in the third figure. The third figure shows the swath width at an altitude of 1225 km and an elevation angle of 20 degrees. All three orbits have a swath width of 4000 km. The overlap of the swaths is something that is desired, as it results in total coverage without coverage gaps. The swath width can be seen in Figure B.2, where the minimum swath width is determined by the maximum Earth central angle and the spacing between the satellites. The minimum elevation angle is determined by the performance of the payload. The performance of the payload is oftentimes contradicting to the constellation design, as a low elevation angle is disadvantageous for the payload, while it results in a higher coverage of the satellites and less costs.

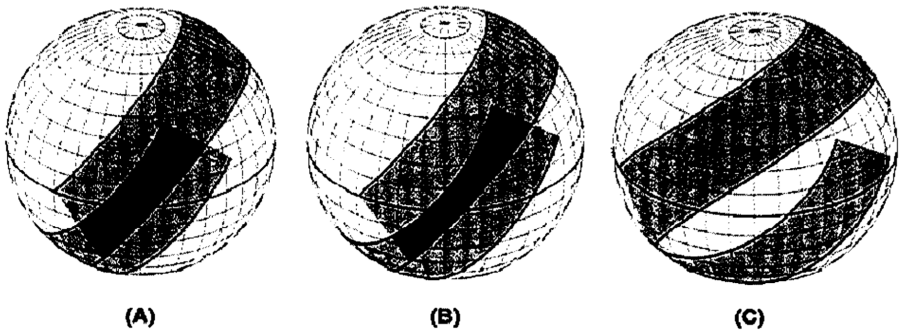

Figure B.1: Similar swath widths at three different altitudes [13]

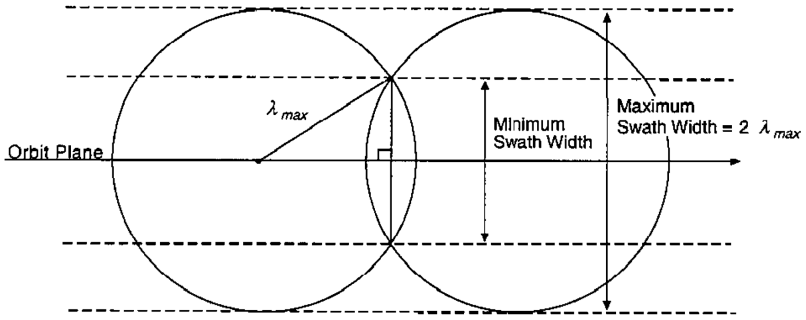

Figure B.2: Minimum and maximum swath width with relation to the width of the street of coverage [13]

B.2. Altitude

For the satellites to have the same orbital period and have the same relationship with respect to each other, the altitude needs to be uniform over the constellation. This will then result in the same pattern over time and therefore repeat itself within a certain number of orbits. Benefits of keeping this altitude similar for all satellites is that it results in less complexity when designing the constellation as well as a similar node rate, therefore maintaining the similar relative orientation. The higher the altitude, the less amount of satellites are needed in the constellation, as was also seen in the swath width. In case the swath width as a result of payload is fixed, the altitude becomes the most important parameter in constellation design. Another important part of constellation design is the number of planes that are needed, which depends on the altitude of the satellites. Figure B.3 shows the altitude that can be achieved with a certain amount of planes at a certain minimum elevation angle to reach full Earth coverage. With an increasing minimum elevation angle, the swath width becomes smaller, hence a higher amount of altitude planes is needed to achieve full Earth coverage. With this increase in plateaus, the costs of the constellation also increases as well as the complexity. On the other hand, with lower inclinations, the spacing between the subsequent nodes at the equator becomes larger and therefore needing less planes. It needs to be noted that the altitudes as shown in Figure B.3 might be lower than is actually needed for the altitude of the satellites, as it needs to comply with the station keeping requirements and thus the station keeping box. Regarding the amount of planes, next to the requirements named in Figure B.3, it depends on a multitude of other parameters and requirements of the constellation. This figure can therefore be used for a first order approximation for the coverage, but depends on the requirements per constellation setup and payload. Another important parameter is the launch capability and the radiation environment. However, as this research looks at satellites that already are in orbit, this is not taken into account in this thesis.

B.3. Inclination

The inclination has a large influence on the total coverage and is a function of the altitude. In constellation design, this is for a large part determined by the oblateness of the Earth and the implications of the J_2 effect.

Minimum Elevation Angle = 0 deg

Inc.	90 deg	75 deg	60 deg
Planes	Altitude (km)	Altitude (km)	Altitude (km)
10	80	74	59
9	98	92	73
8	125	116	93
7	164	153	122
6	225	209	167
5	328	305	241
4	526	486	382
3	987	906	698
2	2,642	2,354	1,690

Minimum Elevation Angle = 5 deg

Inc.	90 deg	75 deg	60 deg
Planes	Altitude (km)	Altitude (km)	Altitude (km)
10	170	162	137
9	200	189	160
8	240	227	192
7	297	281	235
6	384	361	301
5	524	493	406
4	785	734	596
3	1,379	1,275	1,008
2	3,507	3,132	2,276

Minimum Elevation Angle = 10 deg

Inc.	90 deg	75 deg	60 deg
Planes	Altitude (km)	Altitude (km)	Altitude (km)
10	265	253	218
9	306	292	251
8	361	344	295
7	438	416	355
6	552	523	443
5	736	695	582
4	1,069	1,004	828
3	1,821	1,691	1,353
2	4,573	4,078	2,966

Minimum Elevation Angle = 20 deg

Inc.	90 deg	75 deg	60 deg
Planes	Altitude (km)	Altitude (km)	Altitude (km)
10	475	454	397
9	543	519	451
8	633	604	524
7	757	721	622
6	939	892	764
5	1,228	1,163	986
4	1,751	1,648	1,373
3	2,946	2,735	2,197
2	7,804	6,860	4,857

Figure B.3: Reachable altitudes based on varying inclination, elevation angle and orbital planes [13]

This J_2 effect causes the nodes and arguments of perigee to rotate rapidly, which will only result in a larger problem is if this does not occur similarly in the whole constellation. The rate of this rotation is determined by a combination of the inclination, altitude and eccentricity of the satellite orbits. If these three parameters are not uniform throughout the constellation, the rotation of the nodes and argument of perigee will not shift at the same rate in the constellation and will cause offsets.

B.4. Node Spacing

In a constellation the location of the ascending node is oftentimes irrelevant due to the movement of the constellation with respect to inertial space and the Earth surface. Only if the satellites are aimed to have a repeating ground track orbit, the ascending node becomes important.

As was mentioned before, multiple parameters determine the node spacing and rotation of the nodes. This rotation in the nodes and node spacing is not a problem, as long as the constellation rotates at the same rate with respect to itself. Different types of node spacing can be seen, where the coverage becomes a result of the type of node spacing. The mostly evaluated type of node spacing is the equal spacing along the equator. Depending on the application of the constellation, this might not be the best type.

C

Conjunction Event Detection

This chapter discusses the steps in which conjunctions are detected. Even though this is not part of the research, this chapter will provide background on the parameters involved and what criteria need to be passed in order to have a conjunction event.

The first order determination of conjunction events is done in an altitude filter, checking for intersecting orbits. After this the orbit geometry check is done, where the intersecting planes are determined. For these intersecting planes, the closest approach distance is determined. The predicted conjunction events within a spherical control volume of radius R_c are kept as potential fly-bys. This is then stored with a symmetric time window to have a safety distance $|\Delta\overline{r}| \leq R_c$. Using this stored conjunction event in the symmetric time window an orbit phase filter is applied, where the time windows of both the target and risk object will be checked for overlap. If an overlap is detected, the time of closest approach and local minimum distance can be found by analyzing for a zero-transition of the range rate between the two objects ($\frac{\Delta\overline{v}\Delta\overline{r}}{\Delta r} = \dot{\rho} = 0.0$).

A sieving algorithm can be set up to find the close conjunction and conjunction events after the altitude range filter is applied [14]. This sieving algorithm consist of multiple checks, where the volume radius is used to check against the range rate.

The first radius is found by adding an additional safety distance, which includes the escape velocity $v_e = \sqrt{2\mu/r}$ times the time step Δt:

$$R_{c,1} = R_c + v_e \Delta t \tag{C.1}$$

This check is done in the following sequence

$$\rho_X \leq R_{c,1} \tag{C.2}$$
$$\rho_Y \leq R_{c,1} \tag{C.3}$$
$$\rho_Z \leq R_{c,1} \tag{C.4}$$
$$\rho \leq R_{c,1} \tag{C.5}$$

where a close conjunction is not possible if all criteria are met. The orbits that passed these criteria will be checked for a control volume radius which includes the curvature:

$$R_{c,2} = R_c + g(\Delta t)^2 \tag{C.6}$$

where g is the gravitational acceleration of the Earth. This formula is checked as follows:

$$R_{c,2} \leq \sqrt{(\Delta r)^2 - (\Delta\overline{r} \cdot \Delta\overline{v}/\Delta v)^2} \tag{C.7}$$

The third check includes the effective relative velocity as below:

$$R_{c,3} = R_{c,2} + \frac{1}{2}|\Delta\overline{v} \cdot \Delta\overline{r}/\Delta r|\Delta t \tag{C.8}$$

which will be checked against the following criterion:

$$\rho \leq R_{c,3} \tag{C.9}$$

These three sieves are supposed to clear most of the orbits that passed the altitude filter. From the orbits that still passed, the time of closest approach t_{tca} is analyzed and determined with $\Delta r_{tca} = \rho_{tca}$. The time of closes approach is then determined with

$$\Delta\overline{v}_{tca}\Delta\overline{r}_{tca}/\Delta r_{tca} = \dot{\rho}_{tca} = 0.0 \qquad \rightarrow \qquad t_{tca} \tag{C.10}$$

where the final check for the sieving steps is as follows:

$$\rho_{tca}(\dot{\rho} = 0.0) \leq R_c \tag{C.11}$$

These sieving steps altogether reject about 99% of all analyzed conjunctions [14].

For the time of closest approach, the ranges and velocities of the target and risk object can be expressed in the orbit related coordinates $\overline{U}$, $\overline{V}$ and $\overline{W}$. This transformation is done as described in the previous section, where the coordinates will be mapped from $(X, Y, Z) \rightarrow (U, V, W)$. First the position and velocity are expressed in the (X, Y, Z) frame:

$$(\Delta\overline{r}_{tca})_{X,Y,Z} = (\overline{r}_r(t_{tca}) - \overline{r}_r(t_{tca}))_{X,Y,Z} \tag{C.12}$$

$$(\Delta\overline{v}_{tca})_{X,Y,Z} = (\overline{v}_r(t_{tca}) - \overline{v}_r(t_{tca}))_{X,Y,Z} \tag{C.13}$$

In order to then find the relative position and velocity in the (U, V, W) frame, the above vectors can be substituted in the following equations:

$$(\Delta\overline{r}_{tca})_{U,V,W} = (\Delta\overline{r}_t)_{U,V,W} = (R_t)_{U,V,W}(\Delta\overline{r}_{tca})_{X,Y,Z} \tag{C.14}$$

$$(\Delta\overline{v}_{tca})_{U,V,W} = (\Delta\overline{v}_t)_{U,V,W} = (R_t)_{U,V,W}(\Delta\overline{v}_{tca})_{X,Y,Z} \tag{C.15}$$

where $(R_t)_{U,V,W}$ is as described in Equation 3.23.

It was found that the above described sieving algorithm is more efficient and robust than previously found methods where the filters evaluated the altitude, orbital plane intersection, phasing of the orbit and the minimum approach distance.

D

Optimization Verification Worked Out

Following the setup of the optimization (DE method), the code was tested to check the validity. The sections below discuss the results that were found.

First the Beale function will be discussed, follows by the Levi N.13 function. The third function that was tested is the Himmelblau function and last but not least, the McCormick function was used to test the code. A summary of the results can be seen in Chapter 6.4.

D.1. Beale Function

The first function that was used to verify the code was the Beale function, which is described below. This function was chosen as a first check, as it has one global minimum and is made up of two unknowns in the x and y frame.

$$f(x,y) = (1.5 - x + xy)^2 + (2.25 - x + xy^2)^2 + (2.625 - x + xy^3)^2 \tag{D.1}$$

The function can be seen in Figure D.1, where the global minimum can be seen in Figure D.2 with a restriction in the max value in z axis to get a better indication of the minimum.

The global minimum is found on the following points and range:

$$f(3, 0.5) = 0 \qquad [-4.5 \leq x, y \leq 4.5] \tag{D.2}$$

which is also depicted in the two figures above.

Following the written DE algorithm in Matlab, the first test function that was implemented was the Beale Function. With only one clear minimum, convergence was found in the correct data points. The iteration of one of the runs can be seen in Figure D.3, where convergence is reached after about 50 iterations. Figure D.4

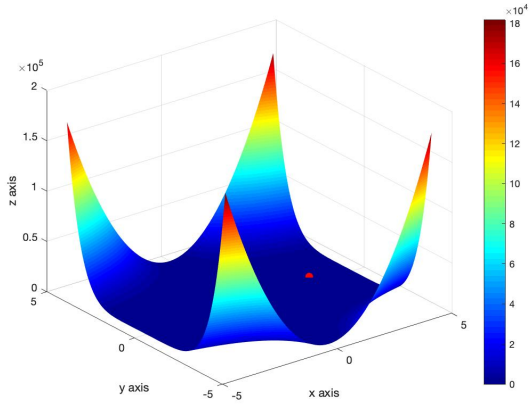

Figure D.1: Beale function

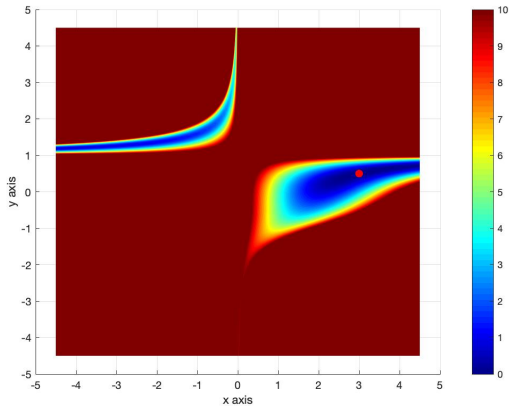

Figure D.2: Global minimum of the Beale function in the (x, y) frame

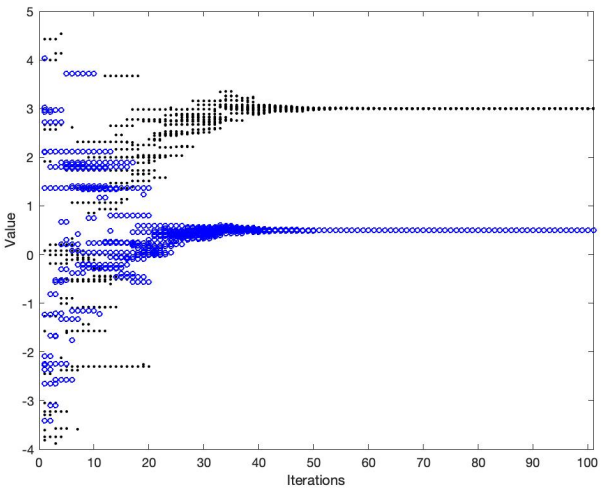

Figure D.3: Convergence to the minimum of the Beale function using the DE algorithm

shows the result of the 50 runs that were done, with each 100 iterations. All 50 tries done in the results shown below were done in 100 iterations, with $N = 15$, $F = 0.5$ and $CR = 0.5$.

The upper two tiles of Figure D.4 show the separate values of x and y respectively for the 50 runs of 100 iterations. It can be seen that still some of the values did not converge (in this case 3 runs of the 50), but that the majority of the runs resulted in the right minimum. From varying some of the parameters that can be set, it can be seen that the smaller the population, the less converged the results are. However, it needs to be noted that a higher value for N does not necessarily mean a higher convergence rate.

Another thing that was found with this function was that a combination of a high CR value and a low number of vectors in the population results in less converged values. On the other hand, a high number of vectors in the population with a low CR value also shows a lower rate of convergence. This means that it takes some runs to get the best values with which the code needs to be ran.

D.2. Levi Function N. 13

The second function that is used to verify the code is the Levi function N. 13, of which the formula is shown below:

$$f(x,y) = \sin^2 3\pi x + (x-1)^2(1+\sin^2 3\pi y) + (y-1)^2(1+sin^2 2\pi y) \tag{D.3}$$

This optimization problem was chosen because of the sinusoids, which causes multiple smaller local minima and one global minimum as shown in Figure D.5 and D.6. Again restricting the maximum value in Figure D.6 shows the global minimum.

The global minimum can be found in the following coordiantes and range:

$$f(1,1) = 0 \qquad [-10 \leq x, y \leq 10] \tag{D.4}$$

Following the own code that was written, Figure D.7 and D.8 were found. Following the sine function, it was tested if the DE algorithm could find the minimum for this optimization problem. It can be seen there that convergence is reached quite early, where also the correct value was found. Figure D.8 in particular shows the result of 50 consecutive tries of 100 iterations. From this it was seen that four x values did not converge to the correct value in 100 iterations, however the y values did.

It was also found by varying the population size, that the amount of times the convergence reached the correct value increased. Varying the CR value then did not make a difference in the amount of times the correct value was found. Only lowering the amount of iterations showed that the minimum value was not reached.

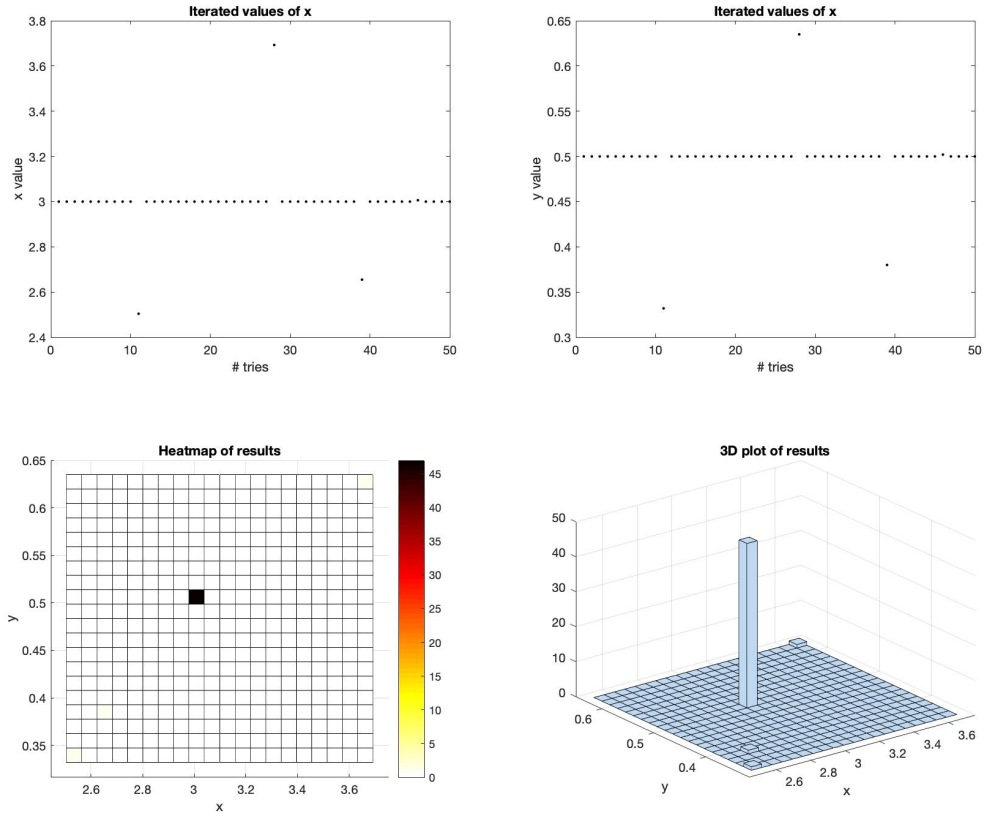

Figure D.4: Final results of multiple runs of the DE algorithm for the Beale function

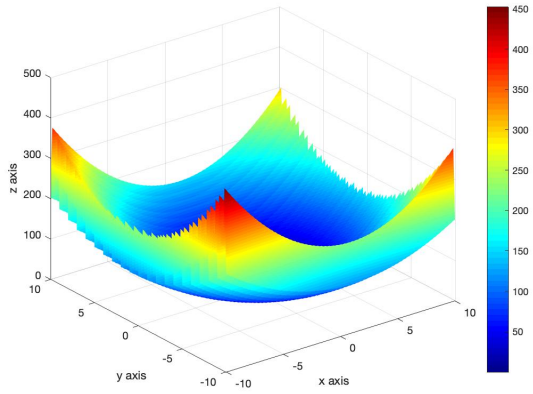

Figure D.5: Levi function N. 13

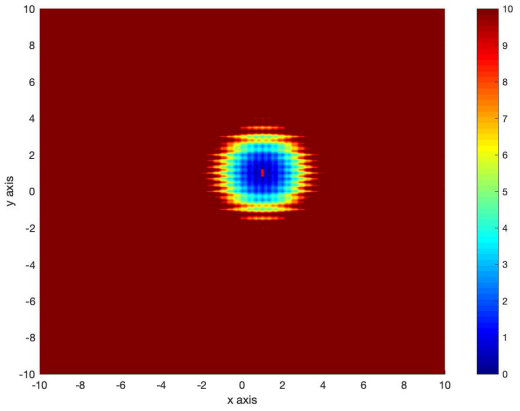

Figure D.6: Global minimum of the Levi function in the (x, y) frame

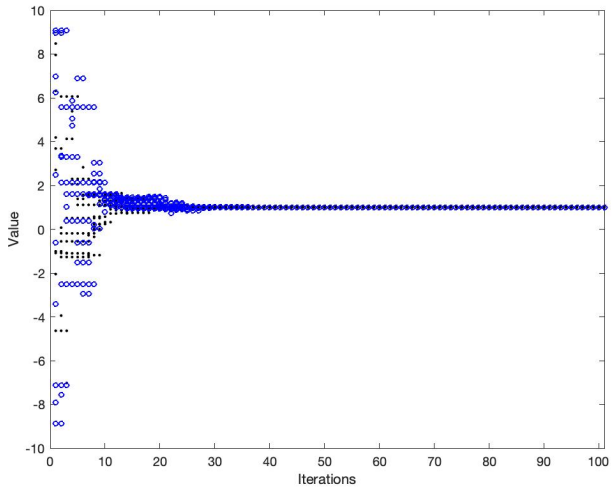

Figure D.7: Convergence to the minimum of the Levi N.13 function using the DE algorithm

D.3. Himmelblau's Function

After the successful test of the previous two optimization function, the Himmelblau's function was used to test the algorithm. The Himmelblau function is described below

$$f(x,y) = (x^2 + y - 11)^2 + (x + y^2 - 7)^2 \tag{D.5}$$

and was chosen because of the four minima it has. As the code can be set to multiple unknowns, it is possible that all unknowns converge to the same local minimum. It is therefore that the code needs to be run multiple times to see what the overall most occurring outcome is, to see the different minima.

The four global minima can be seen in Figure D.9, where the restricted view in the (x, y) frame can be seen in Figure D.10 and shows the minima more clearly.

The four minima are found in the following coordinates and range:

$$\text{Min} = \begin{cases} f(3.0, 2.0) & = 0.0 \\ f(-2.805118, 3.131312) & = 0.0 \\ f(-3.779310, -3.283186) & = 0.0 \\ f(3.584428, -1.8481262) & = 0.0 \end{cases} \qquad [-5 \leq x, y \leq 5] \tag{D.6}$$

The third function that was tested in the written code is the Himmelblau's function, where four minima can be found. As the parameters that need to be found are four variations on the x and y value, it was chosen

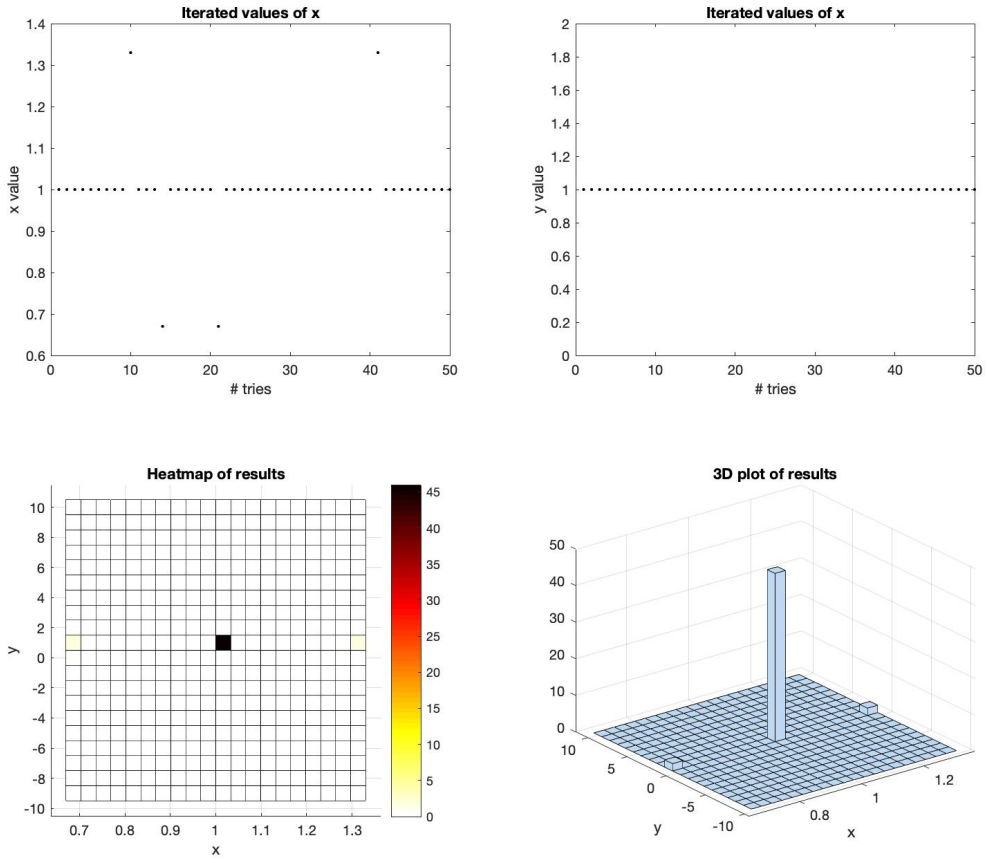

Figure D.8: Final results of multiple runs of the DE algorithm for the Levi N.13 function

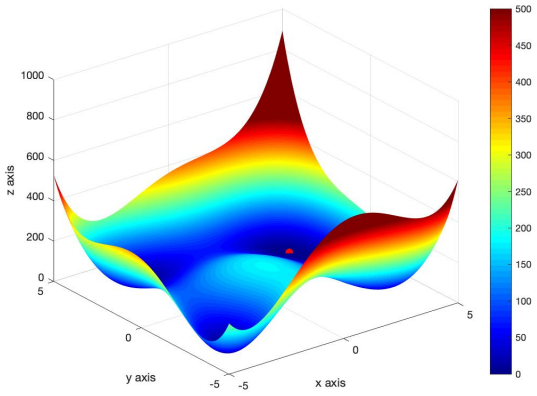

Figure D.9: Himmelblau's function

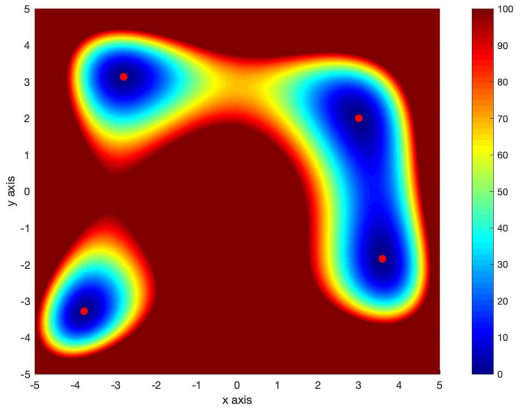

Figure D.10: Global minima of the Himmelblau's function in the (x, y) frame

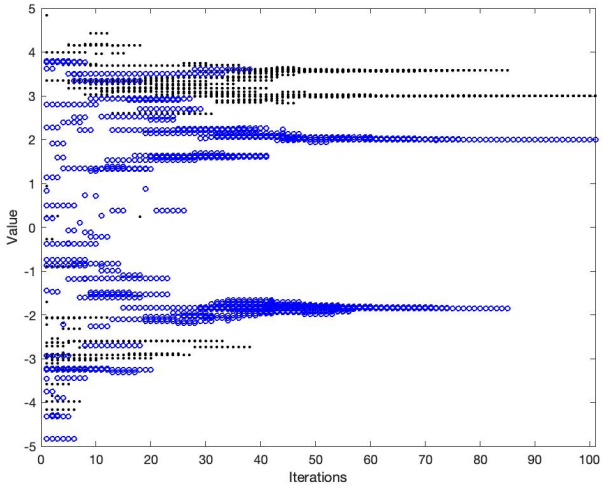

Figure D.11: Convergence to the minimum of the Himmelblau function using the DE algorithm

to perform multiple runs. Multiple runs were found to converge to different values, and in the end would get close to the four minima of the function. D was therefore set to 2, still using 100 iterations and 50 runs.

As is seen in Figure D.11 convergence is only reached in the last few iteration steps, which could be explained by the four different minima that can be found for this function. From the overall results in Figure D.12 it can be seen that all four values are found. However, some were found more often than other values, which also varied per try. The most found value is $(3,2)$, which is also seen when the code is run more often.

When increasing the value for N, it can be seen that less different results are found e.g. only two or three of the four minima is found. The same was found for lowering the CR value, where a lower CR value showed less minima and also a slight increase in converged values. Increasing the value for CR however showed the same results, being that a higher value showed less minima.

From these runs it can be concluded that multiple runs are needed to see if more than one minimum can be found. Additionally, combined with the findings above, a certain range needs to be inspected to have the most favorable convergence rate as well as the correct values.

D.4. McCormick Function

The last function that was used to verify the algorithm is the McCormick function, described below:

$$f(x, y) = \sin(x + y) + (x - y)^2 - 1.5x + 2.5y + 1 \tag{D.7}$$

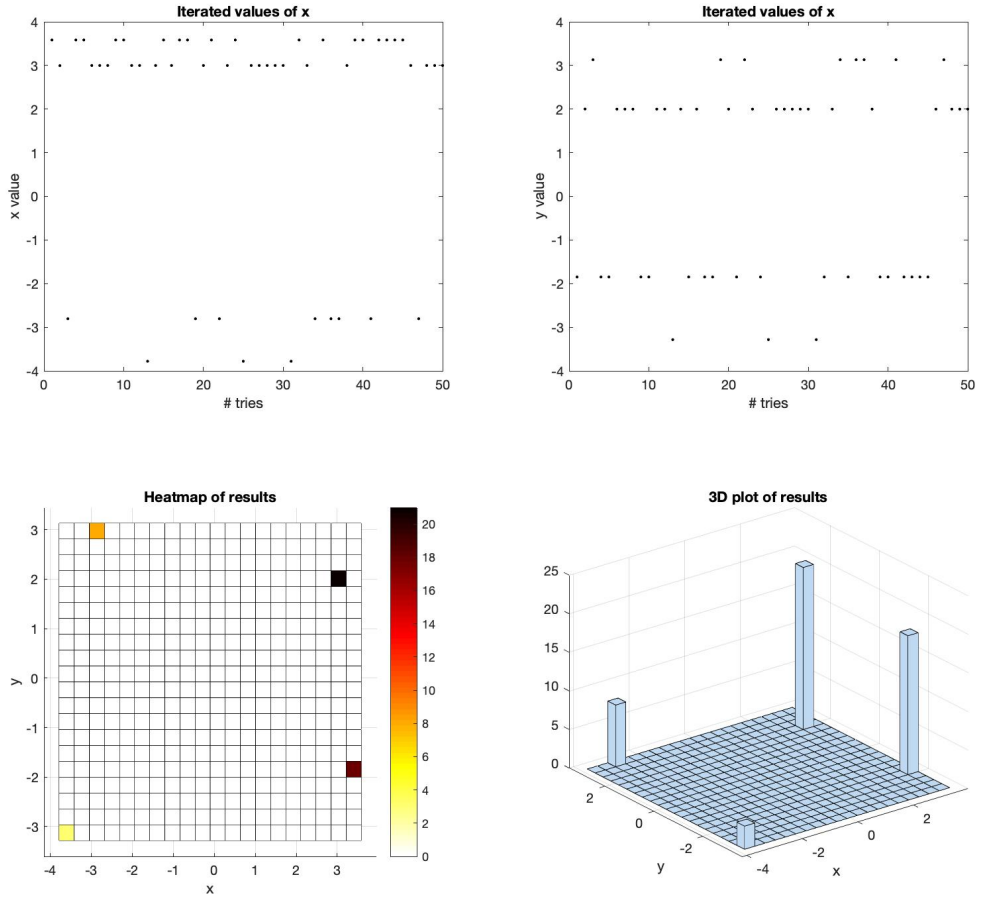

Figure D.12: Final results of multiple runs of the DE algorithm for Himmelblau function

which was chosen because of the non-zero global minimum it has. Additionally, it also has a local minimum that could potentially converted to if the search space is narrowed down too early. This can be seen in Figure D.13, where a more restricted view of the maximum value of the z axis shows the local minimum next to the global minimum in Figure D.14.

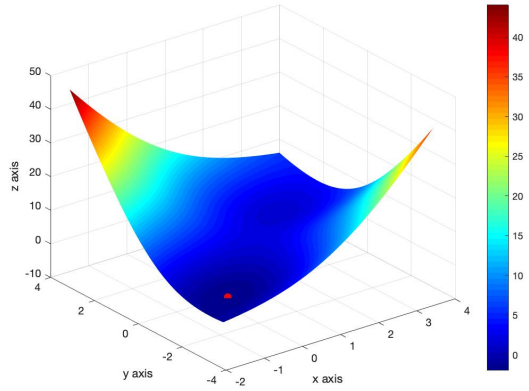

Figure D.13: McCormick function

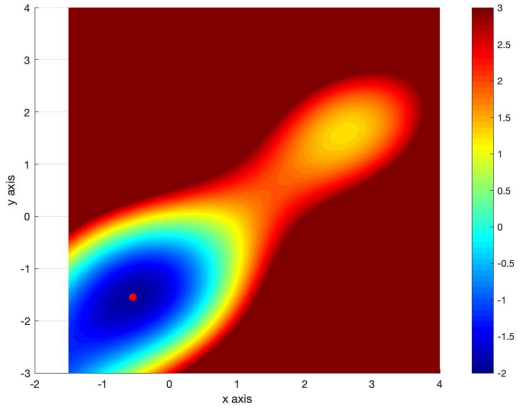

Figure D.14: Global minimum of the McCormick function in the (x, y) frame

The global minimum is seen in the following coordinates and range:

$$f(-0.54719, -1.54719) = -1.9133 \qquad [-1.5 \leq x \leq 4] \tag{D.8}$$

$$[-3 \leq y \leq 4] \tag{D.9}$$

The last function that is tested with the written DE algorithm is the McCormick function, which has a non-zero minimum. As can be seen from the convergence of one of the runs in Figure D.15, the correct value is found quite early on in the iteration process. However, as can also be seen in Figure D.16, the lowest value is not found that easily.

Similarly as above, the amount of iterations was set to 100 with 50 tries. Increasing the amount of tries to 100 shows that indeed the correct value is found more often, however, the minima that are found do seem to have a small off-set. Increasing the amount of tries to 150 shows that the other local minimum is also found.

Increasing the number of vectors in the population shows a wider range of not converged solutions to the global minimum. In contrast, lowering the number of vectors to 4 (which is the minimum number of vectors that is allowed for this algorithm) shows a lower range and also a higher conversion rate. Lowering the CR value shows that a larger amount of iterations converges to the correct value. However, still a small offset can be seen in some of the results. Increasing the value of CR shows results that are overall closer to the global minimum. However, most of the values still have an offset of the global minimum value.

This shows, together with the pervious analyses, that the method is suitable but needs to be tailored and ran a few times to find the global minimum in case the minimum is a non-zero value.

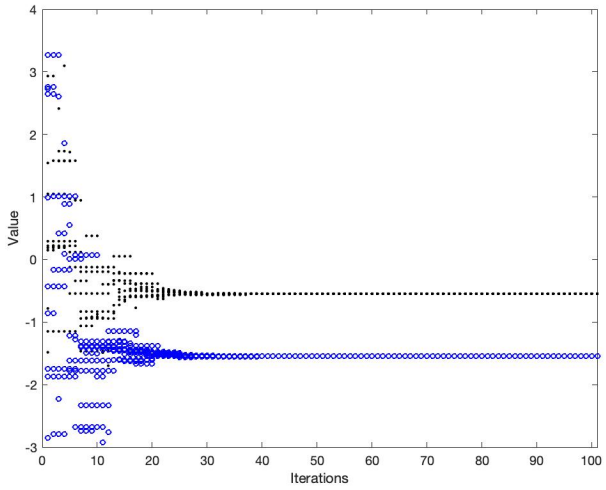

Figure D.15: Convergence to the minimum of the McCormick function using the DE algorithm

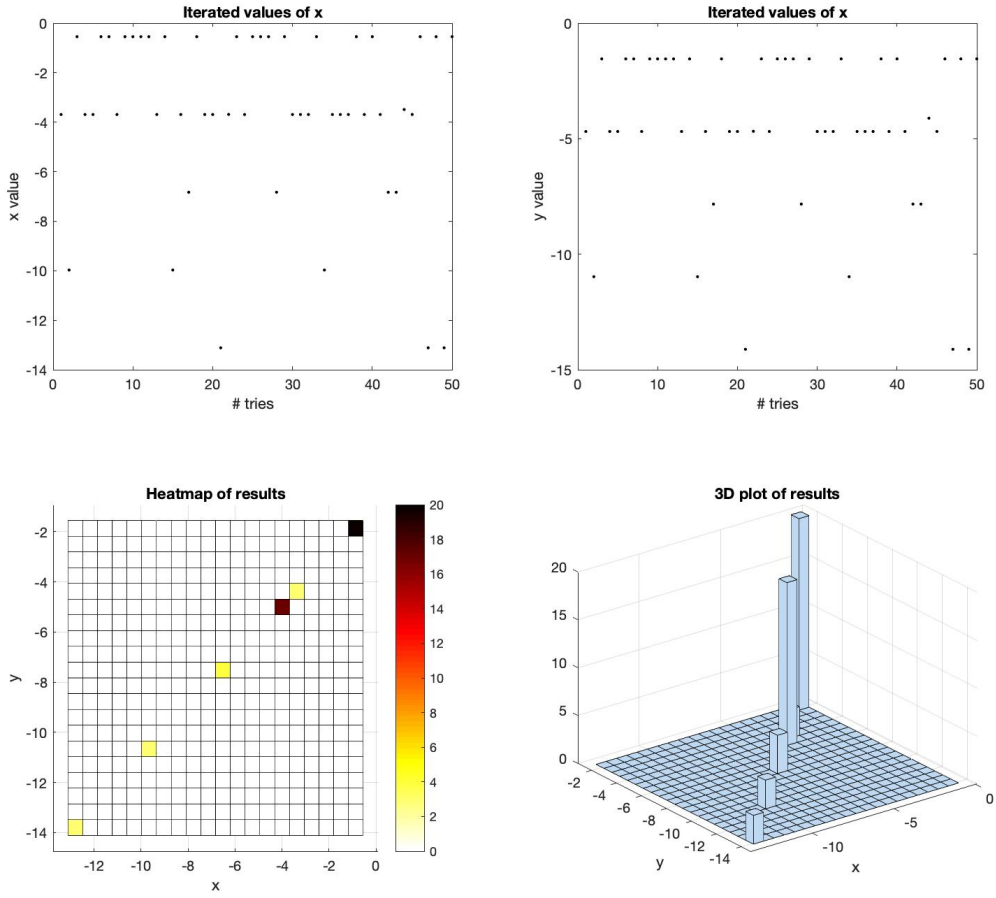

Figure D.16: Final results of multiple runs of the DE algorithm for theMcCormick function

E

CDM Summary

Following the setup of the cost function and the weights for the basic cost function, the CDMs needed to be chosen to do the simulations with. Three CDMs were chosen with differing manoeuvre minima (see Chapter 7). This chapter will give an overview of the data of these three CDMs and what the conjunction geometry looks like.

E.1. CDM Data

The information of the three CDMs can be seen in Table E.1, where the relative position and velocity are shown, as well as the position at TCA (in ITRF frame) and the covariance element values at TCA. The positions and velocities as well as the covariance values are given in the RTN frame, which is the same frame as the RIC frame that was discussed earlier in this thesis.

As was also mentioned in Chapter 7, CDM1 and CDM2 represent the same conjunction event. This can also be seen in the values in Table E.1, where the TCA is at the same time and the position and velocity at TCA. Even though the relative speed is the same, it can be seen that the miss distance is less in the second CDM. Looking at the relative position in RTN, it can be seen that this is mainly a result of different values in the T and N direction as these values are smaller.

Continuing with the position and velocity at TCA, it looks like the difference is small. However, the difference is multiple meters for the position when looking at both satellites. The covariance matrix values have also changed between CDM1 and CDM2, where the largest offset is seen in the elements of the first satellite. Additionally, it can also be seen that the covariance values that have at least one component in the T-direction have significantly larger values compared to the values in the other directions. This indicates that there is a large inaccuracy in the T-direction, which is the in-track direction.

For CDM23 it can be seen that the relative speed is large, compared to the first two CDMs. The relative position on the other hand has lower values compared to the first two CDMs. Comparing the covariance element values with the same analogy can was done above, it is again seen that the elements containing at least one component in the in-track direction have larger values than the other elements.

E.2. Conjunction Location and View

Using the given position and velocity of the satellites, the orbits can be simulated and are shown in Figure E.1, E.2, E.3 and E.4. As the conjunction event is the same for CDM1 and CDM2, Figure E.1 and E.2 show the situation for both events.

In both Figure E.1 and E.2, the second satellite moves in from the left side and the primary satellite moves in from the right side. The conjunction event is indicated where the orbits cross, just north of Madagascar.

Similar as in the two figures depicting CDM1 and CDM2, both Figure E.3 and E.4 depict the orbit and conjunction event for CDM23. Here again the second satellite moves in from the left side and the primary satellite moves in from the right side. The conjunction event is indicated where the orbits cross, on the east of the United States. Comparing the two conjunction events, it can be seen that the angle at which the first conjunction event happens is smaller than that of the second conjunction event.

Looking at these figures, it can be seen that there are two locations in the orbit where a close approach appears. The range between the two satellites of CDM1 is plotted in Figure E.5, with a zoomed in view in

Table E.1: Summary of provided CDM1, CDM2 and CDM23 data needed for simulations

	CDM1	CDM2	CDM23
CREATION_DATE	2020-06-20T02:48:35	2020-06-20T06:33:12	2020-07-31T15:23:36
TCA	2020-06-22T05:07:00.516	2020-06-22T05:07:00.508	2020-08-02T23:53:41.591
MISS_DISTANCE [m]	459	370	211
RELATIVE_SPEED [m/s]	5748	5748	14296
RELATIVE_POSITION_R [m]	96.4	97	107.3
RELATIVE_POSITION_T [m]	415.4	330.7	57.7
RELATIVE_POSITION_N [m]	170.7	135.2	-172.9
RELATIVE_VELOCITY_R [m/s]	4.2	4.3	26.6
RELATIVE_VELOCITY_T [m/s]	-2175	-2175	-13464.4
RELATIVE_VELOCITY_N [m/s]	5321.2	5321.2	-4805.4
COLLISION_PROBABILITY [-]	1.76913E-06	1.76584E-06	5.85055E-06
		Satellite 1	
Exclusion Volume Radius [m]	5	5	5
X [km]	4560.16072	4560.159464	2877.976475
Y [km]	5192.240197	5192.235818	-4758.011392
Z [km]	-501.709793	-501.757873	4122.244762
X_DOT [km/s]	0.756933827	0.756898773	-3.706088763
Y_DOT [km/s]	-1.388219496	-1.388259547	2.988464288
Z_DOT [km/s]	-7.500758917	-7.500755515	6.004896721
CR_R [m^2]	69.83596841	66.64338361	92.62849224
CT_R [m^2]	-1291.603568	-1126.119327	-1920.603491
CT_T [m^2]	175605.4531	148744.3989	299197.3367
CN_R [m^2]	-5.314552666	-4.59813584	16.36909905
CN_T [m^2]	8.585562252	-9.502919227	-30.40769978
CN_N [m^2]	28.53619574	27.90761293	12.37911792
		Satellite 2	
Exclusion Volume Radius [m]	5	5	5
X [km]	4560.116654	4560.138218	2878.133064
Y [km]	5192.365085	5192.349915	-4757.958454
Z [km]	-502.149589	-502.109395	4122.376793
X_DOT [km/s]	-3.346020535	-3.345986888	6.07222365
Y_DOT [km/s]	2.362422075	2.362459702	0.16590118
Z_DOT [km/s]	-6.036413657	-6.036417707	-4.035037439
CR_R [m^2]	40755.55886	40753.50786	69540.75411
CT_R [m^2]	21982041.39	21982303.56	39162530.17
CT_T [m^2]	38482251100	38482328928	30200866406
CN_R [m^2]	-19146.25116	-19146.50225	-24571.81104
CN_T [m^2]	-32995007.54	-32995097.35	-17888975.07
CN_N [m^2]	30832.70946	30832.81486	11961.03291

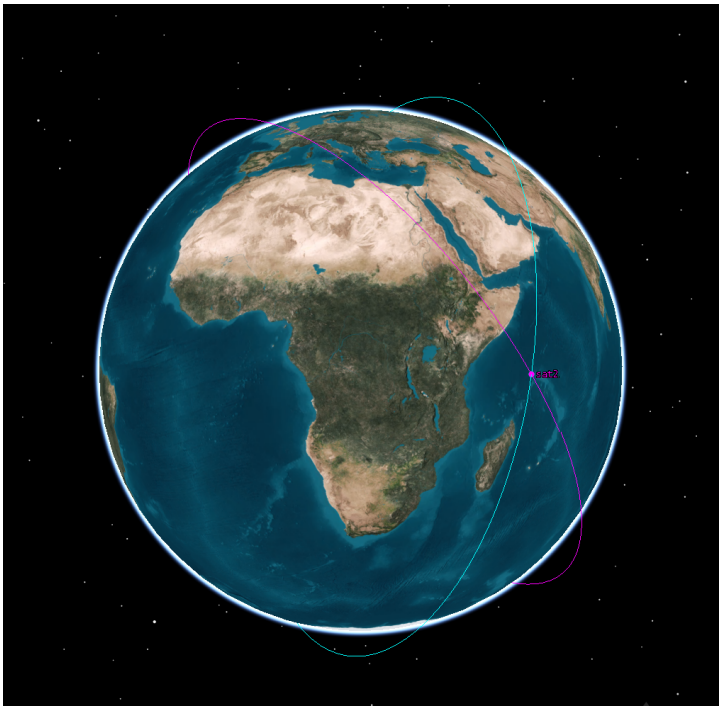

Figure E.1: 3D view of conjunction event of CDM1 and CDM2

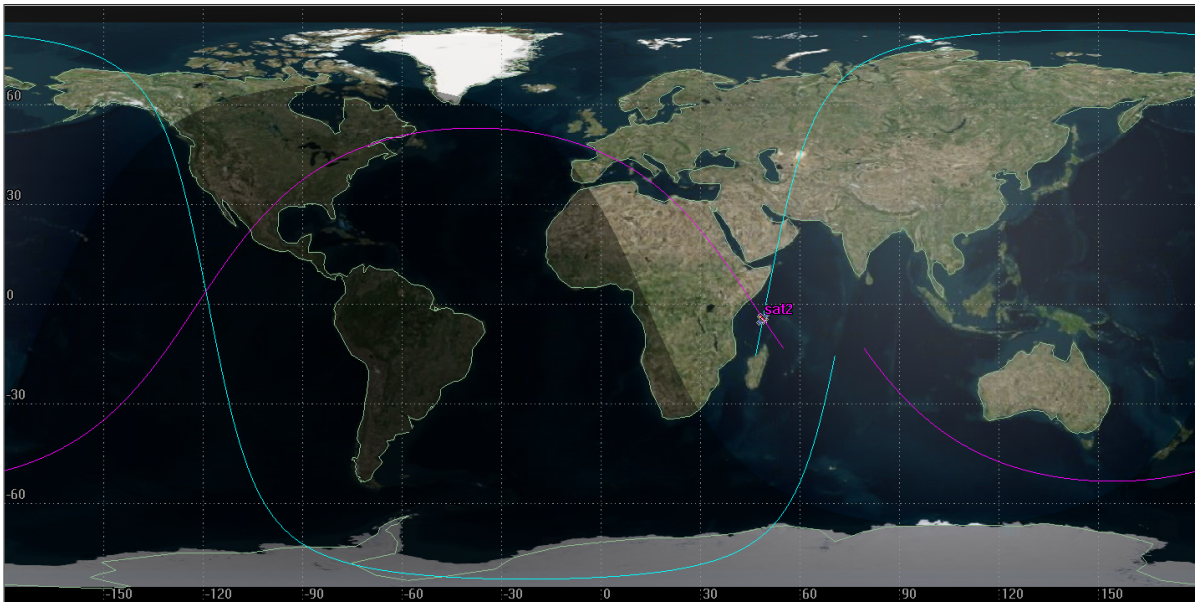

Figure E.2: 2D view of conjunction event of CDM1 and CDM2

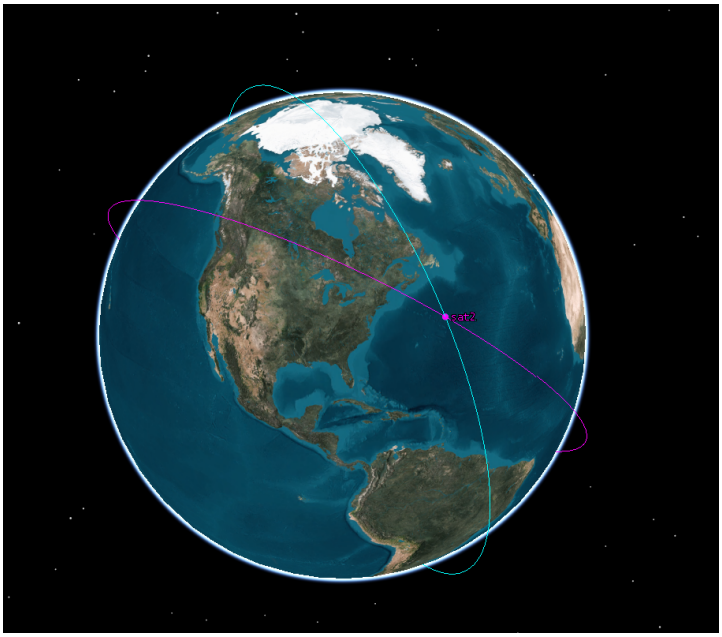

Figure E.3: 3D view of conjunction event of CDM23

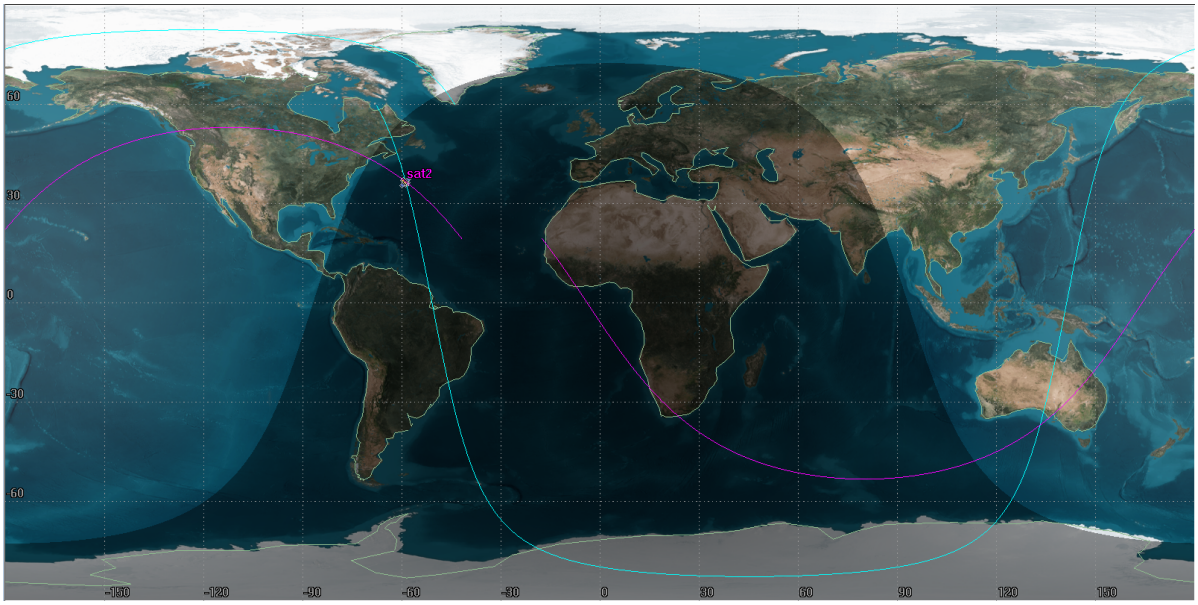

Figure E.4: 2D view of conjunction event of CDM23

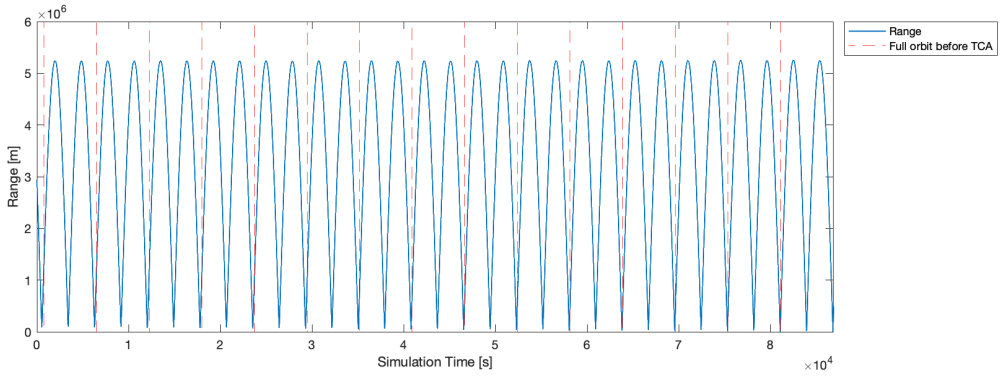

Figure E.5: Range between the primary and secondary satellite during the simulation time of CDM1

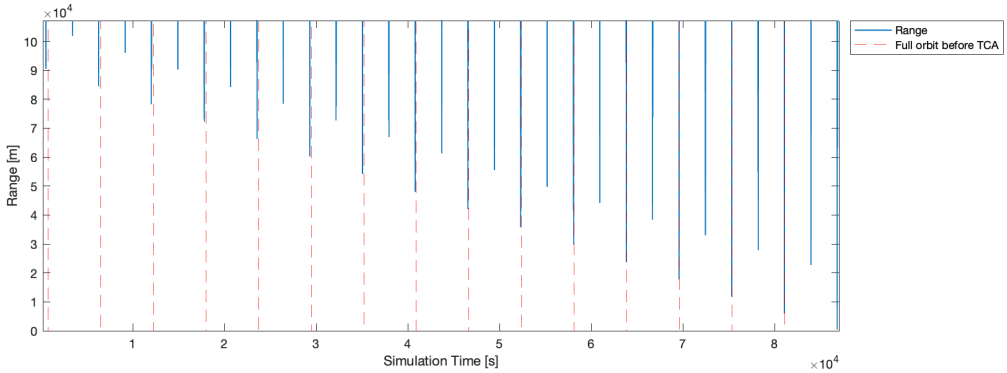

Figure E.6: Zoomed in range between the primary and secondary satellite during the simulation time of CDM1

Figure E.6. Here it can be seen that the close approach at the opposite side of the orbit is larger than the one at the indicated location of TCA.

In the zoomed in figure it is seen that the range gets closer and closer, where the closest is seen at TCA.

Bibliography

[1] ESA Space Debris Office. Esa's annual space environment report. Technical report, European Space Operations Centre, 07 2019.

[2] Donald Kessler, Nicholas Johnson, J.-C Liou, and Mark Matney. The kessler syndrome: Implications to future space operations. *Advances in the Astronautical Sciences*, 137, 01 2010.

[3] Christophe Bonnal, Laurent Francillout, Monique Moury, Ursula Aniakou, Juan-Carlos Dolado Perez, Julien Mariez, and Sylvain Michel. Cnes technical considerations on space traffic management. *Acta Astronautica*, 167:296 – 301, 2020.

[4] NASA Orbital Debris Program Office. Orbital debris quarterly news. Technical report, National Aeronautical and Space Administration, 02 2020. Volume 24, Issue 1.

[5] Ting Wang. Analysis of debris from the collision of the cosmos 2251 and the iridium 33 satellites. *Science & Global Security*, 18(2):87–118, 2010.

[6] Gil Denis, Didier Alary, Xavier Pasco, Nathalie Pisot, Delphine Texier, and Sandrine Toulza. From new space to big space: How commercial space dream is becoming a reality. *Acta Astronautica*, 166:431–443, 2020.

[7] Inter-Agency Space Debris Coordination Committee. Iadc space debris mitigation guidelines. Technical report, IADC Space Debris Mitigation Guidelines, 09 2007.

[8] Holger Krag, Stijn Lemmens, Tim Flohrer, and H Klinkrad. Global trends in achieving successful end-of-life disposal in leo and geo. In *SpaceOps 2014 Conference, Pasadena*, 05 2014.

[9] Carmen Pardini and Luciano Anselmo. Review of past on-orbit collisions among cataloged objects and examination of the catastrophic fragmentation concept. *Acta Astronautica*, 100:30 – 39, 2014.

[10] Jae-Dong Seong and Hae-Dong Kim. Collision avoidance maneuvers for multiple threatening objects using heuristic algorithms. *Proceedings of the Institution of Mechanical Engineers, Part G: Journal of Aerospace Engineering*, 229(2):256–268, 2015.

[11] Eun-Hyouek Kim, Hae-Dong Kim, and Hak-Jung Kim. A study on the collision avoidance maneuver optimization with multiple space debris. *Journal of Astronomy and Space Sciences*, 29:11–21, 03 2012.

[12] 18 SPCS. Spaceflight safety handbook for satellite operators. 2020.

[13] James Wertz. *Mission geometry: orbit and constellation design and management: spacecraft orbit and attitude systems*. Microcosm Press and Springer, 01 2001.

[14] Heiner Klinkrad. Space debris. *Encyclopedia of Aerospace Engineering*, 2010.

[15] Salvatore Alfano and Daniel Oltrogge. Probability of collision: Valuation, variability, visualization, and validity. *Acta Astronautica*, 148:301 – 316, 2018.

[16] Bob Schutz, Byron Tapley, and George H Born. *Statistical orbit determination*. Elsevier, 2004.

[17] MD Hejduk. Neutral atmospheric density modeling and the conjunction assessment problem. 2017.

[18] Sara Miller, Mitchell LR Walker, Jack Agolli, and John Dankanich. Survey and performance evaluation of small-satellite propulsion technologies. *Journal of Spacecraft and Rockets*, pages 1–10, 2020.

[19] Toshinori Ikenaga and Masayoshi Utashima. Study on the stationkeeping strategy for the libration point mission. *Transactions of the Japan Society for Aeronautical and Space Sciences, Aerospace Technology Japan*, 10(ists28):Pd_11–Pd_20, 2012.

[20] Hans J Königsmann, John T Collins, Simon Dawson, and James R Wertz. Autonomous orbit maintenance system. *Acta Astronautica*, 39(9-12):977–985, 1996.

[21] Kelly Fleetwood. An introduction to differential evolution. In *Proceedings of Mathematics and Statistics of Complex Systems (MASCOS) One Day Symposium, 26th November, Brisbane, Australia*, pages 785–791, 2004.

[22] Napapan Piyasatian. Differential evolution.

[23] T. Flohrer, H. Krag, and H. Klinkrad. Esa's process for the identification and assessment of high-risk conjunction events. *Advances in Space Research*, 44(3):355 – 363, 2009.

[24] Matthew D Hejduk. Collision avoidance short course part i: Theory. 2017.

[25] MF Storz, BR Bowman, and JI Branson. Dynamic calibration atmosphere (dca) for the high accuracy satellite drag model (hasdm). AIAA-2002-4886. AIAA/AAS Astrodynamics Specialist Conference and Exhibit . . . , 2002.

[26] Richard Ghrist and Dragan Plakalovic. Impact of non-gaussian error volumes on conjunction assessment risk analysis. In *AIAA/AAS Astrodynamics specialist conference*, page 4965, 2012.

[27] Matthew D Hejduk and Dan E Snow. Ca risk assessment approaches. 2018.

[28] Sal Alfano. Collision avoidance maneuver planning tool. In *15th AAS/AIAA astrodynamics specialist conference*, pages 7–11, 2005.

[29] Matthew D Hejduk and Lauren C Johnson. Approaches to evaluating probability of collision uncertainty. 2016.

[30] B Reihs, F McLean, S Lemmens, K Merz, and H Krag. Analysis of cdm covariance consistency in operational collision avoidance. In *7th European Conference on Space Debris*, 2017.

[31] The White House. Space policy directive-3, national space traffic management policy. In *Infrastructure & Technology*, 2018.

[32] R. Tullmann, C. Arbinger, S. Baskcomb, J. Berdermann, H. Fiedler, E. Klock, and T. Schildknecht. On the implementation of a european space traffic management system. Technical report, DLR GfR, 06 2017.

[33] Veronica Foreman, Afreen Siddiqi, and Olivier de Weck. Large satellite constellation orbital debris impacts: Case studies of oneweb and spacex proposals. In *AIAA SPACE Forum, Orlando*, 09 2017.

[34] David Wright. Orbital debris produced by kinetic-energy anti-satellite weapons. In *Celebrating the Space Age: 50 Years of Space Technology, 40 Years of the Outer Space Treaty - Conference Report 2-3 April 2007, Geneva, UNIDIR, 2007*, pages 155–164, 2007.

[35] Vladimir Akhmetov, Vadym Savanevych, and Evgen Dikov. Analysis of the indian asat test on 27 march 2019, 2019.

[36] Theodore J Muelhaupt, Marlon E Sorge, Jamie Morin, and Robert S Wilson. Space traffic management in the new space era. *Journal of Space Safety Engineering*, 6(2):80–87, 2019.

[37] Grant R. Cates, Daniel X. Houston, Dougles G. Conley, and Karen L. Jones. Launch undertainty: Implications for large constellations. Technical report, The Aerospace Corporation - Center for Space Policy and Strategy, 11 2018.

[38] European Space Policy Institute. Espi report 71 - towards a european approach to space traffic management - full report. Technical report, ESPI, 01 2020.

[39] Luigi Scatteia. Main trends and challenges in the space sector. Technical report, PWC, 06 2019.

[40] NASA Orbital Debris Program Office. Orbital debris quarterly news. Technical report, National Aeronautical and Space Administration, 08 2019. Volume 23, Issue 3.

[41] Erik Kulu. Newspace index. `https://www.newspace.im/`, 2020. Accessed: 2020-01-15.

[42] Inc. Kuiper Systems LLC, Amazon.com Services. Ibfs file no. sat-loa-20190704-00057, 09 2019. Call Sign S3051.

[43] B. Bastida Virgili, J.C. Dolado, H.G. Lewis, J. Radtke, H. Krag, B. Revelin, C. Cazaux, C. Colombo, R. Crowther, and M. Metz. Risk to space sustainability from large constellations of satellites. *Acta Astronautica*, 126:154 – 162, 2016. Space Flight Safety.

[44] J.-C. Liou. Collision activities in the future orbital debris environment. *Advances in Space Research*, 38(9):2102 – 2106, 2006.